Interactions between drag reducing polymers and surfactants

by

Ketan Prajapati

A thesis
presented to the University of Waterloo
in fulfillment of the
thesis requirement for the degree of
Master of Applied Science
in
Chemical Engineering

Waterloo, Ontario, Canada, 2009
© Prajapati, Ketan 2009

AUTHOR'S DECLARATION

I hereby declare that I am the sole author of this thesis. This is a true copy of the thesis, including any required final revisions, as accepted by my examiners.

I understand that my thesis may be made electronically available to the public.

Abstract

Drag reduction in turbulent pipe flow using polymeric and surfactant additives is well known. Although extensive research work has been carried out on the drag reduction behavior of polymers and surfactants in isolation, little progress has been made on the synergistic effects of combined polymers and surfactants. In this work the interactions between drag-reducing polymers and surfactants were studied. The drag-reducing polymers studied were nonionic polyethylene oxide (referred to as PEO) and anionic copolymer of acrylamide and sodium acrylate (referred to as CPAM). The drag-reducing surfactants studied were nonionic ethoxylated alcohol - Alfonic 1412-7 (referred to as EA), cationic surfactant - Octadecyltrimethylammonium chloride in pure powder form (referred to as OTAC-p) and commercial grade cationic surfactant - Octadecyltrimethylammonium chloride in isopropanol solvent - Arquad 18-50 (referred to as OTAC-s). The interactions between polymers and surfactant were reflected in the measurements of the physical properties such as electrical conductivity, surface tension, viscosity and turbidity.

The critical micelle concentration (cmc) of the mixed polymer / surfactant system was found to be different from that of the surfactant alone. The viscosity of a polymer solution was significantly affected by the addition of surfactant. Weak interactions were observed for the mixed systems of nonionic polymer - nonionic surfactant and anionic polymer - nonionic surfactant. Due to the wrapping of polymer chains around the developing micelles, a minimum in the viscosity is observed in these two cases. In the case of nonionic polymer / cationic surfactant system, the change in the viscosity was found to depend on the polymer concentration (C) and the critical entanglement concentration (C*). When the polymer concentration (C) was less than C* ($C < C^*$), the plot of the viscosity versus surfactant concentration exhibited a minimum. When $C > C^*$, a maximum in the viscosity versus surfactant concentration plot was observed. The interactions between nonionic polymer and cationic surfactant were observed to increase with the increase in temperature.

A large drop in the viscosity occurred in the case of anionic-polymer / cationic-surfactant system when surfactant was added to the polymer solution. The observed changes in the viscosity are explained in terms of the changes in the extension of polymeric chains resulting from polymer-surfactant interactions. The anionic CPAM chains collapsed upon the addition of cationic OTAC-p, due to charge neutralization. The presence of counterion sodium salicylate (NaSal) stabilized the cationic surfactant monomers in the solution, resulting in micelle formation at a surfactant concentration well below the concentration where complete charge neutralization of anionic polymer occurred.

Preliminary results are reported on the pipeline drag reduction behavior of mixed polymer-surfactant system. The results obtained using combinations of CPAM / OTAC-p in pipeline flow are found to be in harmony with the interaction study. Due to the shrinkage of CPAM chains upon the addition of OTAC-p, the drag reducing ability of CPAM is compromised.

Acknowledgements

I am highly grateful to my supervisor Prof. Rajinder Pal for his continuous support and guidance during last two years without which this work could not be completed. I am thankful for his understanding, patience and cooperation. It was a learning experience to work with him. I also appreciate his efforts in thoroughly revising the thesis. I would like to thank Prof. Ali Elkamel and Prof. Neil McManus for their reviews and suggestions.

My sincere thanks to Ms. Jennifer Moll and Mr. Mark Sobon for allowing me to use their lab facilities as and when needed. I would also like to thank Prof. Pu Chen for permission to use their lab instrument. Also, with appreciation, I would like to thank Kathy Wang for helping me with experiments to study the polymer- surfactant interactions in tap water. I am thankful to Ali Mohsenipour for allowing me to use his pipeline flow results dealing with mixed polymer-surfactant system.

With great appreciation I would like to acknowledge the samples received from AkzoNobel USA, The Dow Chemicals Company USA, Molekula Ltd. UK, SASOL USA and Hychem Inc. USA. Financial support for this research is provided by Natural Sciences and Engineering Research Council of Canada (NSERC) in the form of a discovery grant awarded to Professor Rajinder Pal.

Very special thanks to Dhatri - my wife, for her love, support and standing by me. I would also like to thank her for helping me with the graphics work to prepare some of the drawings in this thesis with great appreciation. I would also like to thank my parents, my brother and sister for their endless encouragement and support. The beautiful smiles and innocent eyes of my son, Abhi have been my continuous source of energy. At last, I would like to thank God for this beautiful world and such nice people around me.

Dedication

To my parents

For their love, care and encouragement
They are what I am today

and India

My motherland

Table of Contents

List of Figures

List of Tables

Appendix A

Appendix B

Chapter 1
Introduction

1.1 Background for the Study of interactions between Polymers and Surfactants

Due to a broad range of applications of surfactants and polymers, enormous amount of work has been done on the characterization and properties of surfactant and polymer solutions. The balance in interaction between the solvent and hydrophobic and hydrophilic segments of polymer determines the solubility of a given polymer in solvent. The aggregation of surfactant molecules in aqueous solution depends on hydrophobic, hydrophilic and ionic interactions. Due to a wide variety of molecular structures, polymer and surfactant when mixed together in aqueous solution display a wide variety and sometimes even very strange pattern of properties (Rodenhiser, 1998).

In 1940s and 1950s, the study of interaction between proteins and synthetic ionic surfactants recognized the importance of electrical forces of attraction of charged groups. This led to the development of the concept of "binding" of charged surfactants by the polymer macromolecule to explain the conformational changes in polymer macromolecules (Goddard, 1986). The complexes formed due to interaction of polymer and surfactants have a remarkable influence on the system properties leading to renewed interest in the area in recent decades. However, many concepts traditionally used in polymer-surfactant studies need modification in order to be applicable to a wide variety of macromolecules such as hydrophobically modified polymers which are normally considered hydrophilic. In recent years, there has been a growing interest in oppositely charged polymers and surfactants due to their importance in both biological and technological applications. They are also important in fundamental studies related to intermolecular interactions and hydrophobic aggregation phenomena. In the case of oppositely charged polymer and surfactants, both electrostatic and hydrophobic interactions play a role. The properties of such mixtures depend on many factors such as polymer charge density, backbone rigidity, surfactant chain length and concentrations of polymer and surfactant (Trabelsi et al., 2007).

1.2 Brief overview of polymers and surfactants

1.2.1 Polymers

A polymer is a large macromolecule built from a repetition of smaller chemical units called monomers. For example, polyethylene oxide is made up of repetitive units of ethylene oxide. Proteins and polysaccharides are natural polymers whereas commonly used plastics and adhesives are synthetic polymers. As shown in ***Figure 1.1***, polymer could be linear, branched or cross-linked. If the polymer is synthesized with more than one kind of monomer, it is called a copolymer. Based on the distribution of these different monomer units in the polymer chain, they can be classified further as randomly distributed, block or grafted copolymer. Based on the ionic charge of the monomeric groups, the polymers can be further classified as: non-ionic (example – polyethylene oxide), anionic (example – polyacrylic acid) and cationic (example – polyquaterniums) polymers.

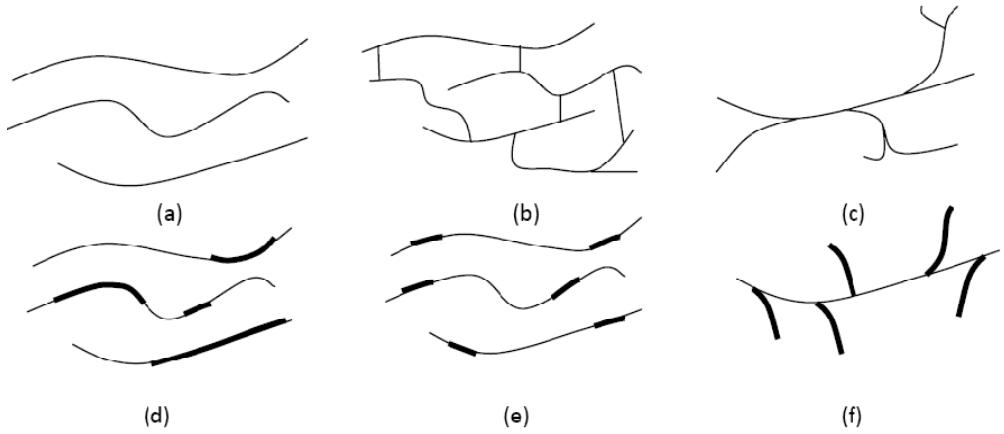

Figure 1.1 Polymer structures: (a) linear (b) cross-linked (c) branched polymer. (d) Randomly distributed (e) block and (f) grafted copolymer.

The physiochemical and rheological properties of polymeric solution are determined by the configuration of polymer chain which mainly depends on the interaction of the monomer blocks with each other and the solvent. When dissolved in a solvent, the polymer chains adopt various forms such as a random coil, an extended configuration or a helix. In good solvents, the polymeric chains expand leading to significant increase in viscosity of the

solution. This change in viscosity depends on type of polymer, and charge density of the polymer (in case of ionic polymer), molecular weight of polymer and polymer concentration.

The polymer molecules are essentially strings of atoms connected to each other via covalent bonds. However, the polymer molecules have the ability to physically associate and interact with spatially separated regions in a solution. They can induce and transfer the effects such as change in stress and structure from one region to another due to attractive interactions between certain regions of different polymer molecules and formation of three dimensional networks. By incorporating more than one type of monomer in the same macromolecule, one can produce a polymer that exhibits more than one kind of affinity or interaction (Goddard & Ananthapadmanabhan, 1993).

The study of polymeric solutions can be helpful in understanding the micro properties of the macromolecules; such as: molecular weight and molecular weight distribution, polymeric chain configuration, the charge density of ionizable polymer, the degree of association of polymer molecule with the solvent molecules; and the effect of other solutes present in the solution on the characterization and configuration of the macromolecule.

1.2.2 Surfactants

Surfactants are surface active agents that have a tendency to absorb at surfaces and interfaces. They lower the free energy of the phase boundary by absorbing at the interface. For example, the surface tension of water is largely reduced when surfactant is added to water as the surfactant covers the water surface in contact with air. The surface density of the surfactant molecules determines the amount of reduction in surface tension of water. There is, however a limit to the reduction of surface tension of the solvent. The lowering of the surface tension of solvent by addition of surfactant stops when surfactant molecules begin to form micelles in the bulk solution. The concentration at which micelles start to form is called critical micelle concentration (cmc).

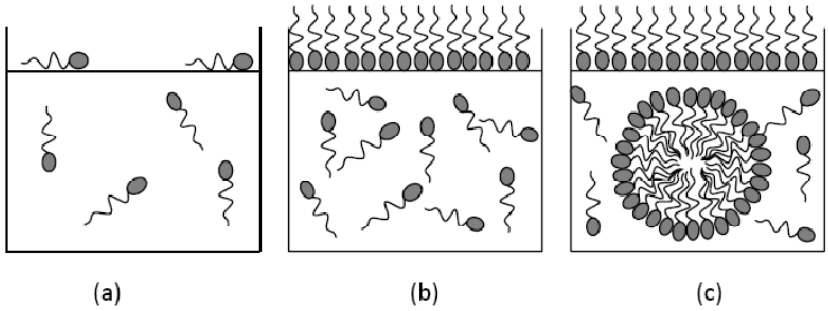

Figure 1.2 Surfactant micelle formation: (a) <cmc, (b) onset cmc, (c) >cmc

The surfactant molecule consists of two parts: the one which is soluble in a solvent is called lyophilic and the one which is insoluble in the solvent is called lyophobic. For example, in the case of water-soluble surfactants, the hydrophilic headgroup is water soluble and the hydrophobic tail is water insoluble. When surfactant is dissolved in water, the surfactant molecule tries to occupy the surface or interface so that the hydrophobic tail of the surfactant molecule is exposed to air and the polar headgroup is exposed to water, forming a uniform layer of surfactant molecules at the surface as shown in ***Figure 1.2***. Similarly, in a micelle, the hydrophobic tails of the surfactant molecules are clustered towards the core of the micellar structure by exposing the polar headgroups towards water.

The hydrophobic tail of the surfactant molecule may be branched or linear alkyl chain with length of 8 – 18 carbon atoms. The polar head group is normally attached to one end of the alkyl chain. The physiochemical properties of surfactant largely depend on the degree of chain branching, polar group position, length of alkyl chain, ionic charge of polar group and size of the polar headgroup. The surfactants can be classified as: non-ionic (example – fatty alcohol ethoxylates), anionic (example - alkyl sulfates), cationic (example – quaternary amines) and zwitterionic (example – amine oxides) depending on the charge of the polar headgroup. Zwitterionic surfactants contain both anionic and cationic charged groups.

1.3 Applications

The usage of polymers and surfactants in combination is found in a very broad range of products such as cosmetics, paints, detergents, foods, polymer synthesis, formulations of drugs and pesticides, and enhanced oil recovery. Here one or more polymer is used in combination with surfactant to achieve different effects, such as emulsification, colloidal stability, viscosity enhancement, gel formation, solubilization, cloud point elevation, catalysis and enzymatic reactions, surface conditioning, wettability improvement, detergency, foaming and phase separation. A very good review of various applications is compiled by Goddard & Ananthapadmanabhan (1993).

1.3.1 Drag Reduction

Besides the conventional uses of polymer and surfactant additives in altering solution properties, both polymers and surfactants are considered and are being used extensively as drag reducers to reduce wall friction in turbulent pipe flow so as to increase pump capacity or to reduce pump power requirement. Although drag reduction is not the main theme of this research, a brief introduction to drag reduction is given here to explain how polymer conformation changes or surfactant micelle formation in solution can affect drag reduction.

1.3.1.1 Drag reduction by polymer additives

In 1948, Toms reported that in straight pipeline flow, the addition of poly (methyl methacrylate) to the solvent monochlorobenzene resulted in less resistance to flow compared to the solvent alone. The drag reduction phenomenon is often referred as “Tom’s Effect” after Toms (Zakin et al., 1998). By adding long chain, flexible polymer molecules in very low concentration (ppm level) to a solvent, turbulent frictional losses can be reduced as much as 80% corresponding to maximum drag reduction asymptote (Virk, 1975). Although there is not a single model available that can explain all aspects of turbulent drag reduction mechanism completely, it is clear that the addition of polymer affects the viscosity and elasticity of the solvent:

1.3.1.1.1 Viscous Effects of polymeric solution

The high shear conditions of turbulent flow induces stretching of polymer chain, which increases effective viscosity in the buffer layer of turbulent flow by increasing elongational viscosity (Hinch, 1977; Metzner & Metzner, 1970). Due to this increase in effective viscosity in the buffer layer of turbulent flow, the buffer layer thickness increases which results in reduction of wall friction (Lumley, 1973). The streamwise and spanwise fluctuations are suppressed, velocity profile is modified and the shear in the boundary layer is redistributed. As shown in ***Figure 1.3***, the nature and strength of vortices formed is modified in the case of polymer solution which results in significant changes in the near-wall structure of the turbulent boundary layer (White & Mungal, 2008).

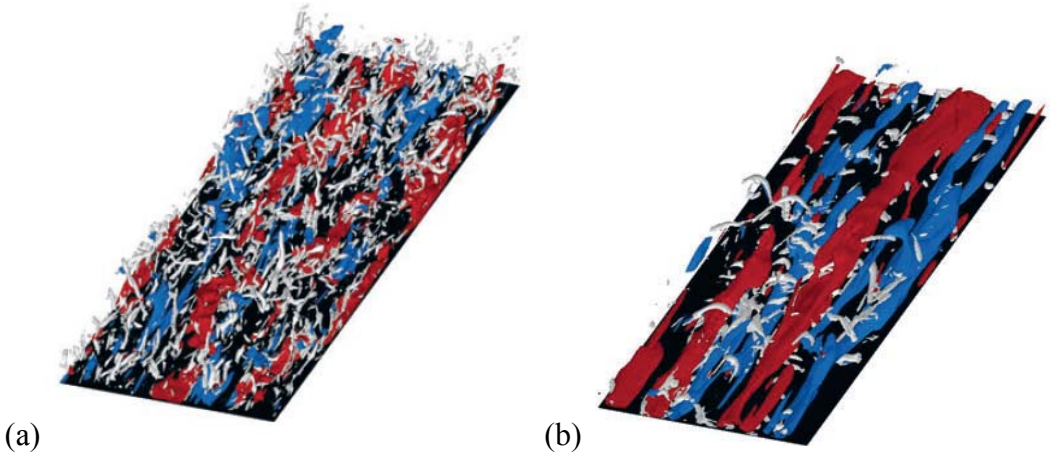

(a) (b)

Figure 1.3 Instantaneous visualization of near-wall vortex structures showing high speed and low speed streaks for (a) Newtonian fluid and (b) polymer solution at 60% drag reduction: : (□) Near-wall vortex structures (■) High-speed velocity steaks and (■) Low-speed velocity steaks (White & Mungal, 2008)

1.3.1.1.2 Elastic effects of Polymer solution

Tabor & de Gennes (1986) developed the idea of elastic energy storage by the partially stretched polymer molecules as playing a critical part in drag reduction. As per elastic theory, drag reduction is observed when cumulative elastic energy stored by these partially stretched polymer molecules reaches the level of kinetic energy in the buffer layer of turbulent flow (White & Mungal, 2008).

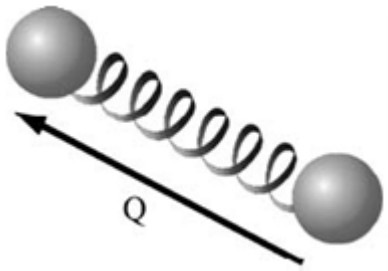

Figure 1.4 Polymer chain represented in Dumbbell in FENE-P model (Tesauro et al., 2007)

The FENE-P (Finite elastic non-linear extensibility – Peterlin) model describes a polymer chain in the form of two spherical beads connected by a massless spring specified as a connector vector **Q,** as shown in ***Figure 1.4***. It is proposed that energy is transported by the velocity fluctuations to the polymer chain in the form of stretching of the polymer chain, which in turn dissipates the energy into heat by relaxation of the polymer chain from its extended state to equilibrium state (Tesauro et al., 2007).

1.3.1.2 Drag reduction by surfactant additives

Drag reduction in turbulent pipe flow using surfactant was first reported by Mysels in 1948. He investigated the effect of aluminum disoaps on gasoline flow (Zakin et al., 1998). Savins (1967) reported drag reduction as high as 80% using 0.2% Sodium Oleate aqueous solution with KCl as counterion. As shown in ***Figure 1.5***, at a surfactant concentration sufficiently higher than the critical micelle concentration (cmc) the surfactant molecules form worm-like micellar structures in turbulent flow. The formation of such shear induced structures largely modifies the solvent properties and the solution exhibits viscoelasticity.

The exact mechanism of drag reduction by surfactants is not known even till today. However, a large number of researchers have proposed that viscoelastic effects of surfactant solution could be responsible for turbulent drag reduction. Bewersdorff & Ohlendorf (1988) showed that both micro and integral scale of turbulence axial velocity fluctuations increase substantially compared to Newtonian solvent. This increase in the size of eddies could be due to an increase in local viscosity resulting from the formation of the shear induced structures.

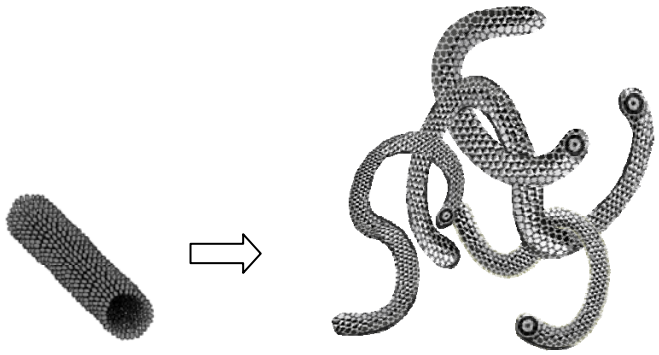

Figure 1.5 Worm-like micellar structures crucial for drag reduction (Adapted from Ezrahi et al., 2000)

In the case of surfactant induced drag reduction, the turbulent energy fluctuations (which are considered responsible for the energy loss in the form of kinetic energy of the small but very strong eddy) are found to be at a larger distance from the wall. These fluctuations are weak and the number of strong fluctuations is less than in Newtonian turbulence (Povkh et al., 1988). Also, the Reynolds stresses are found to be zero or are significantly lower than those seen in the Newtonian solvent (Povkh et al., 1988; Bewersdorff, 1990). These stress deficiencies could be explained by locally increased "effective viscosity" (Zakin et al., 1998). Anisotropic conditions are reported through Small-angle-neutron scattering (SANS) in which the statistically oriented and rotating rodlike micelles completely align in the direction of flow with their long axis almost parallel to the flow direction above critical shear stress (Bewersdorff et al., 1986; Bewersdorff et al., 1989).

1.4 Research Objectives

During the past half century, enormous amount of work has been done to study the drag reduction phenomena; to explore new applications or to explain drag reduction mechanism in turbulent flow. However, almost all of the reported work has been done to study drag reducing polymers and surfactants in isolation. Very little work has been done to study their synergistic effects to serve the purpose of drag reduction. Following is the comparison of polymers and surfactants as drag reducers.

Polymers	Surfactants
➢ Polymers start showing drag reduction at very low concentration. There is no minimum concentration requirement	➢ The surfactant concentration should be sufficiently high to form shear induced structure, in order to observe drag reduction
➢ Polymer drag reduction is not affected by temperature significantly	➢ Surfactant drag reduction is observed only in specific temperature range as micelle formation is largely affected by temperature change
➢ Large number of biodegradable polymers are available which can be used as drag reducers without any environmental issues	➢ There are a lot of uncertainties about surfactant toxicity, long term stability and post application separation techniques
➢ Polymer molecules undergo mechanical degradation under high shear condition and lose their drag reduction capability permanently	➢ Surfactant micellar network undergoes temporary disruption under very high shear conditions. The network structure is rebuilt and the drag reduction capability is regained below the critical stress

Table 1.1 Comparison of drag reduction characteristic of polymers and surfactants

As shown in ***Table 1.1***, both polymers and surfactants have some advantages and disadvantages. The combination of polymer and surfactant could be more effective in reducing drag as:

a. The combined product could improve the long term stability of drag reducer
b. The combined drag reducer can be used over a broader temperature range
c. The combined drag reducer can be used without compromising the performance under conditions in which there are large variations in turbulent shear stress

Surprisingly, after some initial studies of mixed polymer-surfactant system (for example, Patterson & Little (1975) found a drag reduction of almost 75% using polyethylene oxide and carboxylate soap mixtures), the area largely remains unexplored. Recently, Suksamranchit et al. (2006), Suksamranchit et al. (2006), Sirivat & Suksamranchit (2007) and Matras et al. (2008) have initiated research in this area using rheological study.

The broad objective of this work is to study the interactions between drag reducing polymers and surfactants using different combinations of polymers and surfactants and to identify the combinations favorable from drag reduction point of view.

Following are the specific objectives of this work:

1. To study the interaction between drag reducing polymers and surfactants. There are several analytical techniques available which can be employed to study the interaction between drag reducing polymers and surfactants. Four fundamental techniques employed in this study are: Conductivity, Surface Tension, Viscosity and Turbidity.
2. To identify the system that shows high degree of interaction and to study its behavior from a drag reduction point of view. For example, strong interactions are observed between oppositely charged polymers and surfactants suggesting drastic conformational changes.
3. To identify the concentration ranges of the drag reducing polymers and surfactants in which one could combine them to observe favorable interactions from drag reduction point of view.

1.4.1 Outline

In subsequent Chapters, the interaction between drag reducing polymers and surfactants is discussed. **Chapter 2** covers literature review to give a brief outline of early and recent developments in the field of polymer and surfactant interactions. In **Chapter 3**, the materials studied in this work (drag reducing polymers and surfactants) are introduced with their physical properties of interest in drag reduction. **Chapter 3** also sheds light on the experimental procedures and techniques used to study the interactions between drag reducing polymers and surfactants. Some theoretical concepts related to experimental techniques are also introduced in **Chapter 3**. **Chapter 4** describes experimental results in details. The results are discussed in relation to the existing theories. The relevancy of the experimental results from drag reduction point of view is described. **Chapter 4** also presents the pipeline study results of polymer / surfactant combination as drag reducer. **Chapter 5** summarizes the key findings of this study and gives recommendations for further work in this area.

Chapter 2
Literature Review

2.1 Interaction of non-ionic polymers with surfactants

Jones (1967) should be credited for his pioneer work in the study of interaction between polymers and surfactants. By studying the interaction between nonionic polymer - polyethylene oxide (PEO) and anionic surfactant - sodium dodecyl sulfate (SDS) using conductance measurements, surface tension and viscosity data, he identified two transition points, namely: cac (critical aggregation concentration) and psp (polymer saturation point) as shown in ***Figure 2.1***.

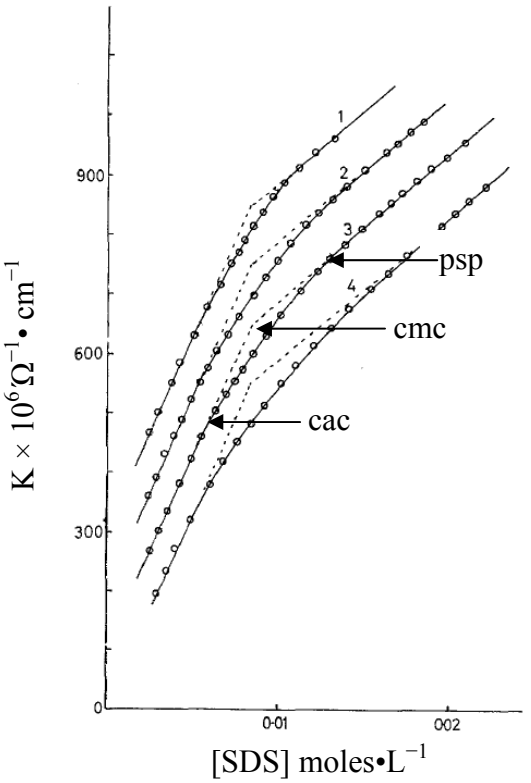

Figure 2.1 Conductance of PEO vs. SDS (curves 1, 2, 3 and 4 at PEO concentration 0.025%, 0.05%, 0.065% and 0.09% (wt./vol.) respectively, displaced by unit scale. Dotted line for pure SDS solution) (Reproduced from Jones, 1967)

No interaction between PEO and SDS is observed below cac whereas roughly stoichiometric interactions are reported between cac and psp. Past the psp, polymer-surfactant aggregates (in the form of polymer loosely adsorbed on micelles) and free micelles exist in dynamic equilibrium (Cabane, 1977; Lissi, 1985).

In contrast to the remarkable interaction of nonionic polymer - polyethylene Glycol (PEG) and anionic surfactant - Sodium hexadecyl sulfate (SHS), Saito (1967) reported very weak interaction between PEG and cationic hexadecyl amine hydrochloride (HAC). Similarly, Schwuger (1973) found no complex formation between PEG and cationic surfactant dodecyltrimethylammonium chloride. However, by increasing number of carbon atoms from 12 to 18 in the hydrophobic tail of the surfactant, he observed a plateau in surface tension plot similar to that found in nonionic polymer / anionic surfactant (Schwuger, 1973) system indicating the presence of interaction between nonionic polymer and cationic surfactant. The interaction of nonionic polymer and anionic surfactant is very well studied and reported. However, due to limited use of anionic surfactants as drag reducers, the interactions of polymers and anionic surfactants are not explored in this study.

2.1.1 Interaction of Non-ionic polymer with Non-ionic surfactant

Hydrophilic polymers such as PVA (polyvinyl alcohol), PEO and PVP (polyvinyl propylene) generally exhibit no interactions with polyoxyethylated nonionic surfactants as verified by various techniques such as dye solubilization, viscosity and surface tension (Saito, 1987). However, Feitosa et al. (1996) reported that high molecular weight PEO forms clusters with polyethoxylated nonionic surfactant ($C_{12}E_5$). Studies dealing with the measurement of hydrodynamic radius of gyration (R_H) of PEO/$C_{12}E_5$ have indicated that the increase of $C_{12}E_5$ in PEO solution induces growth of micellar clusters within the polymer chain domain leading to uncoiling of the polymeric chains of PEO. Also, Fluorescence Quenching measurements indicated significant increase in the aggregation number of the $C_{12}E_5$ micelles upon increasing PEO concentration. This can be due to stabilization of more number of $C_{12}E_5$ monomers in cluster formed by the surrounding polymer segments (Feitosa et al. 1996).

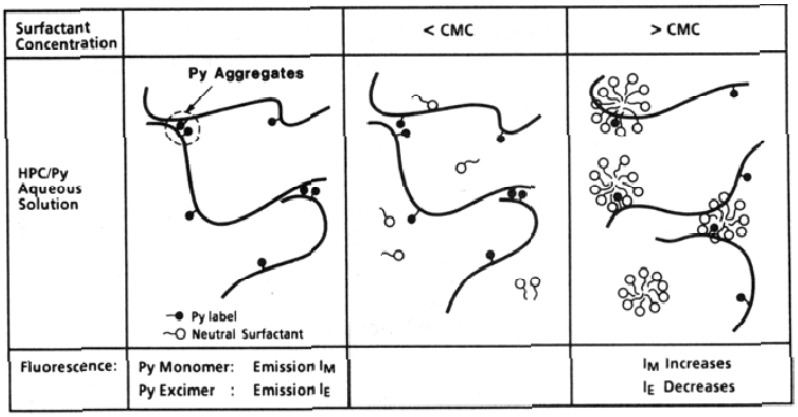

Figure 2.2 Schematic representation of interaction between HPC/Py and nonionic surfactant (Winnik, 1990)

Microcalorimetric studies of interactions of non-ionic surfactant n-octylthioglucoside (OTG) with polyethylene oxide (PEO) and polypropylene oxide (PPO) indicate that PEO resides at the surface of micelles due to hydrophilic nature of the polymer. Hydrophobic polymer (PPO) binds well with the hydrophobic core of the OTG surfactant by penetrating into the micelle (Brackman, 1988). The interactions between nonionic polymer and surfactant observed by Brackman (1988) were further investigated by Winnik (1990) who studied the interactions between Pyrene-labeled hydroxypropyl cellulose (HPC/Py) and OTG using fluorescence measurements. Strong interactions were observed in the concentration range near the cmc of the surfactant. As shown in ***Figure 2.2***, the polymer-polymer aggregates in the presence of surfactant are disturbed and even modified leading to conformational changes of polymeric chains (Winnik, 1990).

By investigating the microstructure of non-ionic surfactant TX-100 and polyethylene Glycol (PEG) complexes using fluorescence resonance energy transfer, Ge et al. (2007) have recently illustrated two possible configurations of TX-100 / PEG complexes for low and high molecular weight PEG (see ***Figure 2.3***): sphere-like clusters for shorter chains and coral-like clusters for long chains of PEG. As shown in ***Figure 2.3***, PEG does not pass through the TX-100 micelles; it either absorbs on to the surface or penetrates into the hydrophilic layer of the micelles. An increase in the micelle size also occurs due to the formation of these complexes.

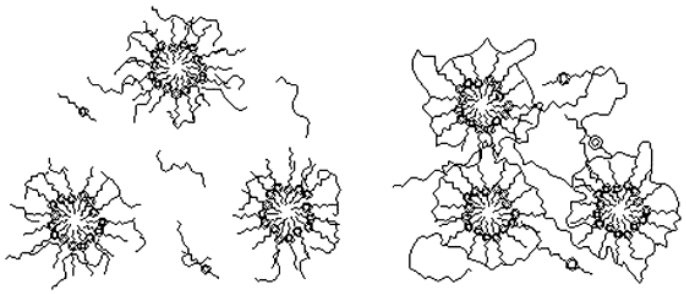

(a) (b)

Figure 2.3 (a) Sphere-like PEG / TX-100 complex for low mol. wt. PEG (b) Coral-like PEG / TX-100 complex for high mol. wt. PEG (Ge et al., 2007)

Qiao & Easteal (1998) studied the variation in cloud point of nonionic surfactant Triton X-114 with the addition of nonionic polymer PEG. Upon addition of PEG to Triton X-114 solution, the cloud point reduces and the effect is more profound in the case of high molecular weight PEG. The short length – low molecular weight PEG chains merely wrap or cover the micelles. Repulsion produced between the wrapped micelles due to the steric and silvation effects of the polymer chains prevents collisions between micelles. Therefore, more energy is required to reach the cloud point. However, in the case of high molecular weight PEG, more than one micellar structure can bind on to a single PEG chain. The exchange of Triton X-114 monomers between neighboring Triton X-114 micelles forms bridges and facilitates collisions among the micelles leading to cloud point reduction. With the increase in molecular weight of PEG, more clusters of polymer-surfactant aggregates are expected to form leading to more opportunities for exchange and micellar collision and hence resulting in lower cloud point.

As shown in ***Figure 2.4 (a)***, the addition of nonionic surfactant Triton X – 100 (TX-100) to aqueous solution of polyacrylamide (PAM) reduces the specific viscosity to some minimum value (Mya et al., 1999). Also, based on diffusion study of aqueous solution of PAM and TX-100, Mya et al. (1999) reported that diffusion co-efficient decrease in the range of 0.1 – 1 mM, which means that the hydrodynamic volume increases (see ***Figure 2.4 (b)***). They suggested that the increase in hydrodynamic volume and the reduction in specific viscosity

are due to a decrease in the number of solute species. The binding of surfactant molecules on to the polymer chains induces the aggregation of chains in the surfactant concentration range of 0.1 – 1mM. The increase in the specific viscosity at very high surfactant concentration can be attributed to formation of free micelles similar to those found in the case of pure surfactant solution.

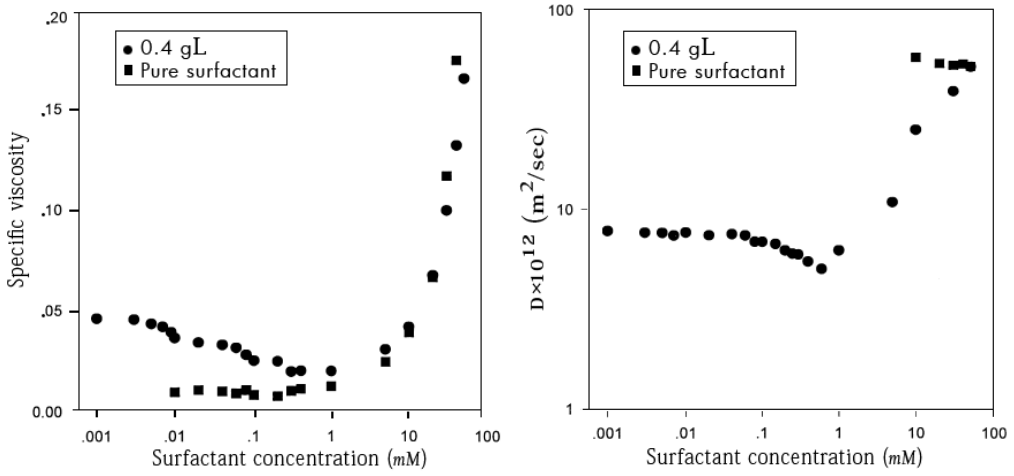

(a) (b)

Figure 2.4 (a) Specific viscosity vs. TX-100 concentration for pure surfactant and 0.4 gm/L PAM solution. (b) Diffusion co-efficient vs. TX-100 concentration for pure surfactant and 0.4 gm/L PAM concentration (Mya et al., 1999)

2.1.2 Interactions of Non-ionic polymer with Cationic surfactant

Early research in this area suggested that there is either complete absence of interactions or very weak interactions are present between nonionic polymer and cationic surfactant (Saito, 1967; Schwuger, 1973; Moroi et al., 1977). Schwuger (1973) observed no interaction between nonionic polyethylene oxide (PEO) and cationic dodecyltrimethylammonium chloride (C_{12}TAC). However, increasing the hydrocarbon tail length of cationic surfactant, the interaction between nonionic PEO and cationic Octadecyltrimethylammonium chloride (C_{18}TAC) became evident. Surface tension and conductivity measurements indicated the presence of two clear inflexion points, one indicating the start of interaction and the other

indicating the end of interaction. The interactions however, were very weak compared to the system of nonionic polymer and anionic surfactant (Schwuger, 1973).

Hydrophobicity is considered to be one of the key factors affecting the interaction between nonionic polymers and cationic surfactant. In aqueous solution of ethyl (hydroxyethyl) cellulose (EHEC), the addition of cationic surfactant dodecyltrimethylammonium bromide (DTAB) in the presence of NaCl induces considerable depression of cloud point. A fairly high concentration of charged surfactant ions and counterions causes the masking of the repulsive interactions of partially charged polymer chains. This results in the cloud point depression. However there exists a minimum cloud point after which the cloud point again starts to increase with further addition of DTAB. The repulsive electrostatic forces overcome the attractive hydrophobic forces leading to an increase in the cloud point at higher concentrations of DTAB (Carlsson et al., 1989). Carlsson et al. (1989) also observed a sharp decrease in the self-diffusion coefficient when DTAB concentration exceeds the cmc point. The obstruction effect (evident by a sharp decrease in the self-diffusion coefficient) is indicative of strong cooperative interaction between DTAB and EHEC. They also reported that high temperatures favor the formation of complex between DTAB and EHEC, as at high temperature polymer becomes more hydrophobic.

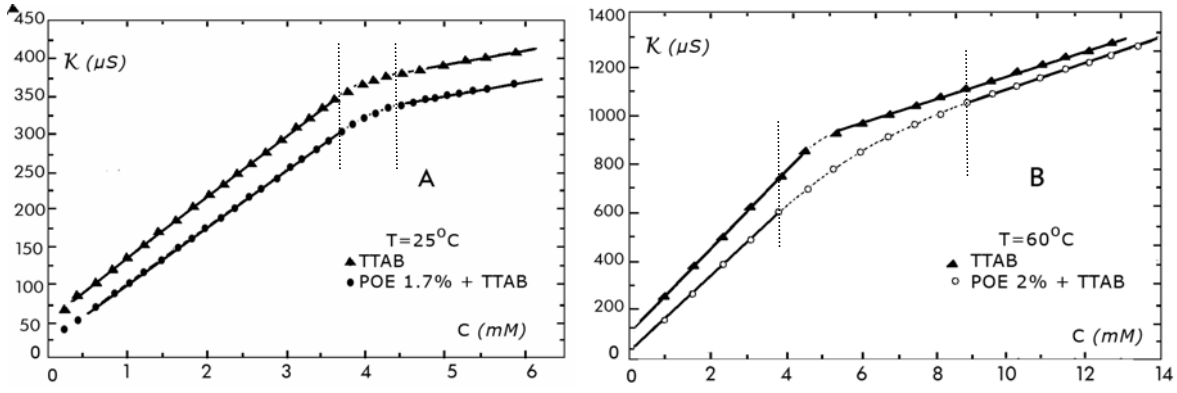

(a) (b)

Figure 2.5 conductivity of aqueous solution of POE and TTAB at (a) 25 °C and (b) 60 °C (Anthony & Zana, 1994)

The effect of temperature on the interaction between nonionic polymer polyoxyethylene (POE) and cationic surfactant tetradecyltrimethylammonium bromide (TTAB) was investigated by Anthony & Zana (1994). In ***Figure 2.5***, the conductivity of pure TTAB solution and mixed POE / TTAB solution at 25 °C and 60 °C is plotted against TTAB concentration. The dotted curved portion on the graphs indicates the interaction between POE and TTAB. The plots indicate strong interactions between POE and TTAB at a high temperature of 60 °C. Further investigation using fluorescence measurements indicated that POE / TTAB complexes are formed above 35 °C at which POE is sufficiently less polar to be able to bind initial free TTAB micelles. Using conductimetry measurements, Benkhira et al. (2000) also reported similar interactions between cationic surfactant dodecyl tetra bromide (DTB) and PEO at 50º C, the interactions were absent at room temperature. The increase in hydrophobic interactions at elevated temperature facilitates the formation of complexes between PEO and DTAB.

Mya et al. (2000) studied the effects of temperature and molecular weight of PEO on the interaction between PEO and cationic surfactant hexadecyltrimethylammonium chloride (HTAC). Conductimetry results revealed that increasing the temperature does not change the cmc point. However, the critical aggregation point (cac) reduces due to lowering of the free energy of micellization in the presence of PEO in the solution (Mya et al., 2000). At higher surfactant concentrations, the polymer chain expands due to electrostatic repulsions between the bound micelles. The electrostatic repulsions tend to decrease at very high surfactant concentration due to shielding of bound micelles by Cl^- counterions.

As shown in ***Figure 2.6***, the increase in viscosity with surfactant addition is more profound for higher molecular weight polymer. The number of micelle attachment sites per polymer chain increases with the increase in the molecular weight of the polymer resulting in strong interactions. Mya et al. (2003) further investigated the effect of counterion KNO_3 on the interaction between nonionic PEO and cationic HTAC. The addition of counterion resulted in the reduction of cac and cmc values. Also, the polymer-surfactant complexes were more stable due to shielding of electrostatic repulsions. However, the increase in the viscosity of

the PEO / HTAC solution due to KNO_3 addition was not sharp. The HTAC concentration at which a maximum in viscosity observed was somewhat higher in the presence of KNO_3. This could be interpreted in terms of the reduction in chain expansion due to shielding of electrostatic repulsion in the presence of counterions. Also, the viscosity maximum observed at higher HTAC concentration is indicative of the increased binding ratio of HTAC to PEO in the presence of KNO_3 counterions (Mya et al., 2003).

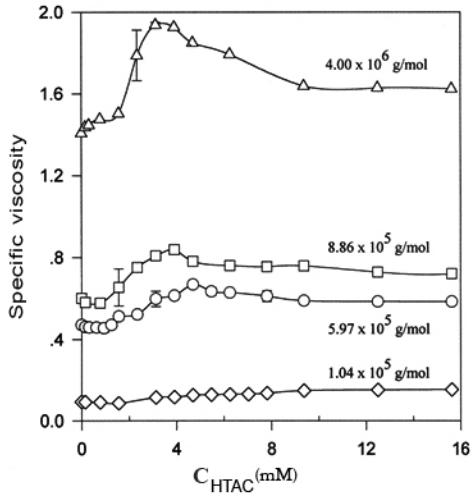

Figure 2.6 Specific Viscosity of PEO / HTAC solution vs. HTAC concentration using different molecular weight PEO (Mya et al., 2000)

In summary, the following factors play a key role in the interaction of nonionic polymer and cationic surfactant:

1. Bulkiness of the headgroup of cationic surfactant
2. Electrostatic repulsions due to protonation of polymers in aqueous solution
3. Degree of counterion binding with the ionic headgroup of micellar surfactant
4. Reduced hydrophobicity of nonionic polymer by increasing the temperature

2.2 Interactions of Anionic polymers with surfactants

2.2.1 Anionic polymer and Non-ionic surfactant

Although the interaction of anionic polymers with nonionic surfactants is extensively studied, the studies have been largely restricted to polymeric acids and nonionic surfactants of PEO type. PEO has shown the tendency to bind protic substances like polycarboxylic acids in water by cooperation of hydrogen bonds and hydrophobic effect. This results in shrinkage of polymer chain and hence reduction in viscosity of the solution.

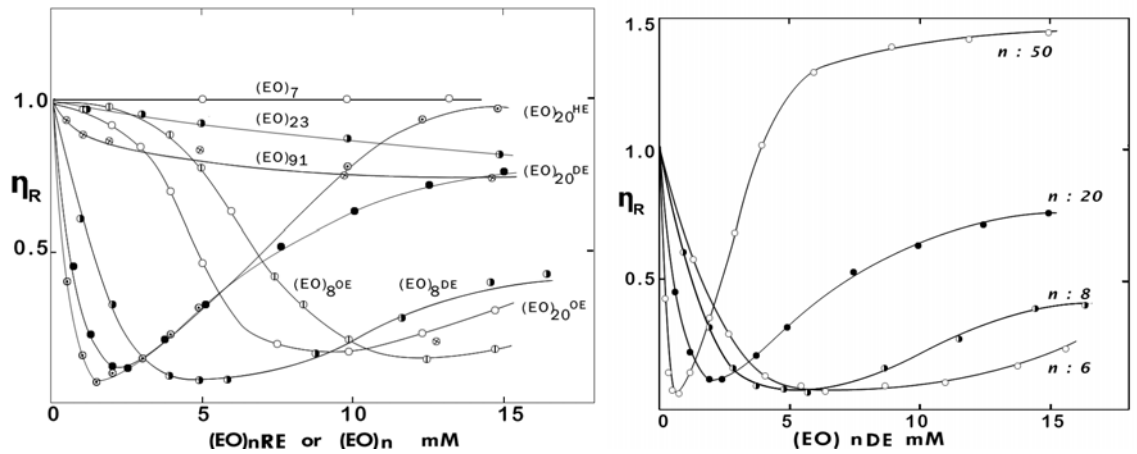

(a) **(b)**

Figure 2.7 (a) Reduced Viscosity ratio η_R of PAA solutions in presence of nonionic surfactants (EO)nRE (R: octyl, dodecyl and hexadecyl; n: 8 and 20) and (EO)n (n:7, 23, 91) to aqueous PAA solution versus surfactant concentration showing the effect of hydrophobic moiety (b) Reduced Viscosity ratio η_R of PAA solutions in presence of nonionic surfactant (EO)nDE (n: 6, 8, 20, 50) to aqueous PAA solution versus surfactant concentration showing the effect of chain length of PEO (Saito & Taniguchi, 1973)

Figure 2.7 shows the relative viscosity data reported by Saito & Taniguchi (1973) indicating the interaction between polyacrylic acid (PAA) and nonionic surfactant $(EO)_nRE$. The interaction between the polymer and surfactant, as reflected in the relative viscosity plot, depends on two factors: nature of hydrophobic moiety (R) and length of hydrophilic tail (EO). Saito & Taniguchi (1973) and Ikawa et al. (1975) further reported that due to interaction between PAA and $(EO)_n$ in the form of hydrogen bonds, some of the protons of

carboxyls are attached to the ether oxygens of $(EO)_n$ leading to an increase in pH. Upon neutralization with NaOH or by increasing pH, the polymer chain of PAA expands. However, by increasing the degree of neutralization of PAA to 0.2 (pH 5.2), the interaction between PAA and $(EO)_{20}$dodecyl almost disappears. This is similar to the findings of Ikawa (1975) for PAA / $(EO)_n$ system.

The complete review of the interactions between anionic polymers such as polymeric acids and nonionic polymers is out of scope of this thesis. Chapter 15 of Surfactant science series, vol. 23, 1987 (edited by Schick) gives further information on this topic.

2.2.2 Anionic polymer and Cationic surfactant

Mixtures of oppositely charged polymer and surfactant have been studied extensively. Hayakawa & Kwak (1982) studied the binding isotherms of Dodecyltrimethylammonium Bromide (DTAB) with anionic polymers - sodium polystryrenesulfonate (NaPS) and sodium dextran sulfate (NaDxS). They suggested that binding of oppositely charged surfactant and polymer is the result of both electrostatic and the hydrophobic interactions. The interaction between DTAB and NaPS starts at a very low concentration compared with DTAB and NaDxS system because of the high hydrophilicity of NaDxS.

Hayakawa et al. (1983) studied the effect of linear charge density of the polymer. For the *linear charge density factor* (ζ) in the order of PAA >> pectate > alginate > NaCMC (sodium Carboxymethyl cellulose), the *cooperative binding constant (Ku)* followed the similar order of PAA >> alginate ≥ pectate > NaCMC. The cooperative binding of surfactant with linear polymer is due to hydrophobic interactions between polymer and bound surfactants. It is affected by the neighboring charge-to-charge distance on polymer chain. NaCMC has longer average separation between neighboring ionic sites and therefore, has smaller cooperative parameter. Polymer chain flexibility (for example, NaCMC is very stiff compared to other polymers mentioned here) and detailed local structure also affect the binding constant in the case of oppositely charged polymer and surfactant (Hayakawa et al., 1983).

Surfactant	Polymer	Ku
TeP	NaPAsp (27800)	2.9
TeP	NaPAsp (4000)	2.0
TeP	NaPAsp (1700)	0.8
DoP	NaPAsp (27800)	30
DoP	NaPAsp (4000)	21
DoP	NaPAsp (1700)	9.9

Table 2.1 cooperative binding constant Ku for the solution of different molecular wt. NaPAsp with TeP and DoP (Liu et al., 1997)

Liu et al. (1997) studied the binding isotherms of anionic polymer - Sodium polyaspartate (NaPAsp) of three different molecular weights with cationic surfactants - tetradecylpyridinium chloride (TeP) and dodecylpyridinium chloride (DoP). As shown in ***Table 2.1***, the cooperative binding constant Ku increases by a factor of about 10 (becomes 10 times) with the increase in surfactant chain length by two CH_2 units. Also, with the reduction in polymer chain length (or molecular weight of the polymer) the polymer- surfactant affinity and Ku decreases. With the decrease in polymer chain length, the electrostatic potential around the ionic polymer decreases resulting in lower polymer-surfactant affinity.

Wallin & Linse (1996) used Monte Carlo simulation to study the interaction between oppositely charged polymer and surfactant. In their model, the micelles are represented by a hard sphere with fixed charge and radius. The ionic polymer (polyelectrolyte) is represented by a flexible chain of charged hard-spheres (beads) connected with each other by harmonic bonds at angle α, as shown in ***Figure 2.8 (A)***. The simulation results indicated that for the polyelectrolyte of low α value, the polymer chain undergoes a large contraction when it forms a complex with a micelle, as shown in ***Figure 2.8 (B)***. Due to the difference in internal stress experienced by flexible and rigid ionic polymers, the interaction of flexible polyelectrolyte with ionic surfactant is stronger in comparison with a rigid polyelectrolyte.

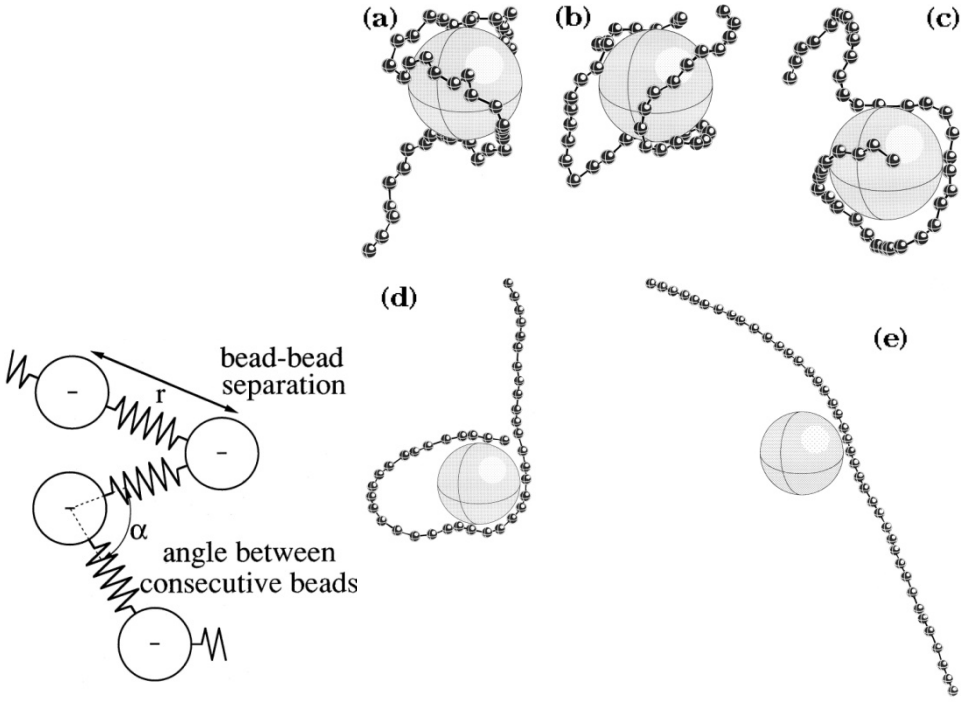

(A) (B)

Figure 2.8 (A) polymer representation used for Monte Carlo simulation (B) simulation images of micelle polymer complex for different polymer flexibility expressed by average angle between polymer beads α for (a) 90° (b) 135° (c) 150° (d) 165° (e) 175° (Wallin & Linse, 1996)

The contraction of the polymer chain can also be verified by the viscosity data. The addition of cationic surfactant to anionic polymer solution results in charge neutralization. Due to the lack of electrostatic repulsive forces, the polymer chains collapse after critical aggregation concentration (cac). Therefore, the viscosity of the polymer solution reduces significantly. As shown in ***Figure 2.9 (a)***, upon addition of cationic surfactants dodecyltrimethylammonium chloride (DTAB), tetradecyltrimethyl-ammonium chloride (TTAB) and hexadecyltrimethylammonium chloride (CTAB) to the aqueous solution of anionic polymer Carboxymethyl cellulose (CMC), the specific viscosity decreases significantly when the surfactant concentration exceeds cac. At high surfactant concentrations, the viscosity of the system reduces to that of water. The decrease in viscosity can be attributed to shrinkage of polymer chains. Also note that by increasing the alkyl chain length of surfactant, the critical

concentration of surfactant required to start interaction with anionic polymer reduces (Mata et al., 2006). The shrinkage in polymer chain is evident in ***Figure 2.9 (b)***. The fluorescence image of T_4 DNA molecule shows that the configuration changes from fully extended to globular form upon addition of DTAB to the solution.

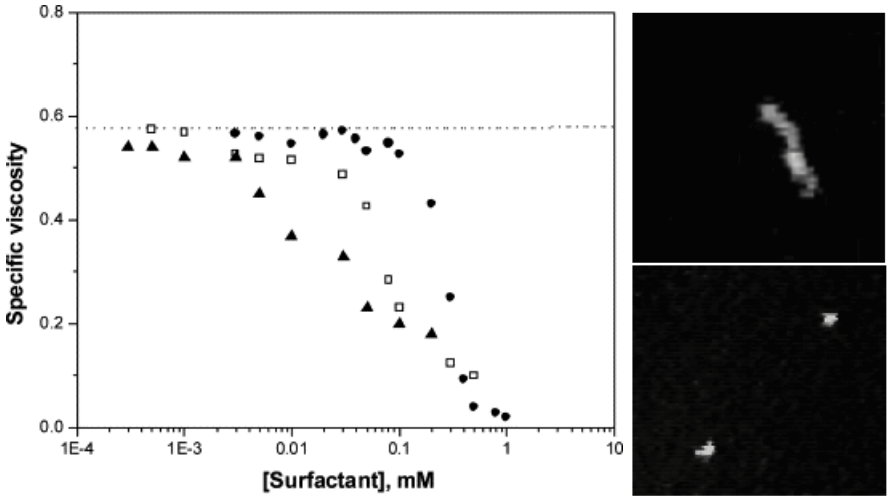

(a) (b)

Figure 2.9 (a) Specific viscosity of aqueous solution of anionic Carboxymethyl cellulose and cationic surfactant (●) DTAB (□) TTAB and (▲) CTAB vs. respective surfactant concentration (Mata et al., 2006). (b) Fluorescence image of T4 DNA molecules; Top: freely moving DNA in 20 mM NaBr solution; Bottom: Globular DNA in presence of 1.9 mM DTAB in 20 mM NaBr solution (Guillot et al., 2003)

Further addition of cationic surfactant to anionic polymer results in phase separation. The complexes formed due to interaction between oppositely charged polymer and surfactant eventually separate out of the solution after complete charge neutralization. At a very high concentration of cationic surfactant, the neutralized polymer / surfactant aggregates become positively charged. This is called charge reversal. Because of charge reversal, the polymer / surfactant aggregates resolubilize (Deo et al., 2007).

In our work, the experiments are limited to concentrations below the point of phase separation and higher concentrations of surfactants are avoided. The polymer / surfactant aggregates should remain in soluble form in order to observe drag reduction. Therefore, the interactions between polymer and surfactant are studied only up to the phase separation point.

2.3 Interactions of drag reducing polymers and surfactants

Patterson & Little (1975) studied the interaction effect of polyethylene oxide and a series of carboxylate soaps on turbulent drag reduction. As shown in ***Figure 2.10***, the drag reducing ability of the polymer reduces initially with the addition of surfactant. With further increase in surfactant concentration the drag reduction ability tends to recover.

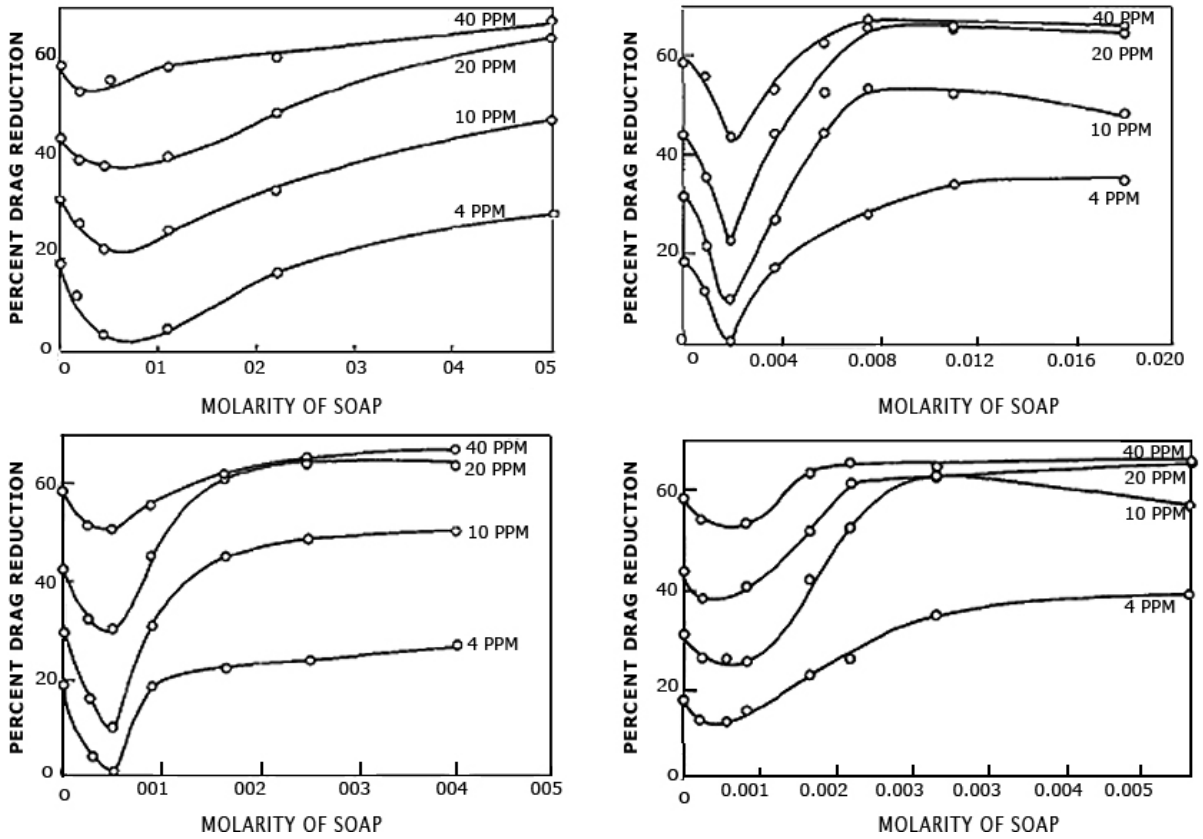

Figure 2.10 Drag reduction of PEO (Polyox WSR 205) in (A) potassium caprylate (B) potassium myristate (C) potassium laurate (D) sodium stearate (Patterson & Little, 1975)

The loss of drag reducing ability of polymer can be attributed to the shrinking of the polymer chains upon the addition of surfactant. The initial dip in the drag reducing ability strongly varies with the type of surfactant. The initial dip could be due to the loss of hydrophilic character of the polymer chain due to adsorption of surfactant ions on the polymer chain. Due to this change in hydrophilic nature of polymer, its configuration in the solvent changes and it shrinks. The shrinkage of the polymer chain is a function of the length of surfactant ion and the number of surfactant ions attached to the polymer. When the surfactant concentration is sufficiently high, the electrostatic repulsive forces, as a result of charge rendered by surfactant ions, overcome the hydrophobic attractions and the polymer chains expand resulting in an increase in drag reduction.

Suksamranchit et al. (2006) studied the effect of polymer-surfactant complex formation on turbulent wall shear stress. The key results reported by them are:

- The critical molecular weight of PEO required to start drag reduction reduces due to interaction with hexadecyltrimethylammonium chloride (HTAC). This means that a low molecular weight polymer in the presence of surfactant can be used to achieve similar drag reduction effect of a high molecular weight polymer in the absence of surfactant.
- Maximum drag reduction can be observed at a surfactant concentration comparable to the maximum binding concentration (mbc) of HTAC to PEO. The turbulent wall shear stress is reduced at surfactant concentrations below the cmc of HTAC, where threadlike micellar network is absent.
- Keeping HTAC concentration at mbc, the maximum drag reduction occurs at a PEO concentration lower than that observed in the case of PEO solution without surfactant.

Suksamranchit et al. (2006) proposed that the interaction between polymer and surfactant starts at a lower surfactant concentration because of stretching of polymer chains by high turbulent shear stress. In subsequent work, Suksamranchit & Sirivat (2007) studied the influence of ionic strength by adding NaCl to the solution of PEO and HTAC. The addition

of NaCl helps in stabilizing the HTAC micelles. At the same time, the cooperative binding between PEO and HTAC improves. In the presence of NaSal counterion, the HTAC micelle size increases due to shielding of electrostatic charge of ionic headgroup of the surfactant. However, the overall hydrodynamic radius of PEO / HTAC complex reduces due to shielding of polymeric charge and dissociation of multi-chain PEO-HTAC complexes (Suksamranchit & Sirivat, 2007). A schematic representation of the effect of ions is given in ***Figure 2.11***.

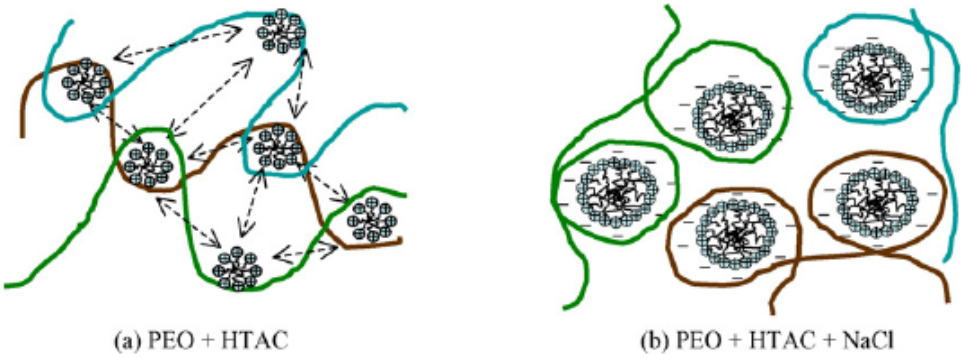

Figure 2.11 Schematic representation of shielding of electrostatic charge due to addition of NaCl counterion leading to increase radius of HTAC micelles and reduced hydrodynamic radius of the PEO / HTAC complex overall (Suksamranchit & Sirivat, 2007)

Recently, Matras et al. (2008) have reported drag reduction results in pipe flow using mixture of PEO and hexadecyltrimethylammonium chloride (CTAB) with sodium salicylate (NaSal) as counterion. The mechanism of aggregate drag reduction is also discussed. According to this study, the PEO/HTAC/NaSal aggregates do not loose their drag reducing ability after the degradation.

Although the interaction between polymer and surfactant is very well documented and studied; a limited amount of research is carried out on the interaction of drag reducing polymers and surfactants. The main focus of our work is to study the interaction between drag reducing polymers and surfactants. The concentration ranges of polymer and surfactant were selected to cover the drag reduction application. Some experiments were conducted in concentration ranges beyond the drag reduction applicability as they are essential from the interaction study prospective.

Chapter 3
Experimental Work

3.1 Chemicals

As shown in ***Figure 3.1***, four different combinations of polymers and surfactants were used to study polymer-surfactant interactions.

After preliminary trial runs and careful consideration, following drag-reducing polymers and surfactants were selected:

a. Nonionic polymer – Polyethylene oxide (referred to as PEO)

b. Anionic polymer – copolymer of Polyacrylamide (referred to as CPAM)

c. Nonionic surfactant – Ethoxylated alcohols - Alfonic 1412-7 (referred to as EA)

d. Cationic surfactant – Octadecyltrimethylammonium chloride (referred to as OTAC)

The details about the drag reduction studies involving these materials are given in ***Table A.1*** and ***Table A.2*** of **Appendix A**.

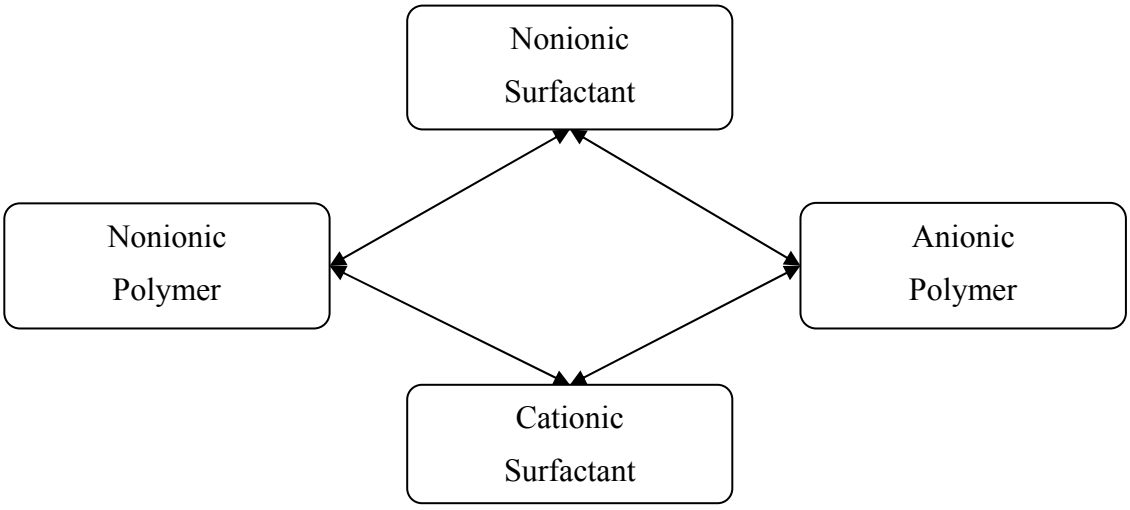

Figure 3.1 Polymer and surfactant combination chart

In what follows, a brief description of the polymers and surfactants used in this work is given.

3.1.1 Polyethylene oxide (PEO)

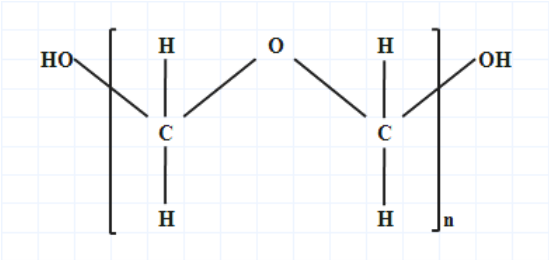

Figure 3.2 PEO formula

The polyethylene oxide (PEO), trade name POLYOX WSR 301, is a nonionic water soluble polymer supplied by Dow Chemicals, USA. The majority of its applications are in cosmetic products. The average molecular weight is 4×10^6 gm/mol. PEO has been extensively studied and applied as a drag reducer. It is a linear polymer made up of ethylene oxide monomers, as shown in ***Figure 3.2***. It is highly hydrophilic in nature due to the arrangement of oxygen atoms in the chain and therefore, its interaction with surfactant is not considered to be very cooperative at room temperature.

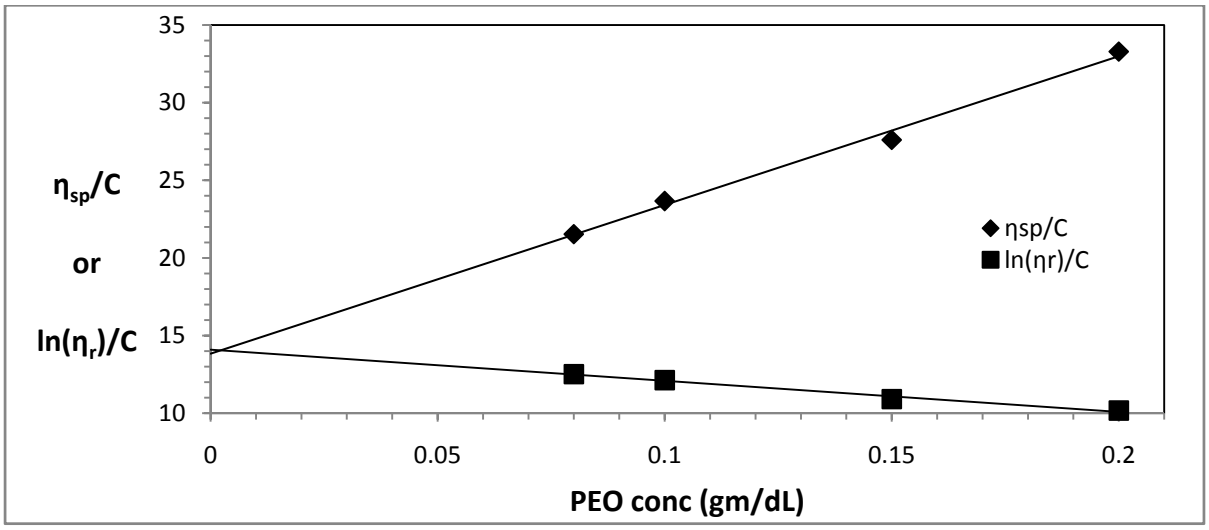

Figure 3.3 Intrinsic viscosity of aqueous solution of PEO in deionized water at 25 °C

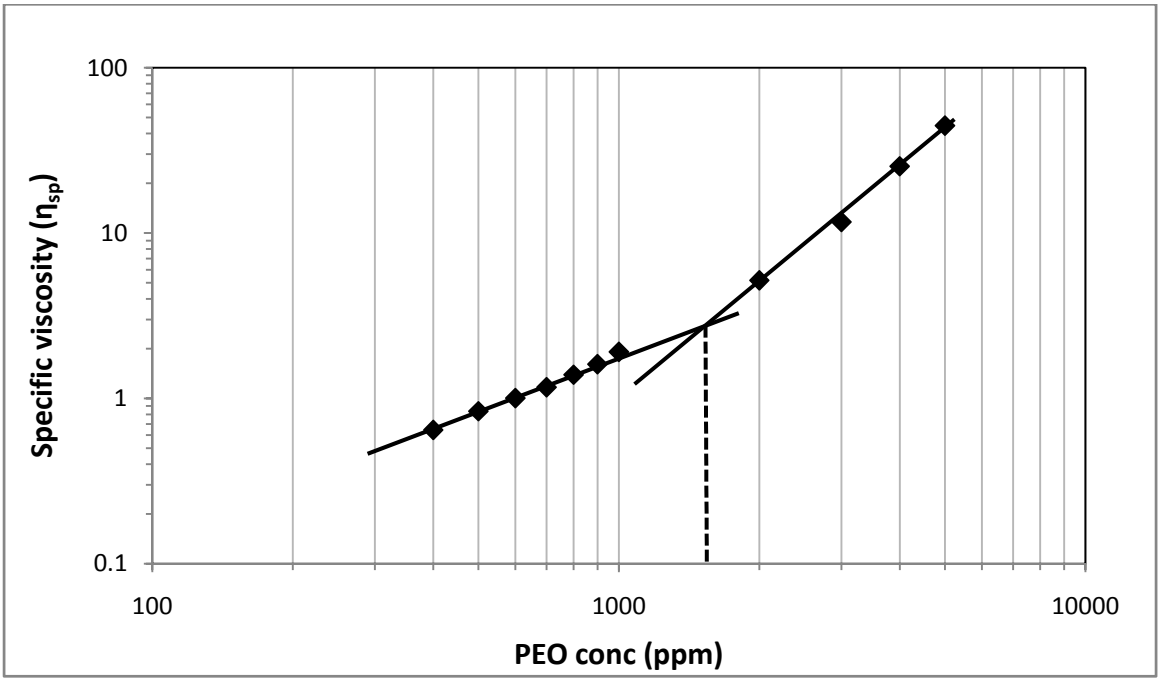

Figure 3.4 Specific viscosity of aqueous PEO solution vs. PEO concentration at 25 °C

In our experiments, the intrinsic viscosity of PEO was found to be 14 dL/gm (715 ppm) as shown in ***Figure 3.3***. The critical overlap concentration (C*) of PEO is approximately 1400 ppm as shown in ***Figure 3.4***.

3.1.2 Polyacrylamide copolymer (CPAM)

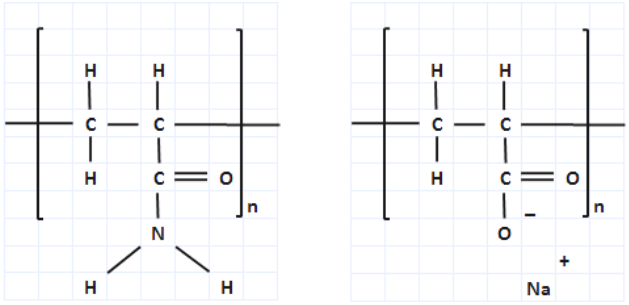

Figure 3.5 copolymers of polyacrylamide (CPAM): acrylamide and sodium acrylate

The copolymer of polyacrylamide (CPAM), trade name Hyperdrill AF 207, is a commercial grade flocculent and drag reducer supplied by Hychem, Inc., USA. CPAM is a copolymer of

acrylamide and sodium acrylate with molecular weight in the range of 11 - 14×10^6 gm/mol and charge density of approximately 30%. When dissolved in water, the sodium acrylate copolymers release Na^+ ions in water, leaving negative charge on the polymer chains of CPAM. The intrinsic viscosity of CPAM was found to be 71.18 dL/gm as shown in ***Figure 3.6*** and the critical overlap concentration C* ≈ 280 ppm at 25 °C is (See ***Figure 3.7***).

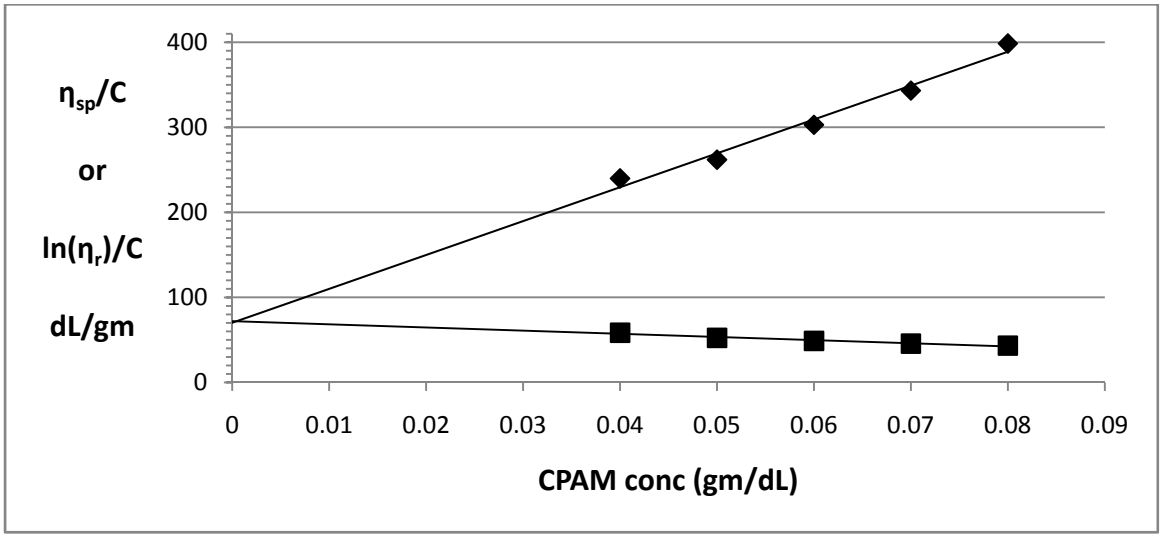

Figure 3.6 Intrinsic viscosity of aqueous CPAM solution in deionized Water at 25 °C

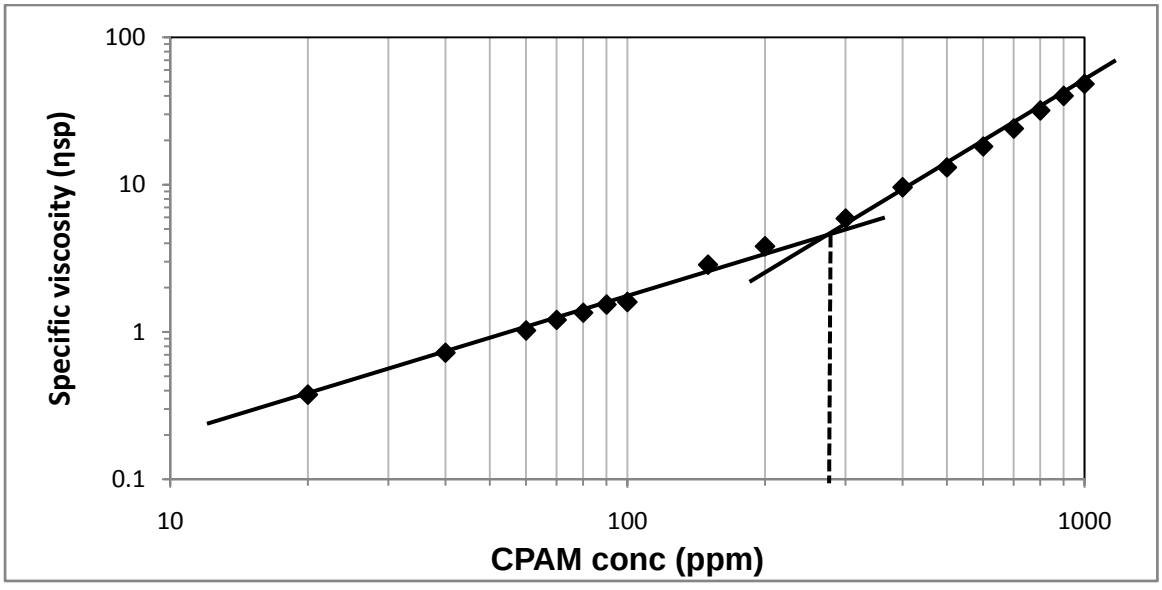

Figure 3.7 specific viscosity of aqueous CPAM solution vs. CPAM concentration at 25 °C

3.1.3 Ethoxylated Alcohol - Alfonic 1412-7 (EA)

Alfonic 1412-7 (referred to as EA) is the mixture of nonionic water soluble linear ethoxylated alcohols of series C_{12}-C_{18}, supplied by Sasol, USA. It is widely used as emulsifier, foaming agent and cleaner in many biodegradable cleaning products. Recently, Seonwook (2003) studied its drag reduction ability.

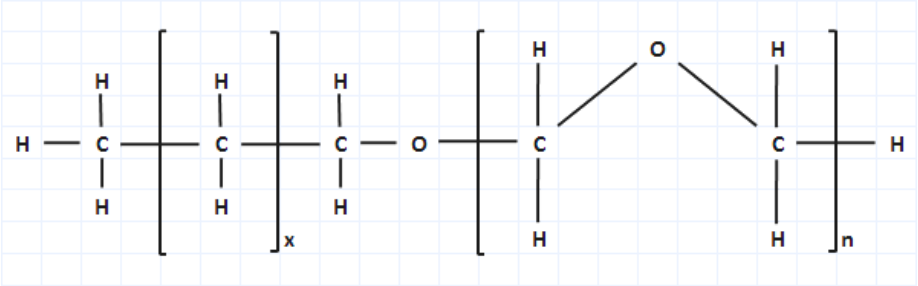

Figure 3.8 EA structure with average x = 12-14 and n=7

In EA, the hydrophobic tail is composed of 12 to 14 alkyl group alcohols. The hydrophilic headgroup is composed of an average of 7 ethylene oxide units, as shown in ***Figure 3.8***. The average molecular weight is 513 gm/mol. The cmc (critical micelle concentration) of EA is around 40 ppm as determined by du Nouy ring method. This value of cmc is reasonable for such a long chain nonionic surfactant.

3.1.4 Octadecyltrimethylammonium Chloride (OTAC)

Two grades of cationic surfactant Octadecyltrimethylammonium chloride (referred to as OTAC) were used. Arquad 18-50 (referred to as OTAC-s) is a commercial grade cationic surfactant (supplied by AkzoNobel, USA) which contains approximately 45-55% active material Octadecyltrimethylammonium chloride, 40% isoporpanol, and 10% water. To avoid the influence of isoporpanol on the interaction between polymer and surfactant, 98% pure Octadecyltrimethylammonium chloride (referred to as OTAC-p) supplied by Molekula, UK was used in majority of our experiments.

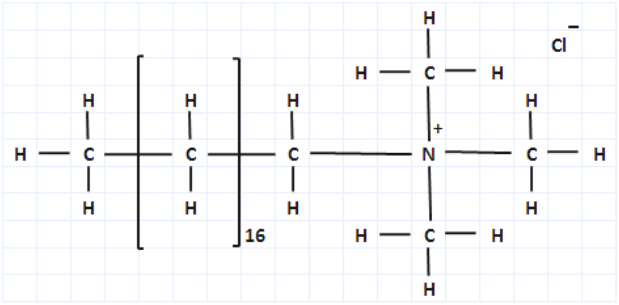

Figure 3.9 Octadecyltrimethylammonium Chloride (OTAC)

OTAC (often referred to as C_{18}TAC in the literature) has a hydrophobic tail consisting of 18 alkyl groups and a comparatively bulky headgroup consisting of trimethylammonium chloride (see ***Figure 3.9***). When dissolved in water, the release of Cl^- ions leaves a positive charge on the surfactant headgroup.

The cmc of OTAC is reported to be in the range of 104 – 139 ppm by Mukerjee & Mysels (1971) and Kang et al. (2001). Aloulou et al. (2004) reported a cmc of around 835 ppm. As shown in ***Figure 3.10 (a),*** the cmc of OTAC-p used in our experiments is found to be around 5700 ppm from conductimetry technique. This value of cmc is very high compared to the literature results. However, as shown in ***Figure 3.10 (b),*** there occurs a small change in the slope of conductivity plot at around 1000 ppm and a large change in the slope around 5700 ppm. The first break in the conductivity plot observed at 1000 ppm can be attributed to cmc_I, when spherical micelles start to form in the solution. The second break in the conductivity plot at 5700 ppm can be attributed to cmc_{II}, where the transformation from spherical micelles to rodlike micelles takes place.

Figure 3.11 shows the surface tension data of OTAC-p in deionized (DI) water obtained from two different methods: du Nouy ring method and pendant drop method. It can be clearly seen that both the methods give cmc somewhere around 5000 ppm (the surface tension levels off above cmc).

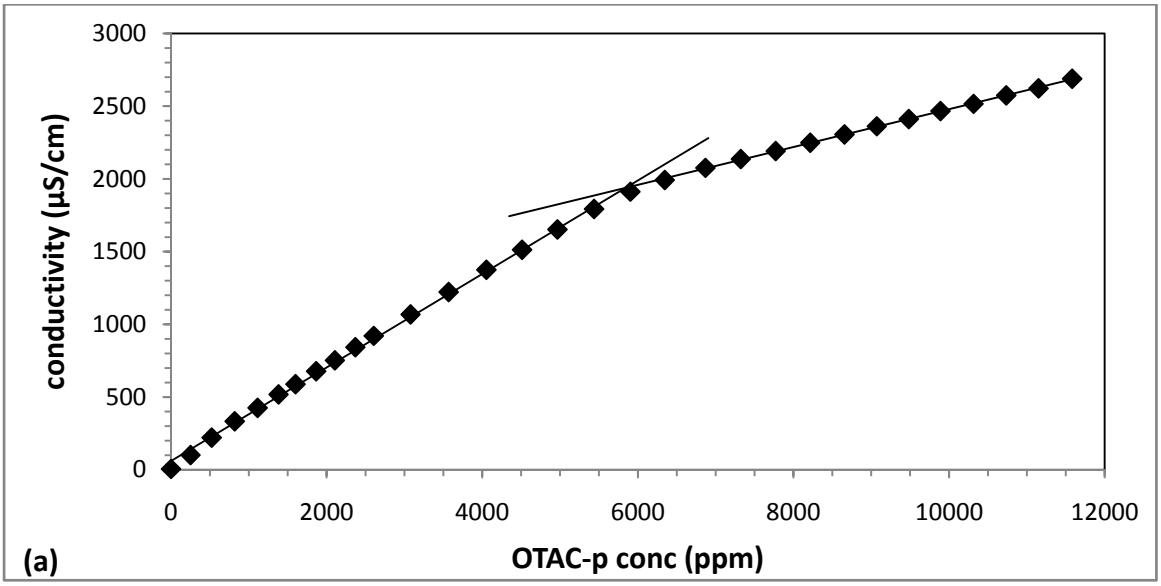

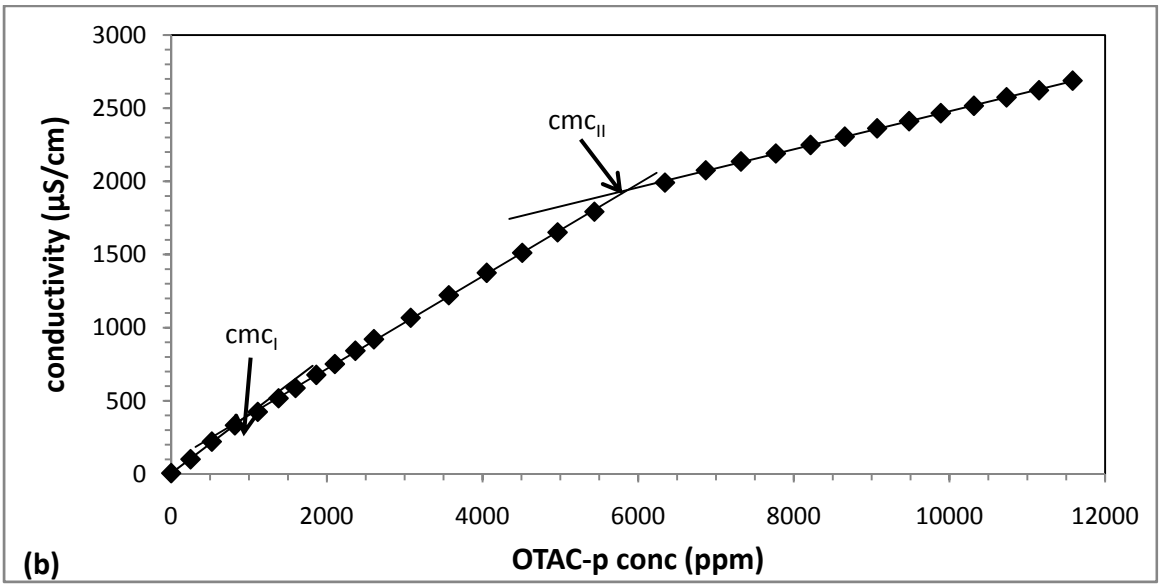

Figure 3.10 Conductivity of OTAC-p aqueous solution vs. OTAC-p concentration: (a) cmc ≈5700 ppm (b) $cmc_I \approx$ 1000 ppm and $cmc_{II} \approx$ 5700 ppm

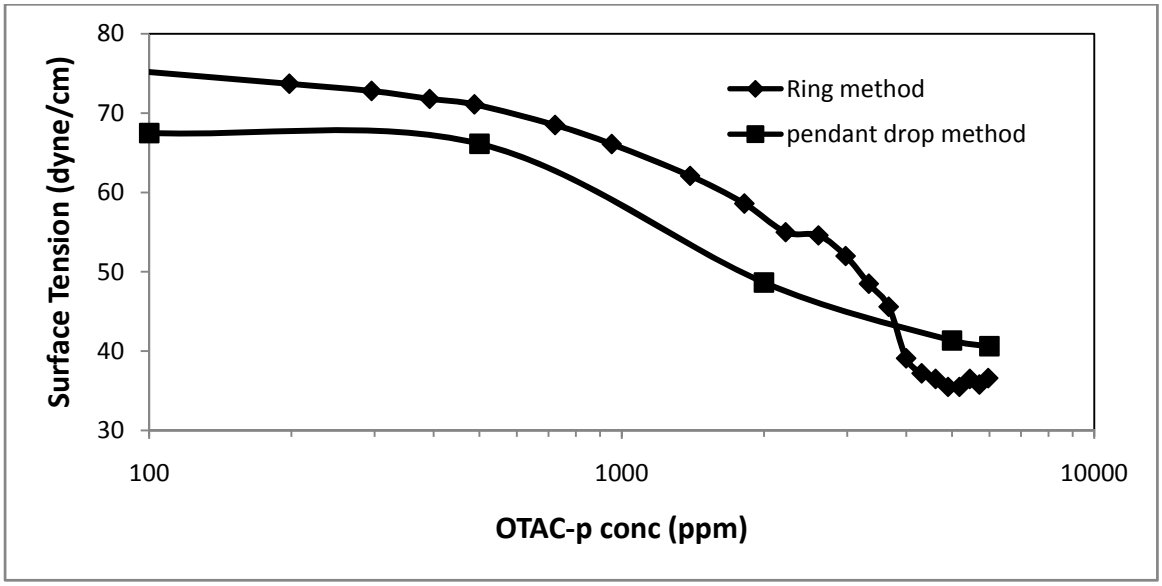

Figure 3.11 Surface Tension data of OTAC-p solution vs. OTAC-p concentration determined using ring method and pendant drop method

To verify the cmc results, similar conductimetry titration was carried out with OTAC-s solution. As shown in ***Figure 3.12***, a change in the slope of conductivity plot is observed at around 233 ppm OTAC-s concentration indicating that the true cmc is about 233 ppm OTAC-s concentration. As OTAC-s consists of approximately 50% active OTAC, the cmc of 100% active OTAC is expected to be around 116 ppm. This cmc of 116 ppm falls well within the range of literature values reported earlier. Also note that no second cmc point is observed in the case of OTAC-s when the concentration is increased upto 18750 ppm.

To find out the true cmc of OTAC is not the aim of this thesis. The intention of this exercise was only to show that there are impurities present in the commercial grade OTAC-p used in our experiments (as per the Certificate of Analysis provided by the manufacturer, the OTAC-p is 98% pure). This point is further discussed in ***section 4.2***, where an attempt is made to show the influence of impurities present in OTAC-p on the interactions between PEO and OTAC-p.

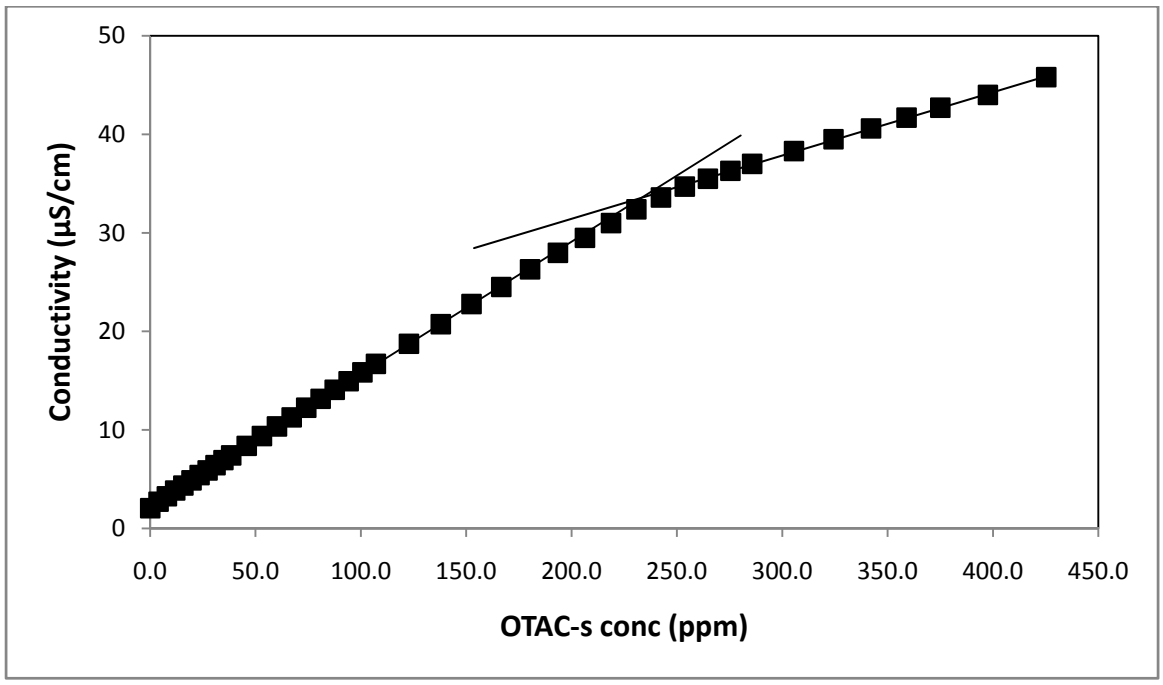

Figure 3.12 Conductivity of OTAC-s aqueous solution vs. OTAC-s concentration

Among the two grades of OTAC (OTAC-p and OTAC-s) considered in this work, OTAC-p is preferred as a drag reducer. During preliminary experiments, it was observed that the addition of a very small amount of OTAC-s to CPAM solution resulted in phase separation. This could be due to side reaction of CPAM with isoporpanol present in OTAC-s. The precipitation of polymer from the solution is not desirable from drag reduction point of view. Therefore, OTAC-s was not used as a cationic surfactant to study the interactions between polymer and surfactant. Only OTAC-p was used in interaction study.

The laboratory grade 99.5% pure Sodium salicylate (referred to as NaSal) was used as a counterion in this study. It was supplied by Sigma Aldrich Chemie Gmbh, Germany.

3.2 Experimental methods

Numerous investigation methods have been utilized to study the interaction between polymer and surfactant. They are based on the measurement of conductivity, surface tension, viscosity, turbidity, fluorescence quenching, nuclear magnetic resonance, binding isotherms using dialysis equilibrium or ion-specific electrodes, fast kinetics, solubilization of dyes, small angle neutron scattering, X-ray diffraction and electron spin resonance A really good survey of all these methods is given by Goddard & Ananthapadmanabhan (1993). Four of these investigation methods were used in this research work. They are briefly discussed here.

3.2.1 Conductivity

Electrical conductivity is one of the widely used methods to study the interactions between polymer and ionic surfactant. In order to use this method to study the interaction between polymer and surfactant, the surfactant has to be ionic. As shown earlier in ***Figure 2.1***, cmc point is identified by a sharp break in the conductivity plot. From the conductivity plots other useful information such as critical aggregation concentration (cac) and polymer saturation point (psp) can also be obtained as illustrated in ***Figure 2.1*** of **Chapter 2**. The conductivity meter used in this work (Orion 3 star) was supplied by Thermo Scientific.

3.2.2 Surface Tension

Electrical conductivity cannot detect the cmc of nonionic surfactant. Surface tension can be used to identify the cmc of both ionic and nonionic surfactants. However, there are limitations of surface tension method as well. For example, if the polymer itself is surface active, then the surface tension data can be misleading. ***Figure 3.13*** shows the surface tension behavior of mixed polymer / surfactant system. The surface tension of pure surfactant follows the dashed line. In presence of interacting polymer, the reduction in surface tension upon addition of surfactant stops at point T_1. This point represents the start of interaction between polymer and surfactant. Due to interaction between polymer and surfactant, the surface tension value reduces gradually (as indicated by a solid line in ***Figure 3.13***) upto T_2.

This point T_2 is the polymer saturation point. After the polymer is saturated with surfactant molecules, free micelles begin to form in the solution and the surface tension value becomes constant.

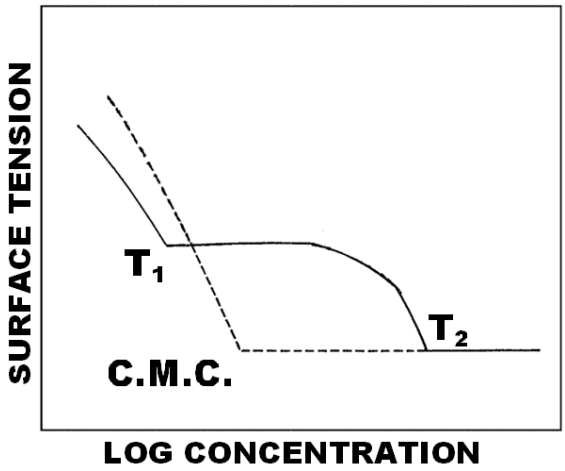

Figure 3.13 Surface tension plot of surfactant with interacting polymer (Goddard, 2002)

For the measurement of surface tension, CSC Du NOUY Tensiometer (Model # 70535) was used. This tensiometer uses a ring method. Some of the results were also verified with pendant drop method (using axismetric drop shape analysis-profile). The difference in results was in the range of ±10 dyne/cm. Although this indicates a relatively high degree of error, the surface tension plots were very similar (see ***Figure 3.11***). Even though there are some limitations of the ring method, the results obtained are in close agreement with the conductivity measurements. As our intension is to study the pattern of interaction between polymer and surfactant, the results of surface tension obtained from the ring method are quite satisfactory.

3.2.3 Viscosity

For the viscosity measurements, a capillary viscometer, Cannon Ubbelhode dilution viscometer (E610- 75) was used. Unless otherwise stated, all the viscosity measurements are reported at 25 °C. In the Ubbelhode viscometer, the times required for the solvent (t_w) and polymer solution (t_p) to pass through the capillary are recorded in seconds and the ratio t_p / t_w gives the relative viscosity. Some of the equations used in the calculations are as follows:

Relative Viscosity

$$\eta_r = \frac{t_p}{t_w} \qquad \textbf{3.1}$$

Specific Viscosity

$$\eta_s = \frac{t_p - t_w}{t_w} \qquad \textbf{3.2}$$

Intrinsic Viscosity

$$[\eta] = \lim_{C \to 0} \frac{\eta_S}{C} = \lim_{C \to 0} \frac{\ln(\eta_r)}{C} \qquad \textbf{3.3}$$

where C is polymer concentration in gm/dL

The polymer configuration in a solution can be explained by the "random walk model". ***Figure 3.14*** shows the repeating monomer of ethylene oxide of unit length of ℓ and the characteristic size of the polymer configuration, represented by end-to-end vector **r.**

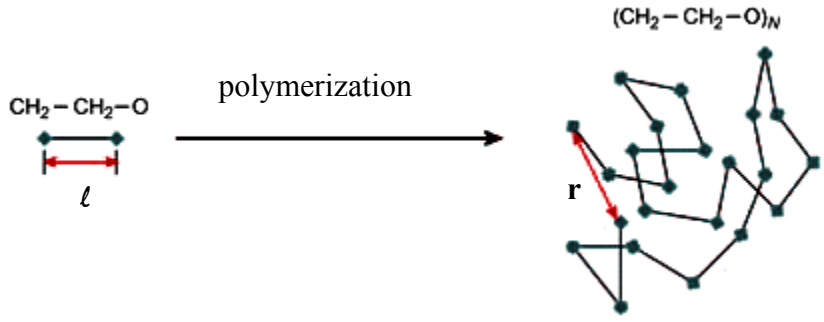

Figure 3.14 Flexible polymer configuration measured by end-to-end distance of polymer chain (Illustrated from White & Mungal, 2008)

The end-to-end vector **r** can be expressed as the sum of individual repeat units as,

$$r = \sum_{1}^{N} \ell i \qquad \textit{3.4}$$

The viscosity of the polymeric solution depends on the end-to-end vector **r**. If the polymer chains are fully extended, then the viscosity of the polymer solution is high. Therefore, the viscosity of the solution can be used to describe the conformational changes in polymer molecule. The root mean square (rms) value of end-to-end distance of the polymer coil $\left(\overline{r^2}\right)^{\frac{1}{2}}$ can be obtained from the intrinsic viscosity [η] value using the Fox-Flory relation (Pal, 1996),

$$[\eta] = \Phi' \frac{\left(\overline{r^2}\right)^{\frac{3}{2}}}{M} \qquad \textit{3.5}$$

where, $\Phi' \approx 2.1 \times 10^{21}$ dL/(mol•cm^3) and M is the molecular weight of the polymer.

3.2.4 Turbidity

The solubility of polymer chain in water depends on the interaction of ionic, polar or hydrogen-bonded hydrophilic blocks of polymer with each other and with water. Upon cooling the polymeric solution of polyacrylamide or polyacrylic acid phase separation occurs as the energy of contact between polymer segments relative to solvent-polymer contact is inversely proportional to temperature. However, a polymer solution of polyethylene oxide or polymethacrylic acid precipitates out when heated. This is mainly due to the differences in thermal expansion co-efficient of polymer and solvent. The measurement of cloud point or turbidity can reveal the interactions between polymer and surfactants depending on energetics of contact between polymer / surfactant aggregates and solvent.

In the cloud point study, the polymer solution is heated until it turns cloudy. In our work, instead of heating the polymer solution, the surfactant concentration is increased at a fixed polymer concentration and the changes in turbidity are recorded. Solutions of PEO / EA, CPAM / EA and PEO / OTAC-p remained clear over a large concentration range of surfactant indicating weak interactions between the polymer and surfactant. However, the solution of anionic CPAM turns cloudy upon addition of cationic OTAC-p. Due to neutralization of anionic charge of CPAM upon addition of cationic OTAC-p, the CPAM / OTAC-p complexes become less polar and hence, less soluble. This reduction in the free energy of CPAM / OTAC-p aggregates is reflected in an increase in the turbidity of the solution.

In order to monitor the turbidity, Hach 2100P Turbidimeter (46500-00) was used in this study. This turbidity meter has a range of 0-1000 NTU. Phase separation of CPAM / OTAC-p aggregates was observed after some maximum value of turbidity.

3.3 Experimental procedure

All the chemicals in this study were used as received without any further purification. The surfactant stock solutions were prepared fresh on the day of experiments by dissolving appropriate amount of surfactant in deionized (DI) water (conductivity 2 – 5.5 μS/cm). The stock solutions of 0.5%, 1.0% and 5.0% by wt. surfactant concentration were prepared as per requirement and used on the same day. The stock solutions of polymer were prepared in the concentration range of 0.05% to 0.5% by wt. by dissolving the appropriate amounts of polymer in DI water at 25 °C. The polymer solution was allowed to mix at low rpm overnight using magnetic stirring plate to ensure homogenization of polymer solution. Fresh polymer stock solutions were prepared for each experiment and were used up within 2 -3 days. NaSal stock solutions containing 1.0% by wt. NaSal were prepared on the day of experiments and were used in equimolar proportion of OTAC-p, unless otherwise specified.

Samples were prepared by dispensing fixed amount of polymer stock solution in all the sample bottles. The appropriate amount of DI water, surfactant stock solution and NaSal counterion stock solution (if necessary) were added to make up 100 - 200 mL total sample quantity. The samples were allowed to mix for sufficient period of time ensuring uniform mixing and then various physical properties such as electrical conductivity, surface tension, turbidity and viscosity were measured at 25 °C, unless otherwise specified in the results.

Although DI water was used in most of the experiments, some experiments were also conducted with tap water (conductivity 650 – 700 μS/cm). They are reported in ***section 4.4.3*** and ***4.5***.

Chapter 4
Results and Discussion

4.1 Interaction of non-ionic polymer with non-ionic surfactant

The highly hydrophilic nonionic polymer polyethylene oxide (PEO) is expected to have a very limited or no interaction with nonionic surfactant Alfonic 1412-7 (EA). Conductivity measurements cannot be used to investigate interactions in a nonionic system of surfactant and polymer. Also, the complexes of PEO and EA remain soluble in the concentration range in which the samples were prepared. Therefore, conductivity and turbidity measurements were not carried out for this system.

4.1.1 Interaction of PEO with EA

4.1.1.1 Surface Tension

It is clear from the surface tension data that the interactions between nonionic PEO and nonionic EA are not completely absent as previously anticipated for nonionic systems. The cmc point of the system identified as the surfactant concentration where the surface tension value becomes constant, is influenced by the polymer. As shown in ***Figure 4.1 (A)***, the cmc for pure EA in DI water is around 40 ppm (in the absence of PEO). However, due to interaction between PEO and EA, the formation of free EA micelles in the solution is delayed. It can be seen from ***Figure 4.1 (B)*** that in the case of 1000 ppm PEO solution, the constant value of surface tension is observed at around 700 ppm EA concentration (marked as T_2 point in ***Figure 4.1 (B)***). The T_2 value is observed to increase with the increase in PEO concentration. This behavior suggests that for the EA molecules, the formation of aggregates on a PEO chain is thermodynamically more favorable than the formation of free micelles. The surface tension of EA solution at cmc is 32.5 dyne/cm. The surface tension value corresponding to T_2 point gradually decreases to 32.3, 32.1 and 32.0 dyne/cm when the PEO concentration is increased to 100, 500 and 1000 ppm respectively. This indicates that PEO is also a surface active agent in its nature.

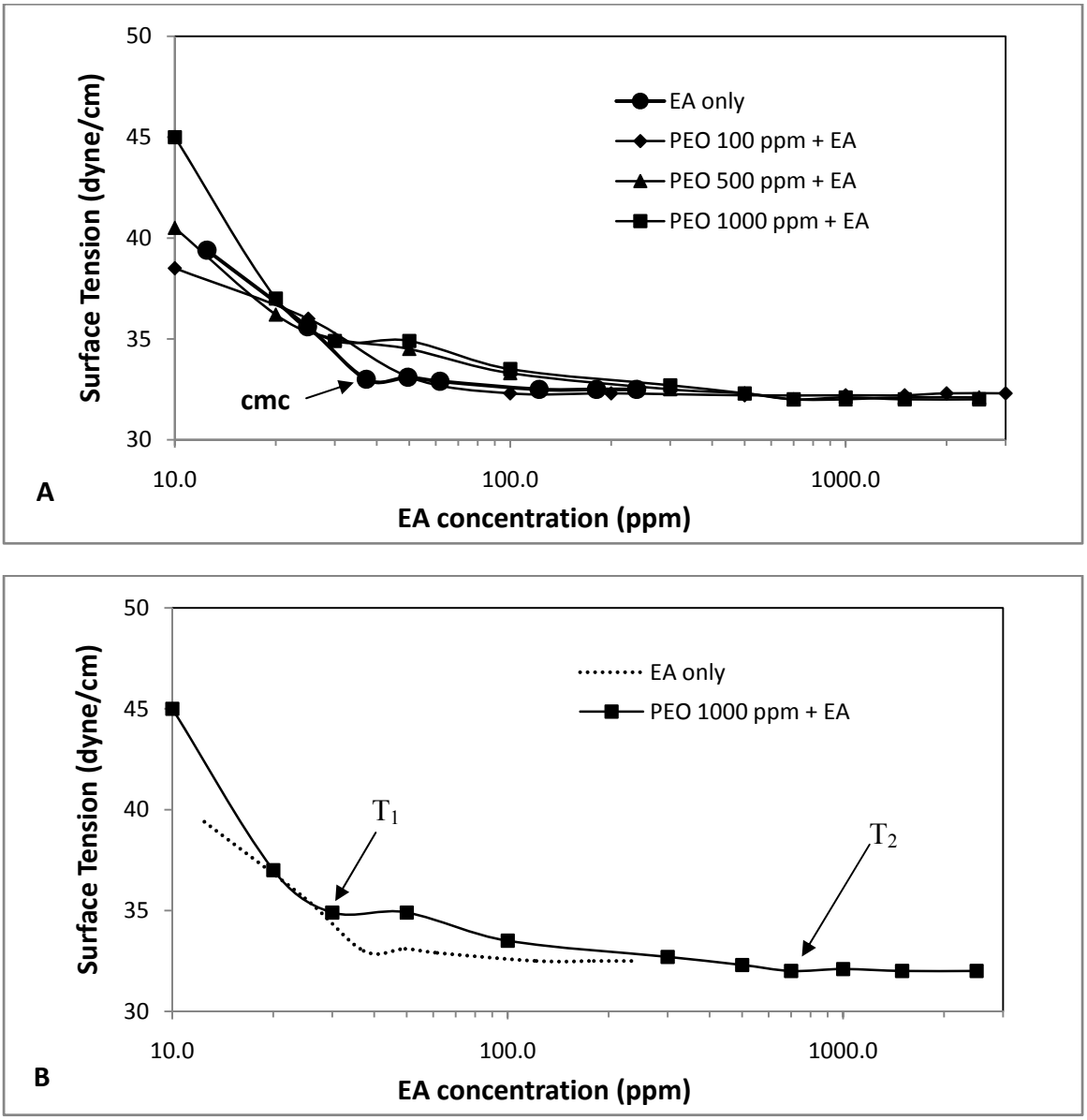

Figure 4.1 Surface Tension plot of PEO / EA aqueous solution in DI water

At a surfactant concentration corresponding to point T_1 of ***Figure 4.1 (B)***, the interaction begins between the polymer and the surfactant. This surfactant concentration is referred to as cac (critical aggregation concentration). After T_1 point, further addition of EA leads to the formation of PEO / EA complexes. Due to the formation of PEO / EA complexes, less number of free EA molecules are available for the solution and therefore, the surface tension

value decreases at a reduced rate in the $T_1 - T_2$ region as observed in ***Figure 4.1(B)***. At the T_2 point, the PEO chains are completely saturated with EA molecules and free EA micelles begin to form in the solution, resulting in a constant value of surface tension. It is also noticeable here that the surface tension plots for 500 and 1000 ppm PEO / EA closely resemble with each other. It is possible that at a sufficiently high concentration; the polymer chains are not easily accessible by the surfactant molecules, limiting the interaction between PEO and EA.

4.1.1.2 Viscosity

As shown in ***Figure 4.2***, a common feature of all the PEO / EA solutions regardless of the PEO concentration is that, the relative viscosity exhibits a minimum point. A larger dip in relative viscosity is found in the case of 1000 ppm PEO concentration. Although a change in the relative viscosity clearly indicates interaction between PEO and EA, it is important to note that the interactions are weak. The changes in the relative viscosity are small.

For a low PEO concentration such as 100 ppm, there is no appreciable change in relative viscosity with the increase in EA concentration initially and the minimum value is observed at an EA concentration of about 400 ppm. At higher PEO concentrations of 500 and 1000 ppm, the relative viscosity increases in the beginning due to interaction between PEO and EA. Due to the scattered nature of the relative viscosity values, the dip in relative viscosity of PEO 500 ppm seems less pronounced compared to PEO 100 ppm. This is likely due to the fact that a simple average of data points can lead to misleading values if the data points are highly scattered. At the same time, to maintain the integrity of data points, outliers cannot be omitted all the times. However, the pattern of relative viscosity plots for PEO 100, 500 and 1000 ppm is the same.

After the T_1 point (see ***Figure 4.1 (B)***), the attachment of surfactant molecules to the hydrophilic portion of the PEO gives some hydrophobicity to PEO, leading to partial expansion of PEO chains as shown in ***Figure 4.3 (a)***.

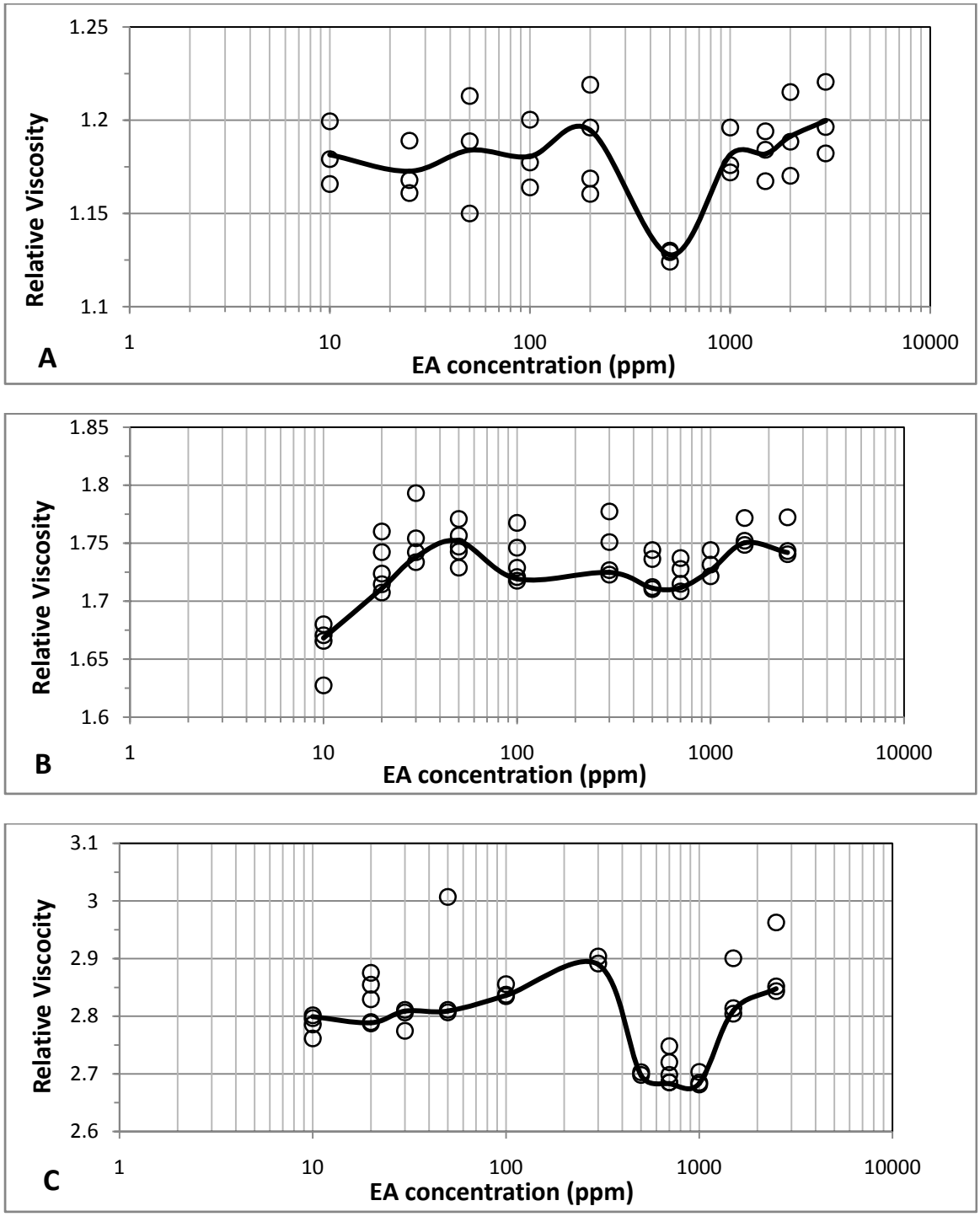

Figure 4.2 Relative Viscosity of PEO / EA solution in DI water at PEO concentrations: (A) 100 ppm (B) 500 ppm (C) 1000 ppm. The solid curve represents the average values (excluding outliners)

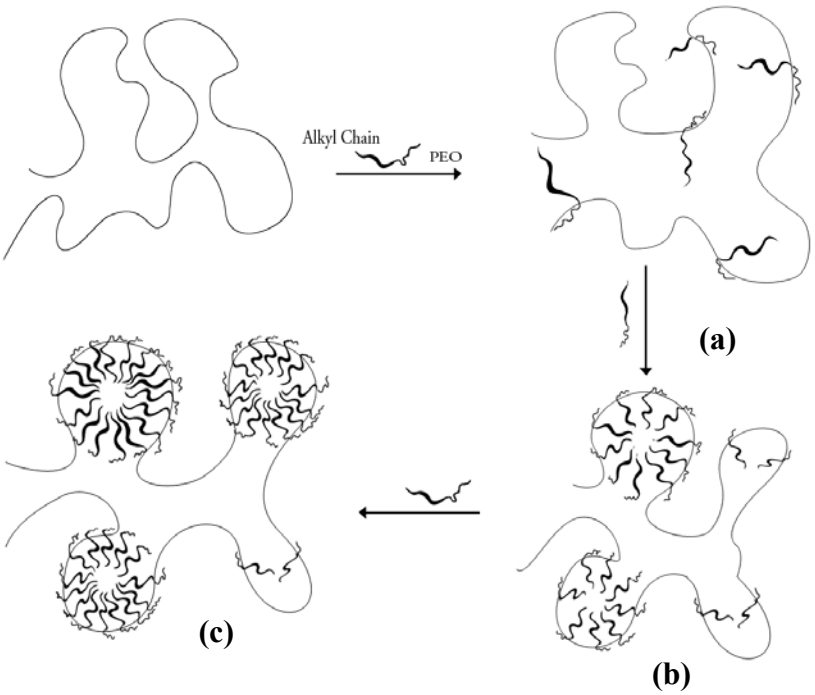

Figure 4.3 PEO / EA complexes in solution

At higher EA concentrations, the aggregates of EA molecules begin to grow on the polymer chain. It has been proposed by many researchers that the PEO chains do not penetrate into the core of EA micelles due to highly hydrophilic nature of the PEO chains (Brackman, 1988; Winnik, 1990; Ge et al., 2007). The PEO chain remains on the surface of the micelles by keeping its hydrophilic portion towards the hydrophilic headgroups of the growing micelles on the polymer chain. As shown in ***Figure 4.3 (b)***, the "wrapping of polymer chains" around the developing EA micelles leads to conformational changes of the polymer chains. The hydrodynamic radius of the polymer chain reduces due to "wrapping of polymer chains" around the developing micelles of EA. This is reflected in the reduction of relative viscosity of the PEO / EA solution.

Interestingly, at high EA concentrations (above 500 ppm EA in the case of 100 ppm PEO, above 700 ppm EA in the case of 500 ppm PEO and above 1000 ppm EA in the case of 1000 ppm PEO), the relative viscosity starts to increase. As shown in ***Figure 4.3 (c)***, above a sufficiently high EA concentration, the polymer chains of PEO begin to expand due to

repulsive forces between adjacent micelles developed on the same polymer chain. The increase in relative viscosity can also be attributed to the formation of free micelles in the bulk solution. There is coexistence of free surfactant micelles and PEO / EA aggregates after the T_2 point. The addition of EA after T_2 (see ***Figure 4.1 (B)***) leads to the formation of free micelles in the solution and therefore the relative viscosity increases further.

For drag reduction application, the polymer and surfactant concentrations in the mixed polymer – surfactant system should be sufficiently high so that the micelles are fully developed and the polymer chains are expanded, as shown in ***Figure 4.3 (c)***.

4.2 Interaction of non-ionic polymer with cationic surfactant

The interaction of nonionic polymer with ionic surfactant is of interest in drag reduction applications as mentioned in ***Chapter 2***. In this work, the interactions between nonionic PEO and cationic OTAC-p, with and without the counterion (NaSal) are studied. Although the interaction between PEO and anionic surfactant - sodium dodecyl sulfate (SDS) is considered to be different from the interaction between PEO and cationic surfactant, some similarities are observed here and are discussed in subsequent sections. The cloud point of the solution of PEO and OTAC-p (with and without NaSal) is above the room temperature and therefore, turbidity measurements were not carried out for this system.

4.2.1 Interaction of PEO with OTAC-p

4.2.1.1 Surface Tension

The surface tension measurements fail to capture any evidence of PEO / OTAC-p interaction. The data shown in ***Figure 4.4*** gives no clear indication of critical aggregation concentration (cac) or polymer saturation point (psp), often observed in the case of nonionic polymer / anionic surfactant system. Also, the curves of 500 ppm PEO and 2500 ppm PEO closely coincide with each other indicating no effect of PEO concentration on the interaction between PEO and OTAC-p. However, the surface tension plots of PEO / OTAC-p solution

and pure OTAC-p solution are quite different. Suksamranchit & Sirivat (2007) reported results on the interaction between PEO and hexadecyltrimethylammonium chloride (HTAC) in the presence of counterion (NaCl). They also identified critical aggregation point (cac) and maximum binding concentration (mbc) using surface tension measurements. However, no such points are observed here.

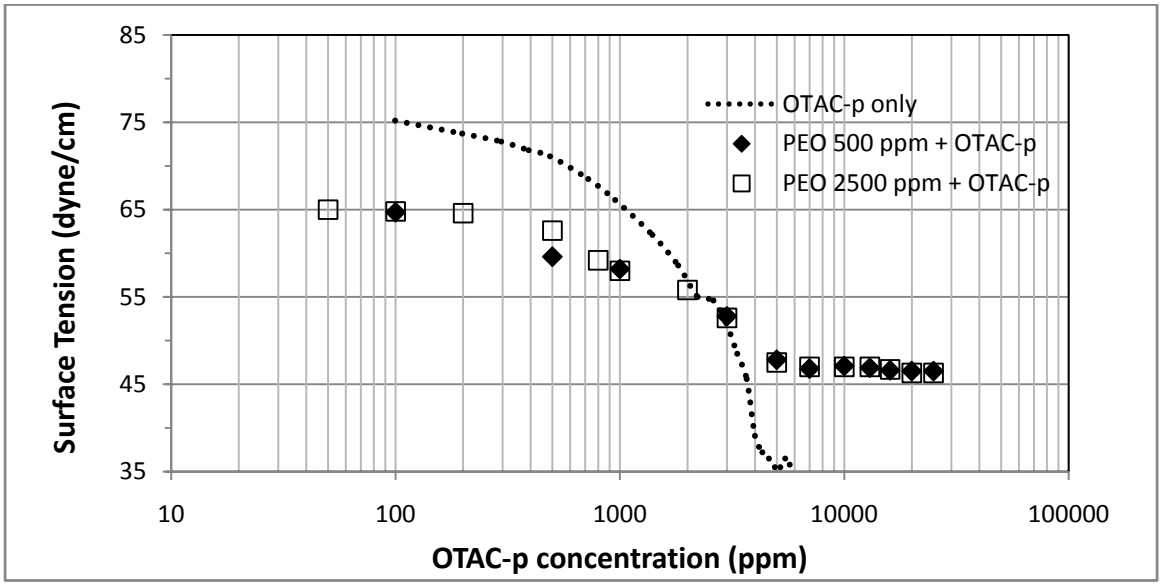

Figure 4.4 Surface Tension of PEO / OTAC-p solution in DI water vs. OTAC-p concentration

4.2.1.2 Conductivity

Consistent with the results of surface tension, the conductivity plots (***Figure 4.5***) show no interaction between PEO and OTAC-p. The "cmc" point is identified by the intersection of conductivity plots as illustrated in ***Figure 4.5***. In the case of pure surfactant solution (without polymer), the cmc point is the true cmc of the surfactant where onset of micellization takes place. In the case of mixed polymer – surfactant system, the intersection point of conductivity plots represents "apparent critical micelle concentration (denoted as cmc'). The

apparent cmc value of PEO / OTAC-p mixture is almost the same as the true cmc of OTAC-p indicating no interaction between PEO and OTAC-p in the solution. This is in contradiction with the results reported by Suksamranchit & Sirivat (2007). They reported a shift in cmc from 1.3 mM for pure HTAC to 1.65 mM for the mixture of PEO / HTAC. The PEO used in this work has a higher molecular wt. than that of the PEO used by Suksamranchit & Sirivat (2007). Also, the hydrophobic tail of OTAC-p is two CH_2 groups longer than HTAC. Both the higher molecular weight of polymer and longer hydrophobic chain of surfactant are favorable for interaction (Schwuger, 1973; Qiao & Easteal, 1998; Mya et al., 2000).

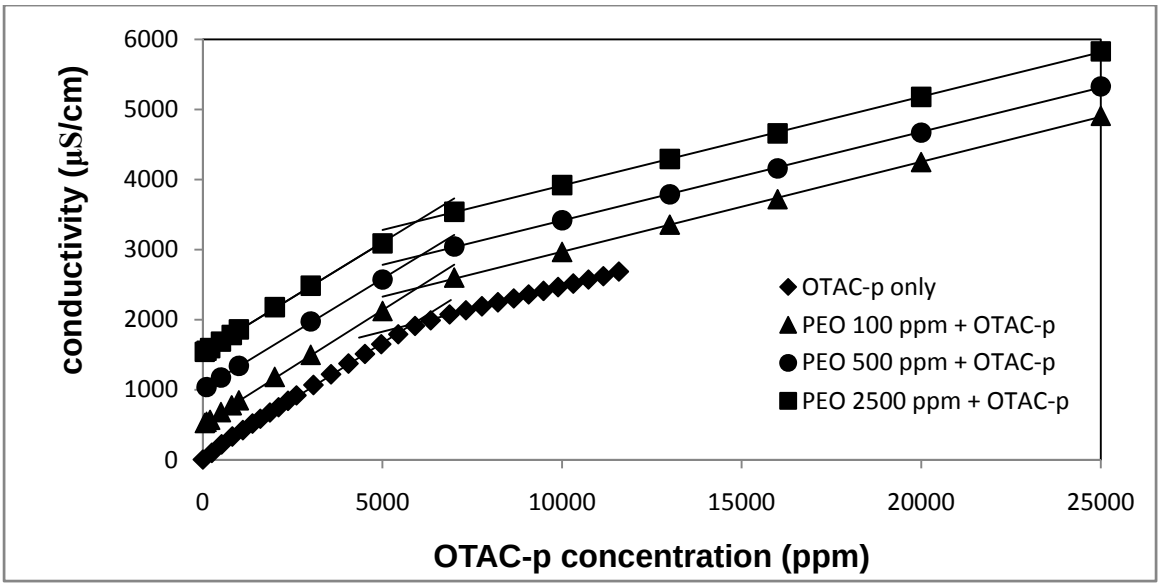

Figure 4.5 Conductivity of PEO / OTAC-p solution vs. OTAC-p concentration (plots of PEO conc. 100, 500 and 2500 ppm moved by unit conductivity for better representation of data)

One possible explanation for the contradiction between our results and the results reported by Suksamranchit & Sirivat (2007) is that they carried out experiments at a temperature of 30°C, whereas, the results reported in this work are at 25 °C. As observed in ***Figure 2.5*** of **Chapter 2**, no interaction between PEO and TTAB was detected at 25 °C whereas clear interaction between PEO and TTAB was detected when the PEO / TTAB solution was heated to 60 °C.

When the PEO / TTAB mixture is heated past 35 °C, the PEO chain becomes sufficiently less polar so that free monomers of TTAB can attach to it (Anthony & Zana, 1994).

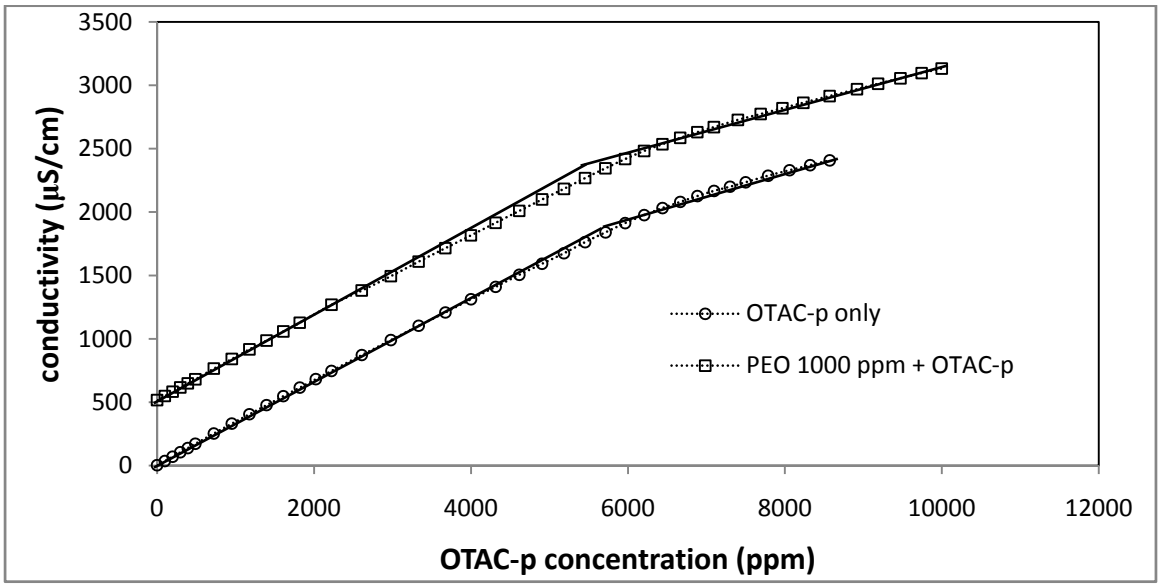

Figure 4.6 Conductivity of pure OTAC-p and OTAC-p / 1000 ppm PEO solution in DI water vs. OTAC-p concentration at 48.5 °C

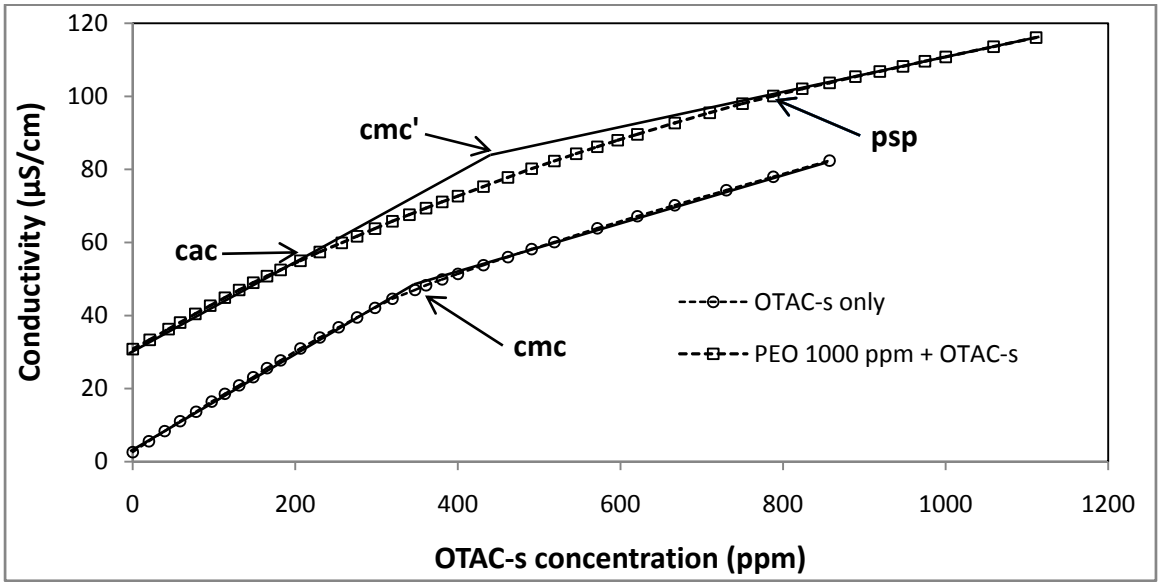

Figure 4.7 Conductivity of OTAC-s and PEO / OTAC-s solution in DI water vs. OTAC-s concentration at 48.5 °C (PEO 1000 ppm plot moved by unit conductivity for better representation of data)

In order to verify the effect of temperature, conductivity measurements of pure OTAC-p solution and 1000 ppm PEO / OTAC-p solution were carried out at 48.5 °C and the results are shown in ***Figure 4.6***. At 48.5 °C, somewhat better interaction between OTAC-p and PEO is observed. However, the shift in cmc value is not as large as reported by Suksamranchit & Sirivat (2007).

To further investigate the effect of temperature, conductimetry of OTAC-s (which contains around 50% of active material – OTAC along with isoporpanol and water) solution containing 1000 ppm PEO was carried out at 48.5 °C. As shown in ***Figure 4.7***, at 48.5 °C highly cooperative interactions between OTAC-s and PEO are observed. The cmc value increases from 320 ppm for pure OTAC-s to 440 ppm for 1000 ppm PEO / OTAC-s mixture. Also, the "cac" point and "psp" points can be seen clearly. The behavior observed in ***Figure 4.7*** is similar to the results reported by Jones (1967) for the PEO / SDS system. Although OTAC-s contains only 50% of active OTAC, OTAC-s shows better interactions with nonionic PEO than OTAC-p. There is, however, a small degree of error associated with the marking of transition points such as cac, cmc and psp. The marking of cac, cmc and psp points can vary somewhat with the data points selected to draw the intersecting lines. This point is discussed further in ***section 4.4.2.1***.

4.2.1.3 Viscosity

The viscosity data for 100, 500 and 2500 ppm PEO solutions as a function of OTAC-p concentration are shown in ***Figure 4.8***. When the surfactant concentration is increased up to the cmc value, the relative viscosity remains almost constant for the 100 ppm PEO solution. The polymer solution consisting of 500 ppm PEO exhibits a behavior opposite to that of 2500 ppm PEO solution. In the case of 500 ppm PEO solution, the relative viscosity first reduces to minimum value and then increases, whereas in the case of 2500 ppm PEO solution, the relative viscosity first increases to some maximum value and then reduces with the increase in surfactant concentration up to the cmc value. The relative viscosity begins to increase at all three PEO concentrations past the cmc point mainly due to the formation of free micelles in the solution.

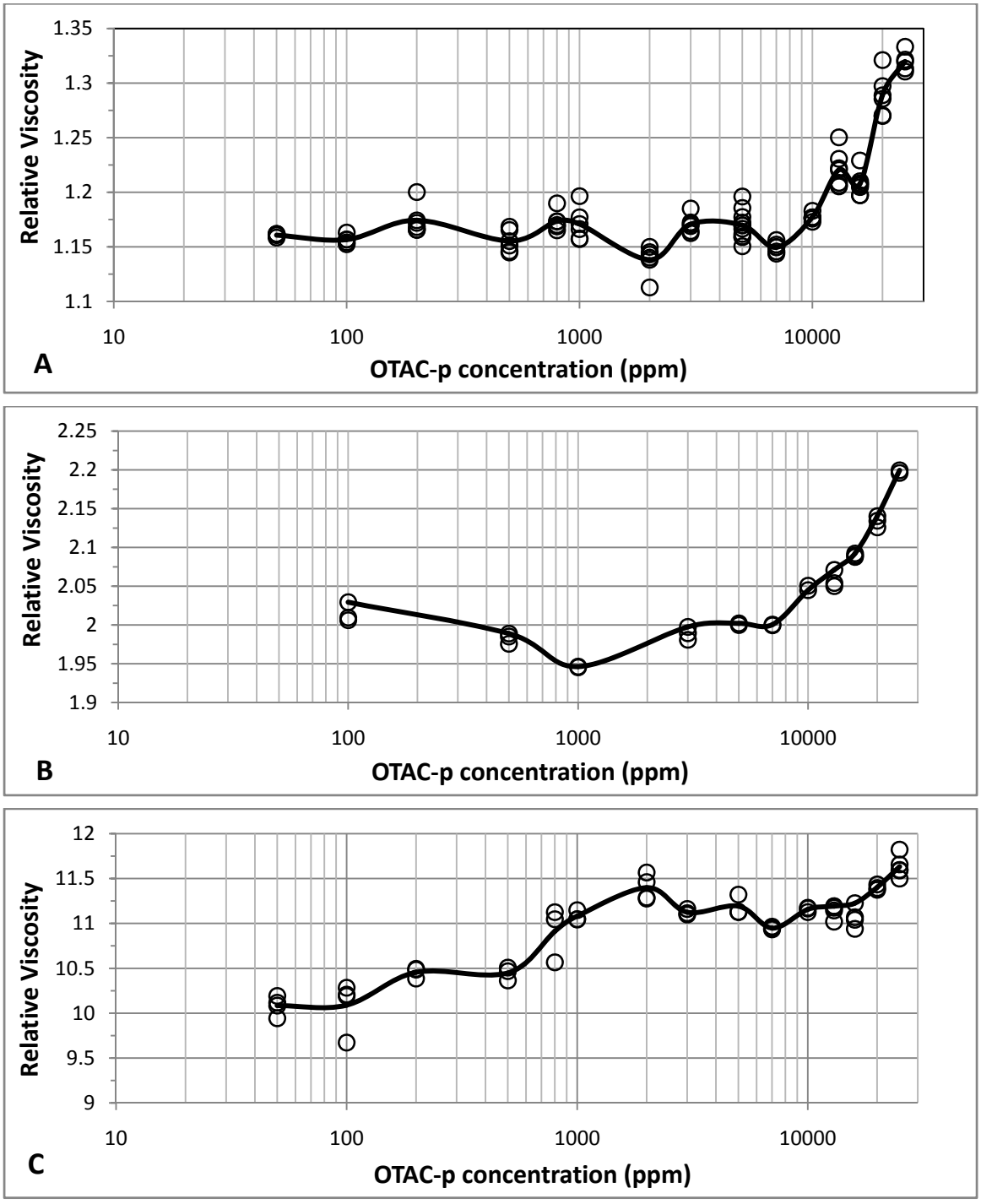

Figure 4.8 Relative Viscosity of PEO / OTAC-p solution in DI water vs. OTAC-p conc. for PEO concentrations: (A) 100 (B) 500 and (C) 2500 ppm. The solid curve represents the average values (excluding outliers)

Nilsson (1995) reported similar results for the nonionic polymer hydroxypropyl methyl cellulose (HPMC) and anionic surfactant (SDS) system and proposed a model illustrated in ***Figure 4.9***, to explain the behavior of polymer / surfactant mixture below and above the critical entanglement concentration (C*) of polymer.

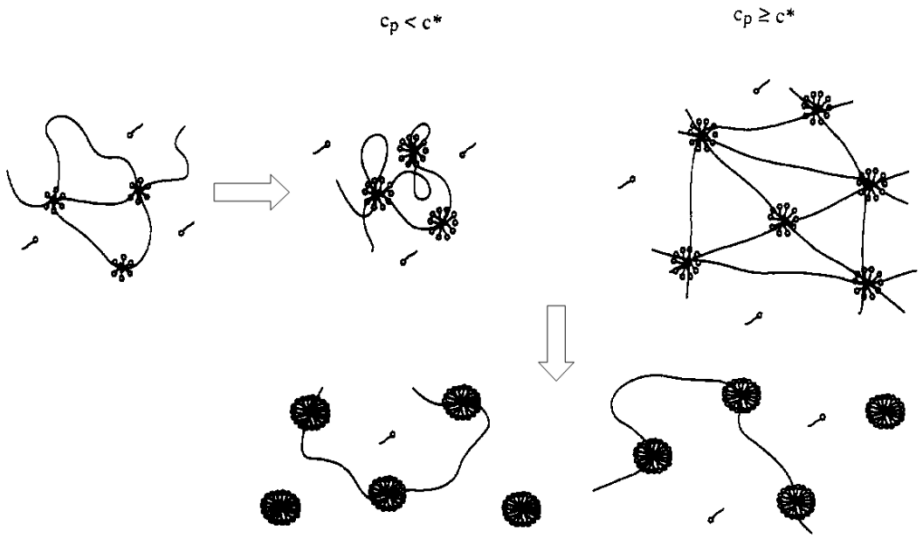

Figure 4.9 Schematic representation of model for nonionic polymer and anionic surfactant clusters formation and development (Reproduced from Nilsson, 1995)

Nilsson (1995) proposed that if the polymer concentration is below C*, the polymer chains are at a distance from each other and so, the chances of forming intermolecular structure of polymer chains are low. As shown in ***Figure 4.9***, when the polymer concentration is less than C*, the polymer chains shrink due to intramolecular interaction of a polymer chain. In this case, different segments of the same polymer chain are attracted to a developing micelle. When the polymer concentration is above C* the intermolecular interactions take place. In this case, various polymer chains are attracted to a developing micelle and form a three dimensional network as shown in ***Figure 4.9***. The formation of a three-dimensional structure results in an increase in the viscosity. The critical entanglement concentration (C*) of PEO is around 1400 ppm and therefore, different behaviors are observed for PEO concentrations of 500 and 2500 ppm.

For the 500 ppm PEO solution (C < C*), further addition of OTAC-p results in the formation of multiple OTAC-p micelles on a single polymer chain. So, the polymer chains start expanding back due to electrostatic repulsion of micelles present on the same polymer chain. For the 2500 ppm PEO solution (C > C*), the number of micelles in the solution increases with further addition of OTAC-p. Therefore, the three-dimensional intermolecular structure disappears and the relative viscosity decreases near the cmc point. The increase in relative viscosity past the cmc point is mainly due to the formation of free micelles in the solution.

To summarize, the conductivity and surface tension data exhibited no interaction between PEO and OTAC-p, whereas the relative viscosity measurements indicated weak interactions due to conformational changes of PEO chains. The interactions were stronger if the PEO / OTAC-p mixture temperature was increased. Therefore, the PEO / OTAC-p combination can be used as an effective drag reducer if the temperature of the mixture is sufficiently high.

4.2.2 Interaction of PEO with OTAC-p + NaSal

The interaction between PEO and OTAC-p was also studied in the presence of the counterion sodium salicylate (NaSal). For all the experiments, NaSal is used in equimolar proportion to that of OTAC-p. For the sake of simplicity, the equimolar combination of OTAC-p and NaSal is represented as OTAC-p + NaSal. The presence of counterion is expected to increase the binding ratio of OTAC-p to PEO. However, the chain expansion could be compromised due to the shielding effect of counterion. Since the PEO/OTAC-p + NaSal solution is clear in the concentration range of experiments, the turbidity measurements were not carried out for this system.

4.2.2.1 Conductivity

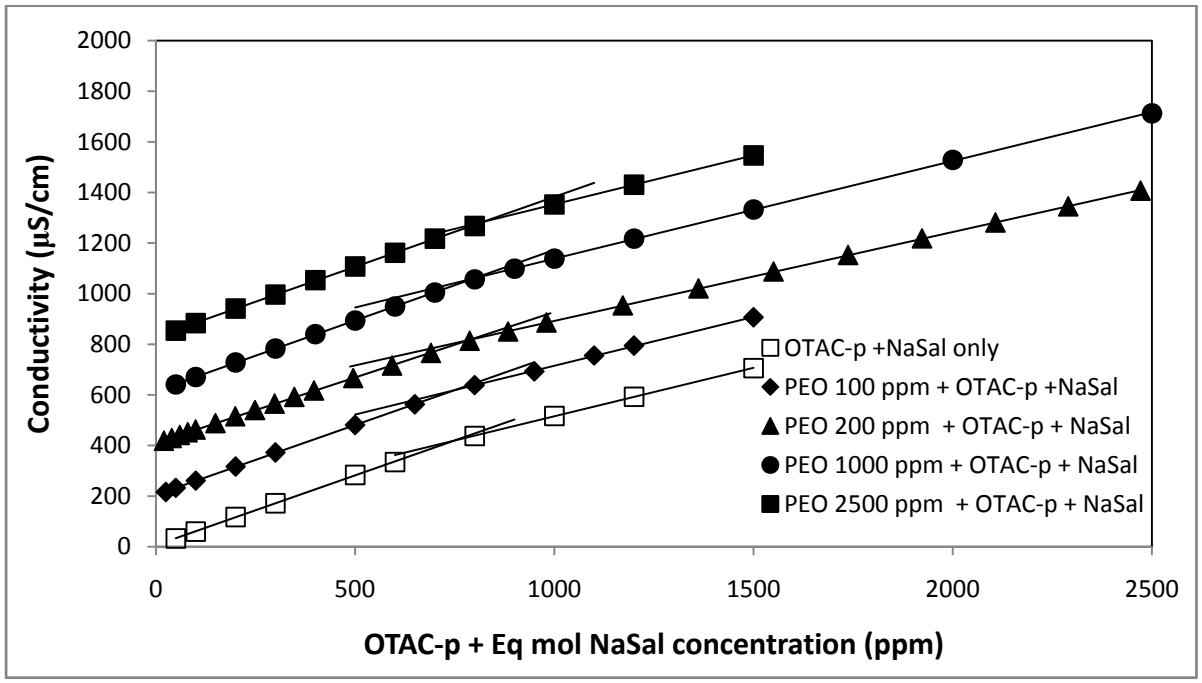

Figure 4.10 Conductivity of PEO / OTAC-p + NaSal solution in DI water vs. OTAC-p + NaSal concentration (Plots for PEO concentrations 100, 200, 1000 and 2500 ppm are moved by unit conductivity for better representation of data)

Although the conductivity data indicated no interaction between PEO and OTAC-p (without counterion) at room temperature, the presence of counterion increases the interaction between PEO and OTAC-p. As shown in ***Figure 4.10***, the cmc value increases from 750 ppm for OTAC-p + NaSal solution (no polymer) to 820 ppm for the solution of PEO / OTAC-p + NaSal at 2500 ppm PEO concentration. Although the change in cmc is not large, it is clear that the interaction between PEO and OTAC-p increases due to presence of NaSal.

Note that, Suksamranchit & Sirivat 2007 reported a change in the cmc from 0.7 mM for PEO / HTAC to 1.2 mM for PEO / HTAC + NaCl whereas in the present case, the change is only from 3.15 mM for PEO / OTAC-p to 3.35 mM for PEO / OTAC-p + NaSal. Also, the starting point of interaction (cac) or the concentration at which polymer is saturated with surfactant (psp) could not be obtained from the conductivity plot.

The temperature of the solution was not raised above the room temperature although it could have a significant effect on the degree of interaction between PEO and OTAC-p.

4.2.2.2 Surface Tension

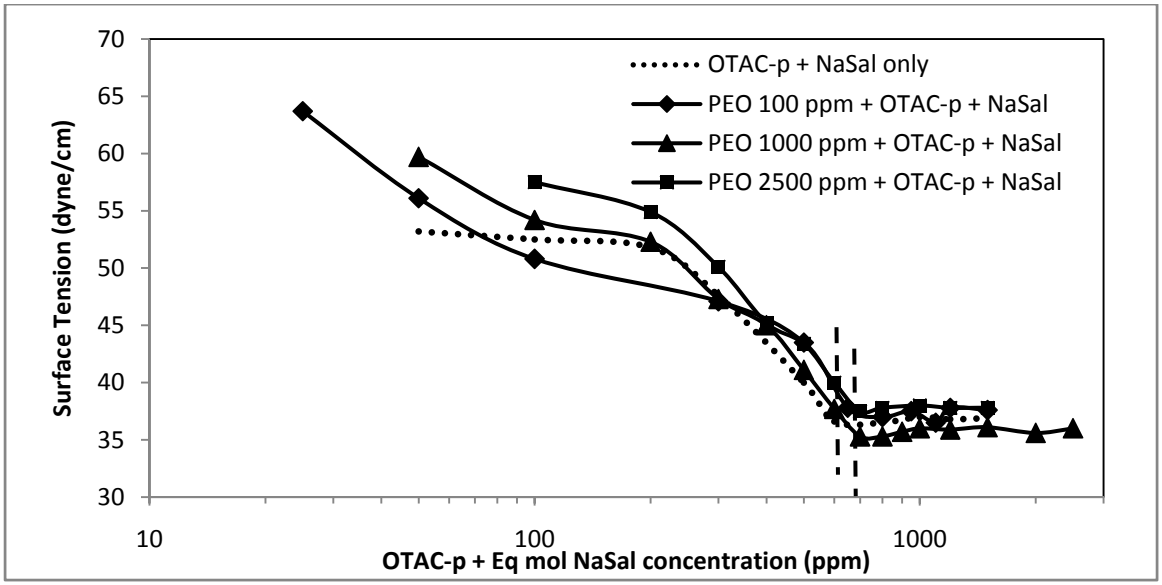

Figure 4.11 Surface Tension of PEO / OTAC-p + NaSal solution in DI water vs. OTAC-p conc. (OTAC-p with equimolar NaSal)

The surface tension data shown in ***Figure 4.11*** are in agreement with the findings of conductivity measurements. The shift in the cmc point due to the addition of PEO is very small and is evident in the graph (indicated by dashed line). If we compare ***Figure 4.11*** with ***Figure 4.4***, there is gradual shift in cmc by increasing PEO concentration in presence of NaSal, whereas, no change in cmc is observed by increasing PEO concentration in absence of NaSal. Thus, the binding of OTAC-p on polymer chains is enhanced due to presence of the counterion.

4.2.2.3 Relative Viscosity

The relative viscosity plots of PEO / OTAC-p + NaSal system are shown in ***Figure 4.12***. The plots are very similar to those of PEO / OTAC-p (without counterion) as shown in ***Figure 4.8***. A common feature of all the plots of ***Figure 4.12*** is that there occurs an increase in relative viscosity past the cmc' point. This can be attributed to the formation of free micelles in the solution past the cmc' point.

Unlike the PEO / OTAC-p mixture (without NaSal), the relative viscosity changes are observed here even at a low PEO concentration of 100 ppm. A reduction in viscosity is observed when the surfactant concentration is increased up to the cmc point. After the cmc point, the viscosity starts increasing. The initial reduction in relative viscosity can be explained as per the model proposed by Nilsson (1995), discussed earlier in ***section 4.2.1.3***, with the added effect of counterion. Due to the presence of counterion NaSal, the binding of OTAC-p on PEO chain is enhanced and so, better interactions are observed even at a low PEO concentration of 100 ppm.

It should be noted that in the case of 2500 ppm PEO / OTAC-p solution, the relative viscosity increased from about 10.0 to 11.5 whereas in the case of 2500 ppm PEO / OTAC-p + NaSal solution, the increase in relative viscosity is observed to be somewhat smaller, from about 9.5 to 10.5. This indicates that the hydrodynamic radius of polymer-surfactant complex is reduced in the presence of counterion. These findings are in agreement with the results reported by Suksamranchit & Sirivat (2007) and can be explained by the model illustrated in ***Figure 2.11***.

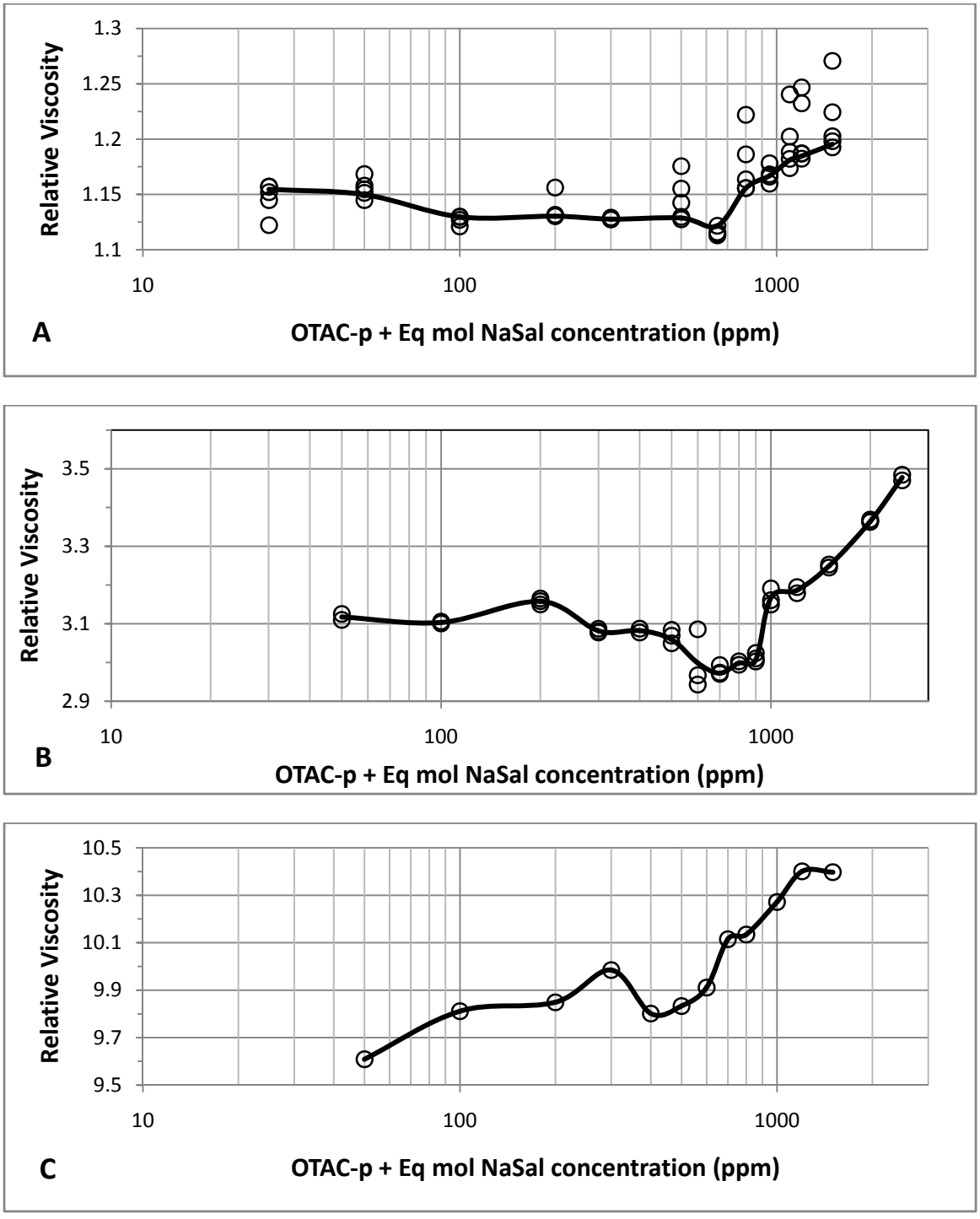

Figure 4.12 Relative Viscosity of PEO / OTAC-p+NaSal solution in DI water vs. OTAC-p conc. (with equimolar NaSal) for PEO conc.: (A) 100 (B) 1000 and (C) 2500 ppm. The solid curve represents the average values (excluding outliers)

4.3 Interaction of anionic polymer with non-ionic surfactant

The interaction of proton-donor polymeric acids with hydrophilic headgroup of ethoxylates is considered highly cooperative leading to conformational changes of the polymeric chain. The interactions between anionic CPAM (containing 30% sodium polyacrylate) and nonionic EA are studied here with the aid of surface tension and viscosity measurements. Due to nonionic nature of the surfactant, conductivity measurements do not reveal any useful information. Also, the solution is clear for the entire concentration range of the experiments. Therefore, conductivity and turbidity measurements are not carried out for this system.

4.3.1 Interaction of CPAM with EA

4.3.1.1 Surface Tension

As shown in ***Figure 4.13***, the cmc value increases with the increase in CPAM concentration due to interaction between CPAM and EA. For example, the cmc value increases from 40 ppm for pure EA to 100 ppm (marked as T_2 in ***Figure 4.13 (B)***) for 50 ppm CPAM solution. The starting point of interaction (T_1) is almost the same for all three CPAM concentrations. After T_1 further addition of EA leads to interaction between CPAM chains and EA as evident by a gradual decrease (at a rate lower than the rate before T_1) in the surface tension value. The location of point T_2 depends on the CPAM concentration; it moves to higher values as CPAM concentration increases. Upon increasing the CPAM concentration, the number of available sites for EA molecules to attach to CPAM molecules increases. Therefore, point T_2 moves to higher values at higher CPAM concentration. After the T_2 point, the polymer sites are saturated with surfactant and therefore, any further increase in the surfactant concentration results in the formation of free micelles in the solution.

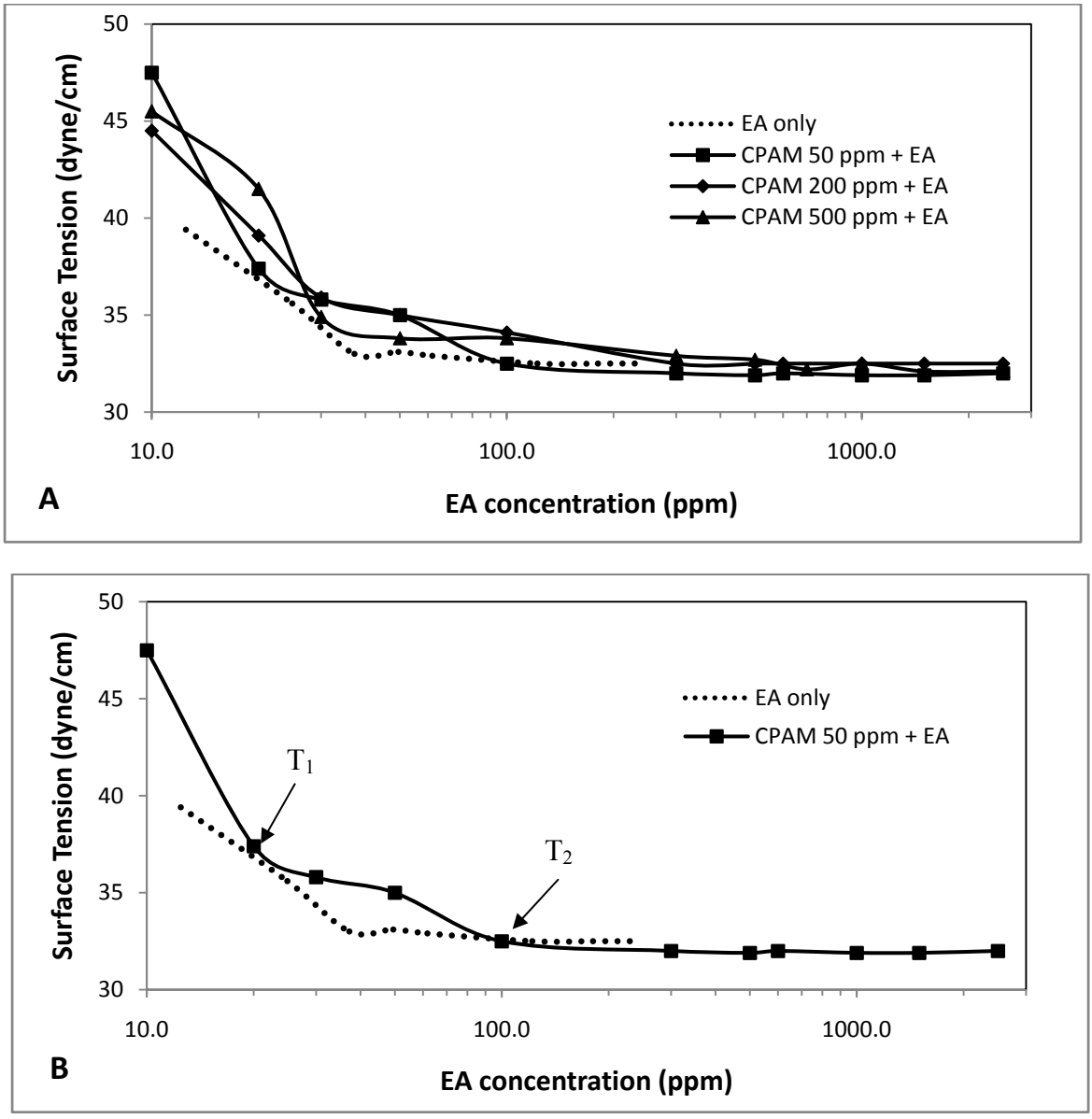

Figure 4.13 Surface tension of CPAM / EA solution in DI water vs. EA concentration

4.3.1.2 Viscosity

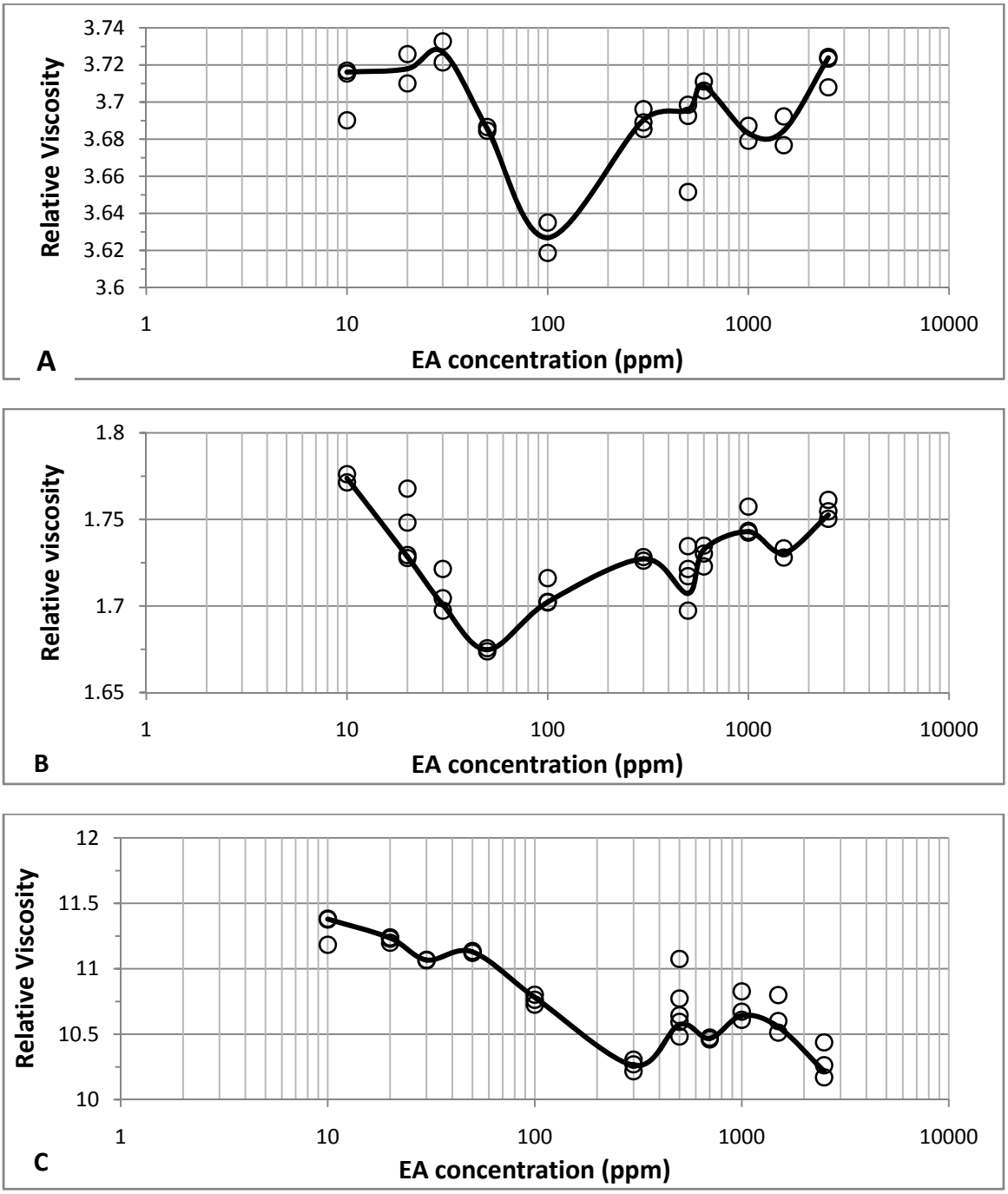

Figure 4.14 Relative Viscosity of anionic CPAM / EA solution in DI water vs. EA concentration for anionic CPAM concentration (A) 50 (B) 200 and (C) 500 ppm. The solid curve represents the average values (excluding outliers)

The relative viscosity data shown in ***Figure 4.14***, indicates a reduction in relative viscosity to a certain minimum value due to interaction between CPAM and EA. This reduction in viscosity can be attributed to cooperative binding between proton donating anionic CPAM and EO (ethylene oxide) units of nonionic EA. Apart from the Na^+ bridging between anionic CPAM and EO units of nonionic surfactant EA, the presence of long hydrophobic alkyl chain (C_{14}) results in additional hydrophobic attractions. However, the shrinkage of anionic CPAM can be attributed mainly to Na^+ bridging between anionic CPAM and EO units leading to a reduction in viscosity. The anionic CPAM chain is wrapped around the micellar aggregates via Na^+ bridging and hydrophobic attractions.

The minimum in relative viscosity is observed around T_2 point (see ***Figure 4.13***). The relative viscosity starts to increase with further addition of EA due to the formation of free micelles of EA. The increase in relative viscosity after point T_2 is mainly due to the formation of free micelles in the solution. Note that the surfactant (EA) concentration corresponding to T_2 point (where relative viscosity is minimum) first decreases and then increases when the CPAM concentration is increased from 50 ppm to 500 ppm. The initial decrease in EA concentration (corresponding to T_2 point) could be due to scattering of data points.

It is likely that the polymer chain shrinkage seen here (corresponding to a sharp reduction in viscosity) is irreversible. The Na^+ bridging bond between anionic CPAM and EO units of EA leads to shielding of electrostatic repulsive forces between charged sites on anionic polymer. Due to a strong nature of this bond, the polymer chains are not expected to expand upon further addition of EA.

From the drag reduction point of view, the combination of CPAM and EA may not be suitable due to permanent contraction of anionic CPAM. However, it may be interesting to examine the effect contraction of CPAM chains on drag reduction.

4.4 Interaction of anionic polymer with cationic surfactant

Interactions between oppositely charged polymer and surfactant have gained great interest in recent years to understand the colloidal chemistry and to explore new applications. In the case of oppositely charged polymer and surfactant – both Coulombic and hydrophobic interactions are involved. The addition of ionic surfactant to oppositely charged polymer leads to the formation of a neutralization product due to strong interaction. Polymer chains tend to collapse resulting in a sharp reduction in viscosity. The polymer chains lose polarity due to charge neutralization. The neutralized polymer / surfactant aggregates precipitate out of the solution. Further addition of ionic surfactant to the neutralized polymer / surfactant aggregates imparts the charge of the ionic surfactant to the polymer chain. This phenomenon is called charge reversal. This results in resolubilization of polymer / surfactant aggregates precipitated out previously due to charge neutralization. Phase separation, as a result of charge neutralization, is not desired from drag reduction point of view. Also, resolubilization occurs only at a high surfactant concentration, which is impractical from drag reduction point of view. Therefore, the interactions between anionic CPAM and cationic OTAC-p (in absence and presence of counterion NaSal) are studied here in the low range of surfactant concentration.

4.4.1 Interaction of CPAM with OTAC-p

4.4.1.1 Conductivity

As shown in ***Figure 4.15***, the conductivity plots of anionic CPAM / cationic OTAC-p system suggest strong interactions between CPAM and OTAC-p. The cmc value moves from 5700 ppm for pure OTAC-p to 6800 and 7100 ppm in the presence of 500 and 1000 ppm CPAM, respectively.

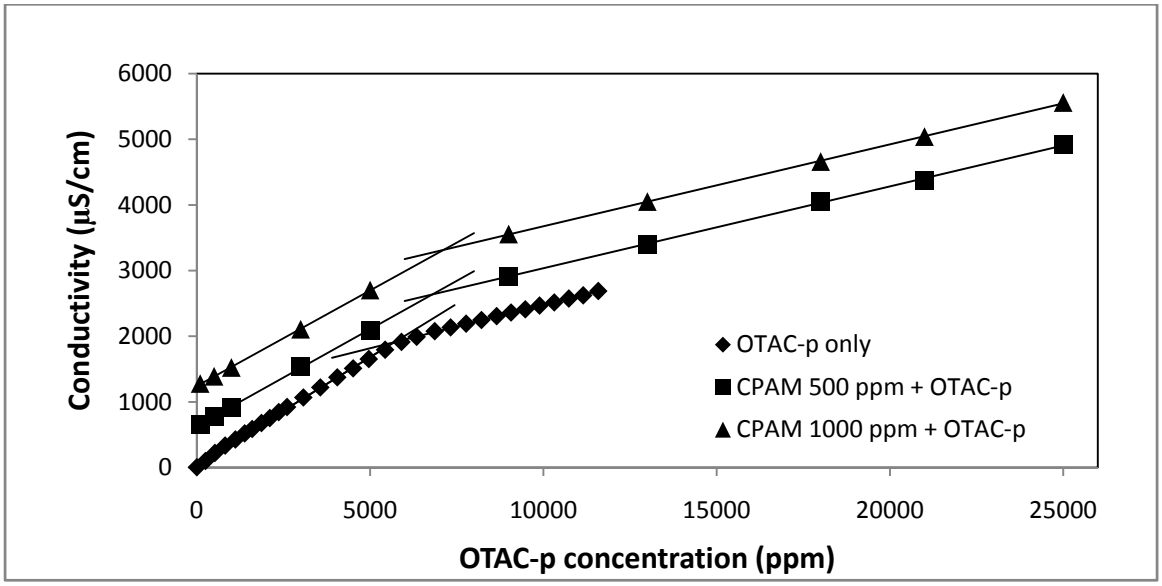

Figure 4.15 Conductivity of CPAM / OTAC-p solution in DI water vs. OTAC-p concentration (CPAM 500 and 1000 ppm concentration data points moved by unit conductivity for better representation of data)

The slope of the conductivity plot before the cmc point reduces from 0.325 for pure OTAC-p to 0.294 and 0.291 for 500 and 1000 ppm CPAM concentrations, respectively. This decrease in slope can be interpreted as a "loss" of free OTAC-p monomers due to fixation of OTAC-p monomers on the anionic CPAM chains. The slopes of the conductivity plots of 500 and 1000 ppm CPAM / OTAC-p mixtures have the same value of 0.124 after the cmc point. This indicates that the primary reaction here is the neutralization of polymeric charge. The OTAC-p monomers start forming micelles only after complete charge neutralization. Also, the charge neutralization of polymer and surfactant does not occur in stoichiometric proportion. For example, when CPAM concentration is doubled from 500 ppm to 1000 ppm, the cmc does not increase in stoichiometric proportion (cmc increases from 6800 ppm to 7100 ppm). This indicates that upon increasing the CPAM concentration, the cmc does not increase linearly, rather it levels off at sufficiently high CPAM concentration. This point will be discussed further in ***section 4.4.2.2***.

4.4.1.2 Turbidity

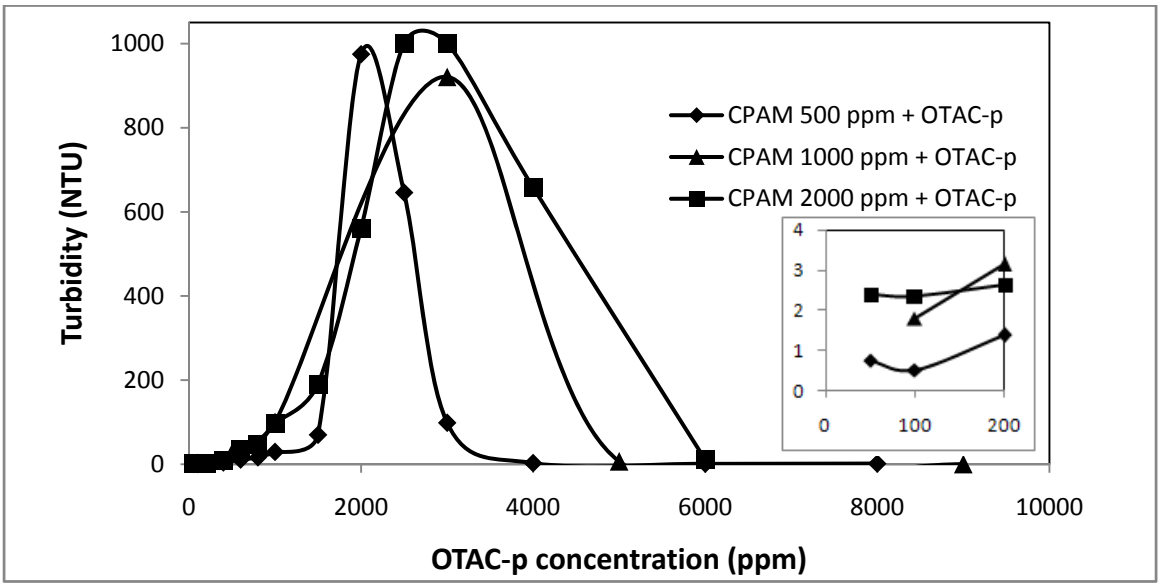

Figure 4.16 Turbidity of CPAM / OTAC-p solution in DI water vs. OTAC-p concentration

The addition of cationic OTAC-p to the aqueous solution of anionic CPAM leads to neutralization of charge on the polymer chains and therefore the polymer becomes less polar. This charge neutralization continues as OTAC-p concentration increases until the phase separation point after which, the polymer / surfactant complexes precipitates out of the solution. The addition of OTAC-p to the anionic CPAM solution turns the solution cloudy resulting in an increase in the turbidity value (see ***Figure 4.16***). As shown in the inset of ***Figure 4.16***, the turbidity starts increasing at a very low OTAC-p concentration, about two orders of magnitude less than the cmc. The point where interaction between polymer and surfactant starts is referred to as cac point. Based on the turbidity data, it seems that the cac point could be around 100 ppm. However, the viscosity data suggested that the interaction between anionic CPAM and cationic OTAC-p started well below 50 ppm OTAC-p.

The maximum turbidity occurs at around 2000 ppm OTAC-p for 500 ppm CPAM solution and at around 3000 ppm OTAC-p for both 1000 and 2000 ppm CPAM solutions. Also, the width of the turbidity plot seems to increase upon increasing the CPAM concentration. It is important to note that the reduction in turbidity after the maximum value is not due to

resolubilization of the polymer / surfactant complexes. The reduction in turbidity after the maximum value is due to phase separation of polymer / surfactant complexes from the solution.

In order to observe drag reduction, it is necessary to have a homogeneous mixture of polymer and surfactant. Therefore, for drag reduction applications, the concentration of OTAC-p in the mixture of CPAM and OTAC-p should not be increased more than that corresponding to the maximum turbidity.

4.4.1.3 Relative viscosity

Upon increasing the OTAC-p concentration the relative viscosity of CPAM /OTAC-p system reduces sharply (see ***Figure 4.17***). The changes in the relative viscosity can be attributed to strong interactions between oppositely charged polymer and surfactant. The Na^+ ion of the sodium polyacrylate copolymer is replaced by the cationic surfactant ion OTA^+ at the anionic binding site of CPAM. Due to electrostatic attractions between the oppositely charged ions, the binding of surfactant on the polymer chain is highly favorable. As indicated by the turbidity data, the binding process starts at a very low surfactant concentration.

Figure 4.18 compares the relative viscosity, turbidity and physical appearance of 1000 ppm CPAM / OTAC-p solution in DI water. It can be seen here that the reduction in relative viscosity is accompanied by an increase in the turbidity (also indicated by dark grey area on the bar near X-axis). Further addition of OTAC-p leads to complete charge neutralization. The relative viscosity reaches a value of unity and the neutralized product precipitates out of the solution.

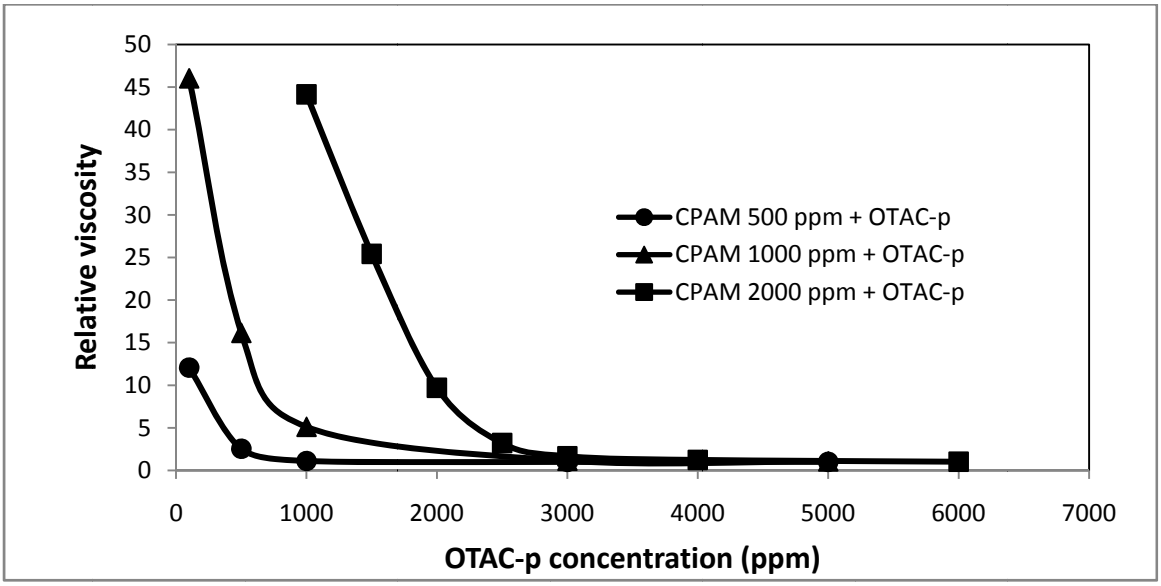

Figure 4.17 Relative viscosity of CPAM / OTAC-p solution in DI water vs. OTAC-p concentration

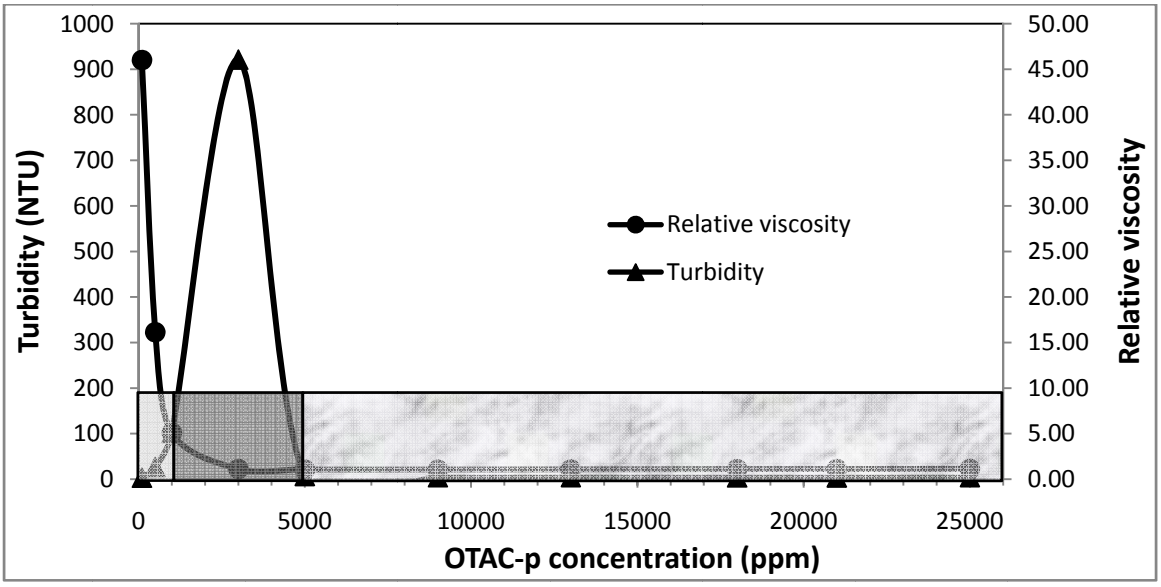

Figure 4.18 Relative viscosity, Turbidity and physical appearance box-plot of 1000 ppm CPAM / OTAC-p solution in DI water.

The schematic representation of interaction between anionic CPAM and cationic OTAC-p is shown in ***Figure 4.19***. The anionic CPAM chains are initially fully extended in the solution due to electrostatic repulsive forces between the charged anionic sites of the polymer chain.

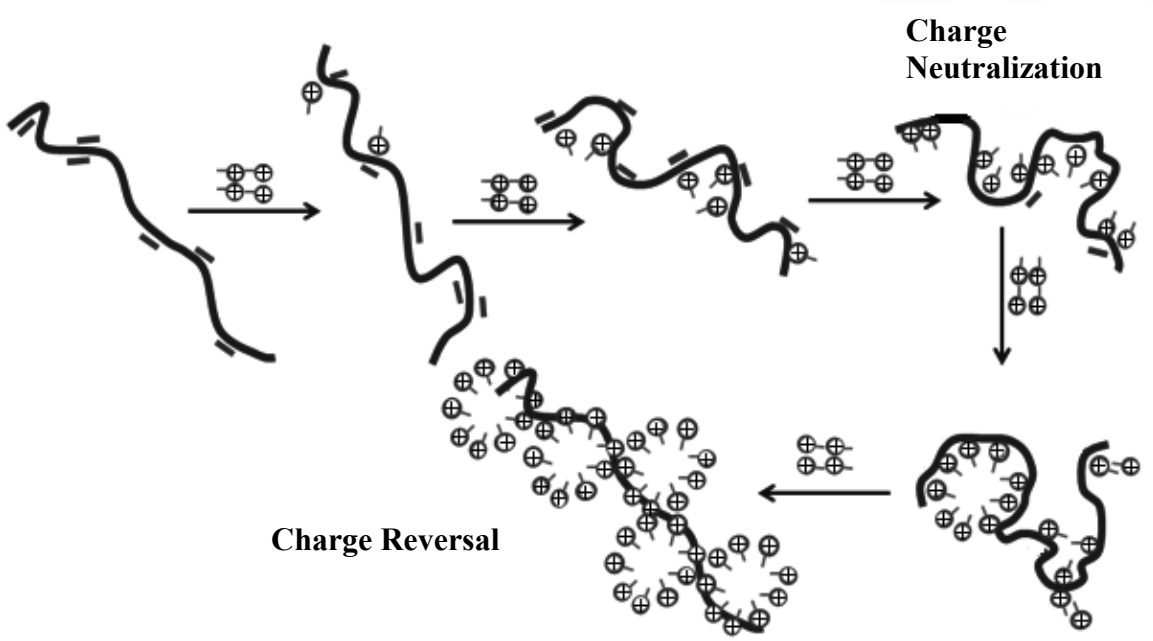

Figure 4.19 Schematic representation of interaction between anionic CPAM and Cationic OTAC-p (Modified from Deo et al., 2007 and Goddard, 2002)

Upon addition of OTAC-p, the anionic charge of the polymer chains begins to neutralize. Due to this charge neutralization, the electrostatic repulsive forces disappear. Therefore, the polymer chains collapse. Also, due to charge neutralization, the polymer chains become less polar and the solution begins to turn cloudy. After complete charge neutralization, the CPAM / OTAC-p aggregates become insoluble and precipitate out.

However, further addition of cationic OTAC-p to the solution leads to the phenomena called "Charge Reversal". The neutralized CPAM OTAC-p complexes became positively charged resulting in resolubilization of the precipitates.

4.4.2 Interaction of CPAM with OTAC-p + NaSal

4.4.2.1 Conductivity

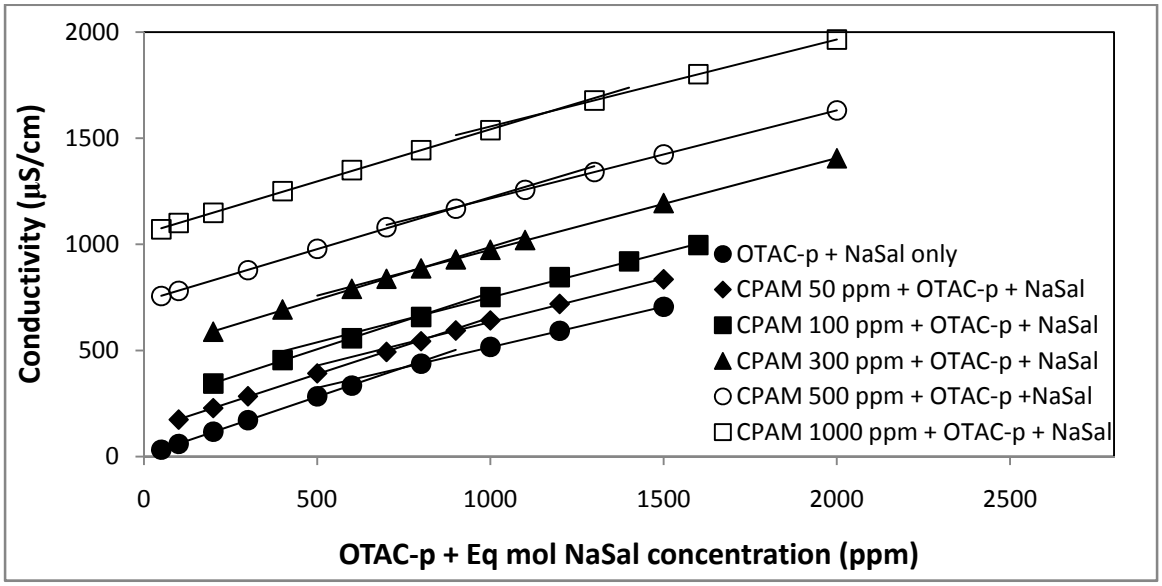

Figure 4.20 Conductivity of CPAM / OTAC-p + NaSal solution in DI water vs. OTAC-p concentration (with equimolar NaSal) (the plots of various CPAM concentrations moved by unit conductivity for better representation of data)

As shown in ***Figure 4.20***, cmc values (determined from the intersection of conductivity plots) increases with the increase in CPAM concentration. As some of the added OTAC-p is used up in neutralizing the anionic charge of the polymer, more of OTAC-p is required to form micelles. However, the change in the slope of the conductivity plot observed at a cmc point is very low due to the presence of counterion. In the present case, the counterion concentration used is equimolar concentration of OTAC-p. At higher concentrations of counterions it is often impossible to judge the cmc point based on the conductivity plot as the change in the slope is very small. Also, note that the increase in the cmc point is not in stoichiometric proportion; this point is discussed further in the following section.

The marking of cmc value on conductivity plots can vary to some extent with the data points selected to draw the intersecting lines. For example, if we compare ***Figure 4.21 A*** and ***B***, the cmc point identified in ***Figure 4.21***A is 859 ppm, whereas ***Figure 4.21 B*** indicates a cmc

value of 948 ppm. The results reported in this work have been compared with surface tension measurements to identify the cmc values.

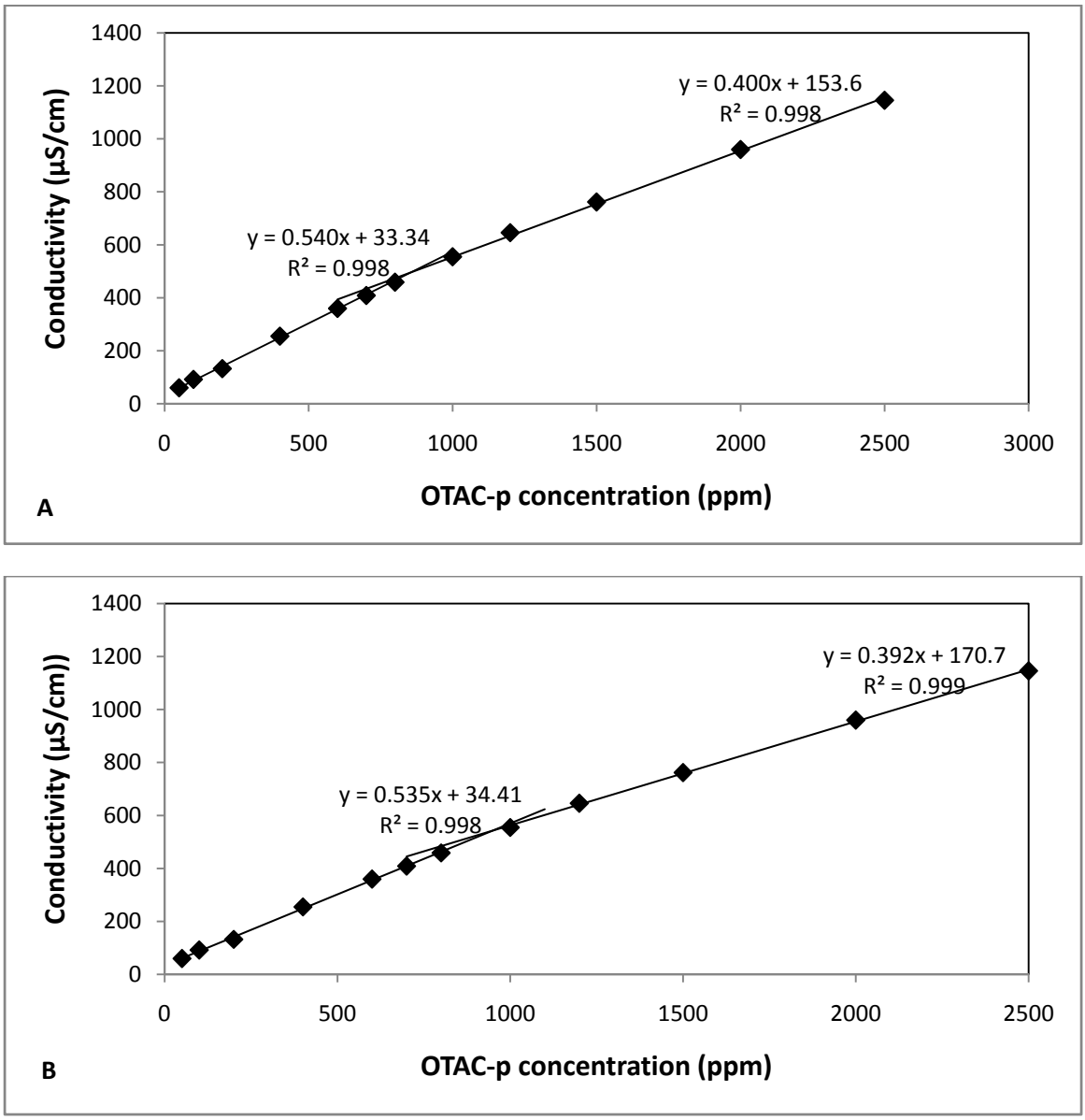

Figure 4.21 Conductivity plots of 100 ppm CPAM / OTAC-p (with equimolar NaSal) in DI water

4.4.2.2 Surface Tension

As shown in ***Figure 4.22***, the surface tension of CPAM / OTAC-p + NaSal solution decreases upon increasing the OTAC-p concentration. The cmc value of OTAC-p + NaSal mixture is around 600 ppm. Higher values of cmc are observed in the presence of CPAM due to the reason explained in the preceding ***section 4.4.2.1***. These results are in agreement with the conductivity data.

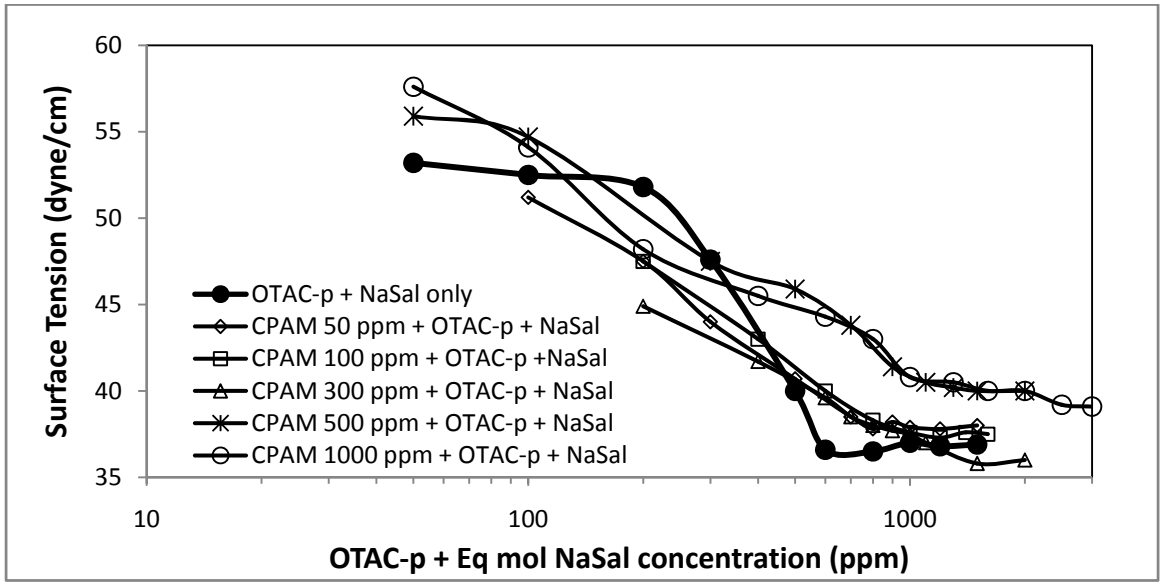

Figure 4.22 Surface Tension data of CPAM / OTAC-p + NaSal solution in DI water vs. OTAC-p concentration

The cmc values obtained from both conductivity and surface tension methods for the solutions at different CPAM concentrations are summarized in ***Figure 4.23***. As shown in ***Figure 4.23***, the cmc does not increase linearly with the increase in CPAM concentration. This indicates that the charge neutralization of anionic CPAM due to the addition of OTAC-p is not in stoichiometric proportion. The onset concentration of entanglement (C*) of polymer CPAM is about 280 ppm. Therefore, at CPAM concentrations higher than 280 ppm, the CPAM chains in the solution are entangled with each other. Due to entanglement of CPAM chains, some portions of the CPAM chains become inaccessible to the OTAC-p monomers. Therefore, at concentrations of CPAM higher than C*, the cmc value tends to level off.

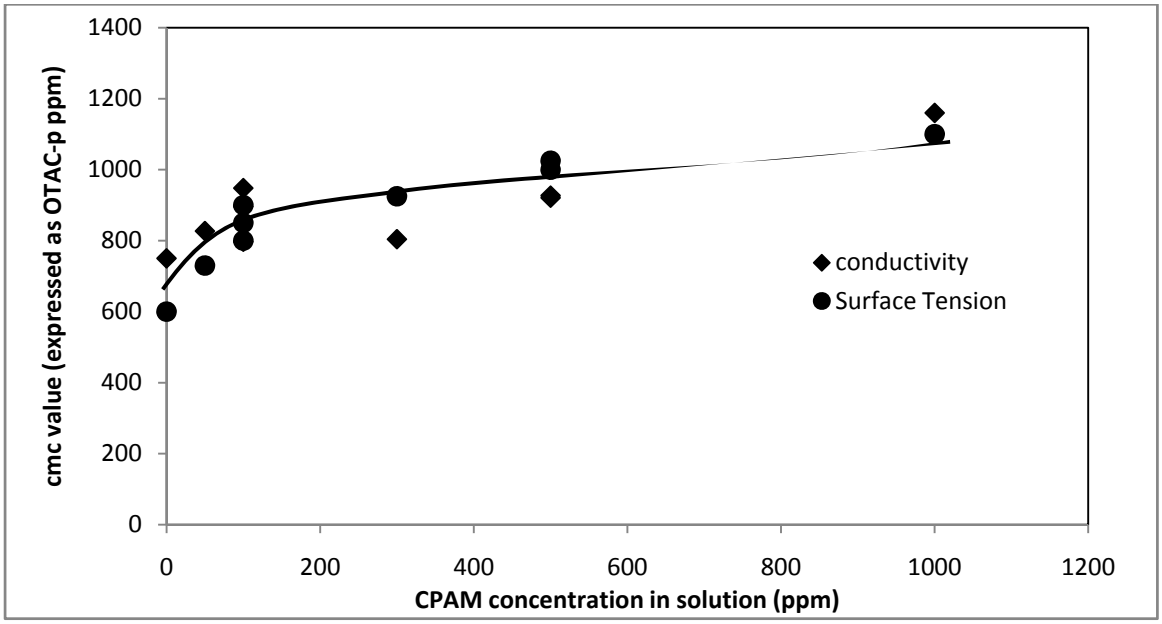

Figure 4.23 cmc values of CPAM / OTAC-p + NaSal solution in DI water vs. CPAM concentration

4.4.2.3 Turbidity

The turbidity data of CPAM / OTAC-p + NaSal (shown in ***Figure 4.24***) are very similar to the turbidity data of CPAM / OTAC-p without NaSal (see ***Figure 4.16***). Interestingly, the OTAC-p concentration where the turbidity maximizes is almost the same for the CPAM / OTAC-p system with and without NaSal. However, the maximum turbidity point (where phase separation occurs) in the case of CPAM / OTAC-p system (without NaSal) is well below the cmc point, whereas in the presence of NaSal, the maximum turbidity point (where phase separation occurs) is above the cmc point.

It was previously suggested that charge neutralization of the polymer chains is favored over the micelle formation in the case of CPAM / OTAC-p system without NaSal. However, in the presence of NaSal, micelle formation of the OTAC-p molecules occurs well below the complete charge neutralization concentration.

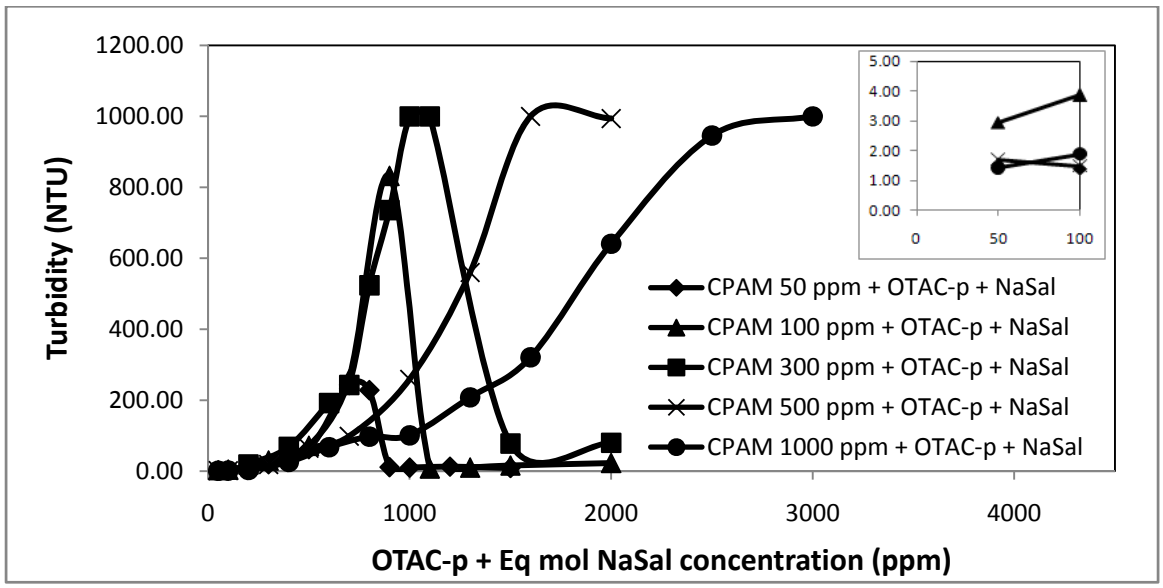

Figure 4.24 Turbidity of CPAM / OTAC-p + NaSal solution in DI water vs. OTAC-p concentration

The onset concentration of interaction, often referred to as "cac" is very similar in both cases – with and without NaSal. Although the interaction between CPAM and OTAC-p is not greatly influenced by the presence of NaSal, The presence of NaSal stabilizes OTAC-p monomers and facilitates the formation of micelles.

4.4.2.4 Relative Viscosity

The relative viscosity data for CPAM / OTAC-p + NaSal system are plotted in ***Figure 4.25***. The relative viscosity behavior is similar to that observed in the case of CPAM / OTAC-p without NaSal. The anionic charge on the polymer chains is neutralized due to the addition of cationic OTAC-p. The intra molecular electrostatic repulsive forces disappear due to charge neutralization leading to a sharp reduction in the relative viscosity of CPAM / OTAC-p + NaSal solution.

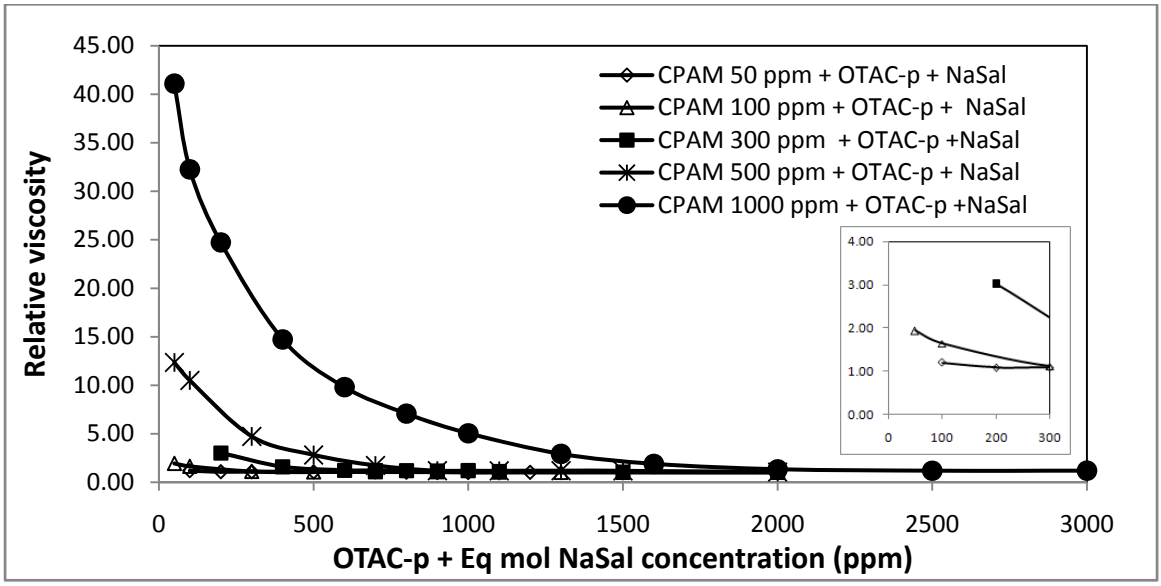

Figure 4.25 Relative viscosity of CPAM / OTAC-p + NaSal solution in DI water vs. OTAC-p concentration

The comparison of ***Figure 4.25*** and ***Figure 4.17*** reveals that the relative viscosity reduces more sharply upon addition of OTAC-p when NaSal is not present. In the presence of NaSal, the drop in relative viscosity of CPAM upon addition of OTAC-p is less sharp. The presence of NaSal stabilizes the highly active OTAC-p molecules and leads to the formation of micelles at low concentrations. Consequently, less or a lower amount of OTAC-p is available to react with anionic charge of CPAM in the low OTAC-p concentration range. Therefore, the drop in relative viscosity is not very abrupt as seen in the absence of NaSal. The inset of ***Figure 4.25*** shows that the reduction in relative viscosity starts at a very low OTAC-p concentration and the onset point of interaction between CPAM and OTAC-p is nearly independent of the CPAM concentration.

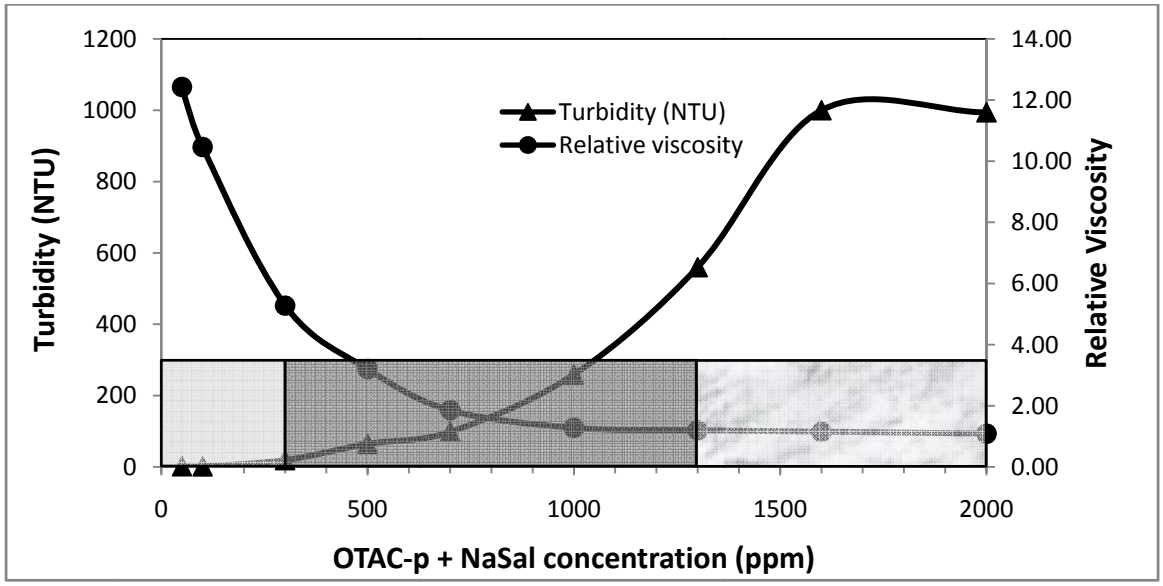

Figure 4.26 Relative viscosity, Turbidity and physical appearance box-plot of 500 ppm CPAM / OTAC-p + NaSal solution in DI water.

Figure 4.26 compares the relative viscosity, turbidity and physical appearance of CPAM / OTAC-p + NaSal solution at 500 ppm CPM concentration. The phase separation of CPAM / OTAC-p + NaSal complexes occurs after OTAC-p concentration of 1300 ppm. Also, the relative viscosity reaches a value of unity near the phase separation point. It is interesting to note here that the phase separation point is well above the cmc value of about 950 ppm for 500 ppm CPAM solution. Therefore, fully developed micelles are expected in the OTAC-p concentration range from cmc (950 ppm) to phase separation point (1300 ppm) in the 500 ppm CPAM solution.

The intrinsic viscosity of a polymer solution can precisely capture the conformational changes of the polymer chains. An attempt is made here to provide evidence of the collapse of CPAM chains due to presence of OTAC-p. The intrinsic viscosity [η] of anionic CPAM is reported to be 71.18 dL/gm (see **Chapter 3, *Figure 3.6***).

The Mark-Houwink correlation is given as,

$$[\eta] = K\overline{M}_v^a \qquad \textbf{4.1}$$

where, a and K are the constants depending on type of polymer and solvent at a given temperature and $\overline{M}_v$ is the viscosity-averaged molecular weight.

Using $K = 6.5\times10^{-3}$ mL/gm and $a = 0.82$ (Kurata & Tsunashima, 1989), we get $\overline{M}_v = 23\times10^6$ gm/mol and using the correlation proposed by Schwartz & Francois (1981) $[\eta] = 5\times10^{-3}\overline{M}_v^{0.9}$ (Vlassopoulos & Schowalter, 1994), the viscosity-average molecular weight $\overline{M}_v$ is found to be 6.87×10^6 gm/mol. The molecular weight of anionic CPAM reported by the manufacturer is $11\text{-}14\times10^6$ gm/mol, which is within the range of viscosity-average molecular weight obtained from two different sets of Mark-Houwinck constants.

Similarly, one can calculate the viscosity averaged molecular weight of PEO. For PEO $K = 12.5\times10^{-3}$ mL/gm and $a = 0.78$ (Kurata & Tsunashima, 1989), and $[\eta] = 14$ dL/gm. Thus, $\overline{M}_v = 2.9\times10^6$ gm/mol for PEO. This $\overline{M}_v$ is in close agreement with 4×10^6 gm/mol specified by the manufacturer.

The end-to-end distance of the polymer coil $\left(\overline{r^2}\right)^{\frac{1}{2}}$ can be obtained from the intrinsic viscosity [η] value using the Fox-Flory Equation:

$$[\eta] = \Phi'\frac{\left(\overline{r^2}\right)^{\frac{3}{2}}}{M} \qquad \textbf{4.2}$$

where, $\Phi' \approx 2.1\times10^{21}$ dL/(mol•cm^3) and M is the molecular weight of the polymer.

Figure 4.27 shows the plots of reduced viscosity (η_{sp}/C) of CPAM / OTAC-p + NaSal solution as a function of polymer (CPAM) concentration at different OTAC-p concentrations. The y-intercept of the plot is the intrinsic viscosity [η].

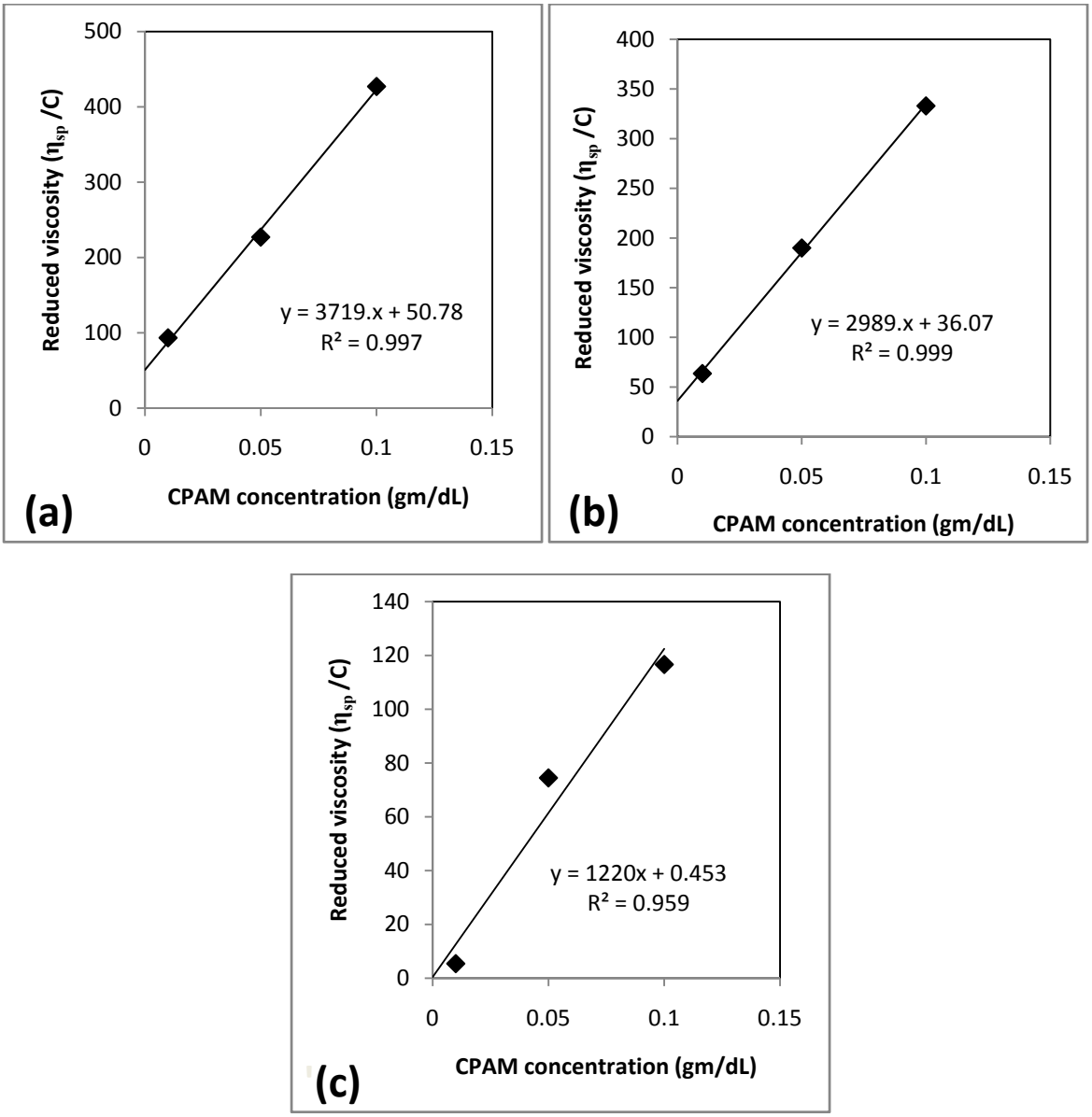

Figure 4.27 Reduced viscosity of CPAM / OTAC-p solution in DI water vs. CPAM concentration : (a) 50 ppm (b) 100 ppm and (c) 500 ppm OTAC-p with equimolar NaSal

Table 4.1 shows the intrinsic viscosity values and the corresponding end-to-end distance values of polymer chains. The average molecular weight of anionic CPAM used in the calculation is 12×10^6 gm/mol. It can be seen from the table that upon addition of OTAC-p to anionic CPAM, the end-to-end distance of the polymer chain decreases from 0.74 μm at 0 ppm OTAC-p to 0.14 μm at 500 ppm OTAC-p concentration (with equimolar NaSal).

Solvent - OTAC-p (with equimolar NaSal) ppm	[η] dL/gm	$\left(\overline{r^2}\right)^{\frac{1}{2}}$ μm
0	71.18	0.74
50	50.78	0.66
100	36.07	0.59
500	0.453	0.14

Table 4.1 Change in end-to-end distance of CPAM chain upon addition of OTAC-p

This suggests large conformational changes of the CPAM chains due to neutralization of anionic charge on the CPAM chains. The polymer chain length is reduced to almost 20% of the fully extended size in DI water.

The reduction in the size of CPAM chains due to interaction with OTAC-p is not favorable from drag reduction point of view. The full extension of the polymer chains are considered to be more effective in drag reduction. The shrinking of CPAM chains due to strong electrostatic attractions between oppositely charged polymer and surfactant (as shown in ***Figure 4.19***) may have an adverse effect on drag reduction. However, the presence of NaSal induces the formation of OTAC-p micelles at OTAC-p concentration well-below the OTAC-p concentration where complete charge neutralization of CPAM takes place. It would be interesting to see the effect of aggregates, formed due to interaction between CPAM and OTAC-p, on drag reduction since the linearity of CPAM will change to branched-type structure.

4.4.3 Interactions of CPAM with OTAC-p in Tap Water

All the results reported so far are with DI (deionized) water. It is important from industrial application point of view to study the interaction between anionic CPAM and cationic OTAC-p in tap water. The tap water in Waterloo contains approximately 11 to 200 ppm of sodium ions (Na^+) [Source – Region of Waterloo, Public Health web-site: *http://chd.region.waterloo.on.ca/web/health.nsf/$All/802C4278C3E2C63885256B14006407A4?OpenDocument*; visited on 08/01/09]. When anionic CPAM is dissolved in DI water, it releases Na^+ and the polymer chain assumes anionic charge. Due to electrostatic repulsions between the charged sites of the anionic CPAM, the polymer chain becomes fully extended giving a high value of viscosity. In tap water, the anionic charge of the CPAM chains is largely shielded by the cationic charge present in the tap water (mainly in the form of Na^+). Due to the lack of electrostatic repulsive forces, the anionic CPAM chains are only partially expanded and therefore, the viscosity of anionic CPAM in tap water is low compared to the viscosity corresponding to DI water. In the following section, the interaction between anionic CPAM and cationic OTAC-p is discussed. The experimental data presented in the following section are produced in collaboration with Prof. Rajinder Pal's co-op student Kathy Wang.

4.4.3.1 Conductivity and surface tension

The conductivity plots of CPAM / OTAC-p (without NaSal) in tap water are shown in ***Figure 4.28***. As can be seen in ***Figure 4.28***, the presence of Na^+ ions in tap water induces counterion effect such that the cmc point of OTAC-p solution in tap water is reduced to 4800 ppm from a value of 5700 ppm found in the case of DI water. Due to the presence of Na^+ counterions in tap water, the OTAC-p monomers are stabilized. Therefore, the formation of micelles in tap water starts at a lower OTAC-p concentration compared with DI water. The cmc value also increases with the increase in CPAM concentration of the solution. The cmc value increased from 4800 ppm at zero CPAM to 6300 ppm at 1000 ppm CPAM.

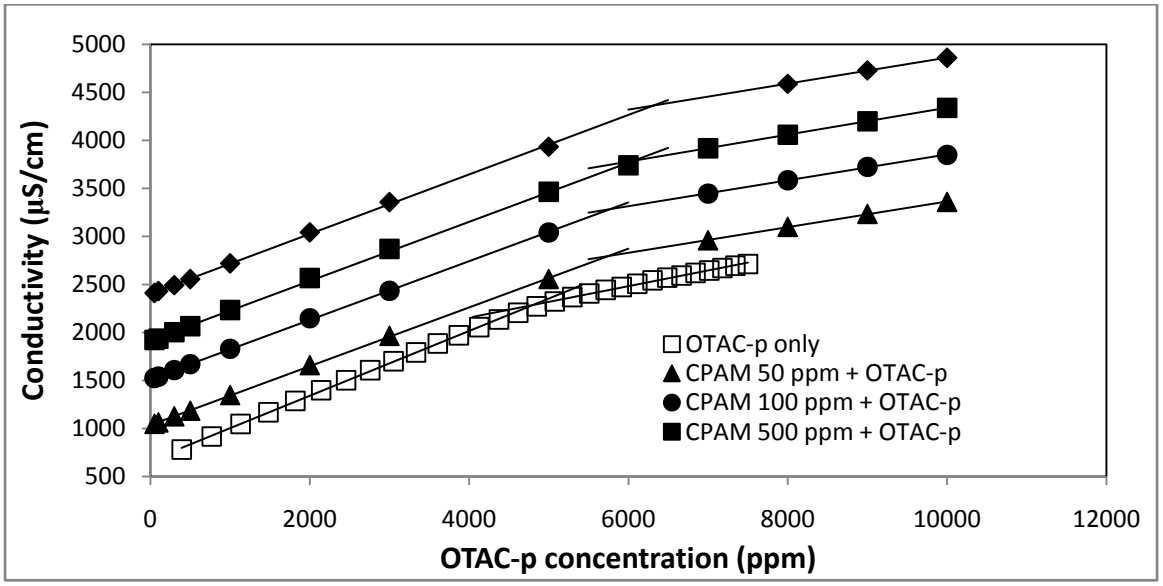

Figure 4.28 Conductivity of anionic CPAM / OTAC-p solution in TAP WATER vs. OTAC-p concentration

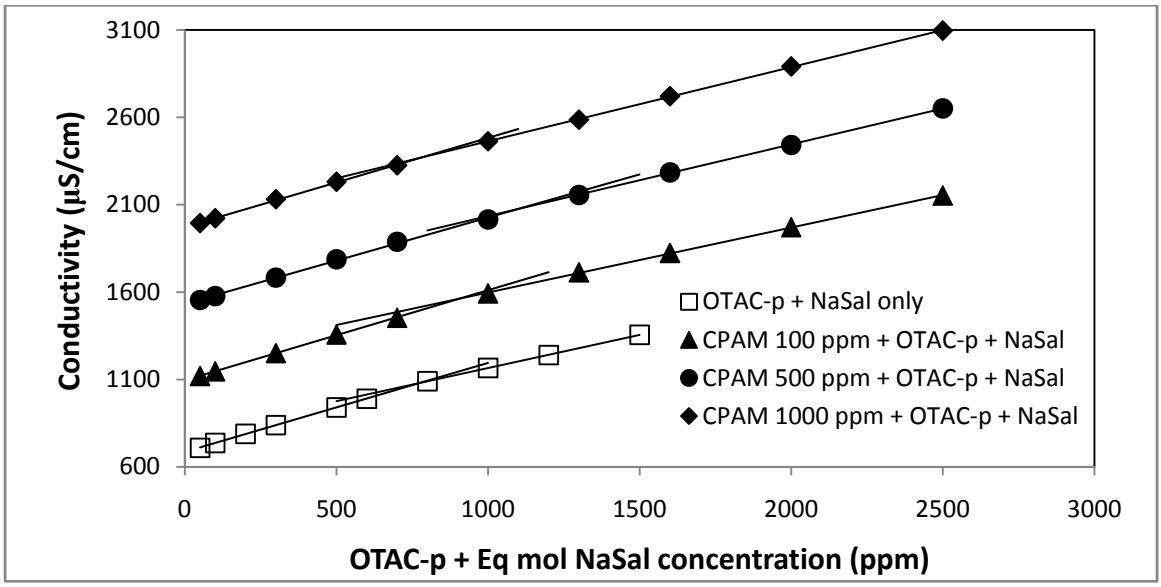

Figure 4.29 conductivity data of CPAM / OTAC-p + NaSal solution in TAP WATER vs. OTAC-p concentration

The effect of Na^+ ions present in tap water is largely nullified upon the addition of equimolar NaSal to the tap water (see ***Figure 4.29***). The cmc of OTAC-p + NaSal is 780 ppm in tap water; it was 750 ppm in DI water. However, the conductivity plots shown in ***Figure 4.29***

reveal that the change in slope at cmc point is very low and therefore, the cmc point obtained from the conductivity data can be erroneous. The surface tension data, shown in ***Figure 4.30***, indicates that the cmc value tends to increase slightly with the increase in CPAM concentration. The nonideal behavior observed in the surface tension plots can be attributed to the surface active property of the CPAM.

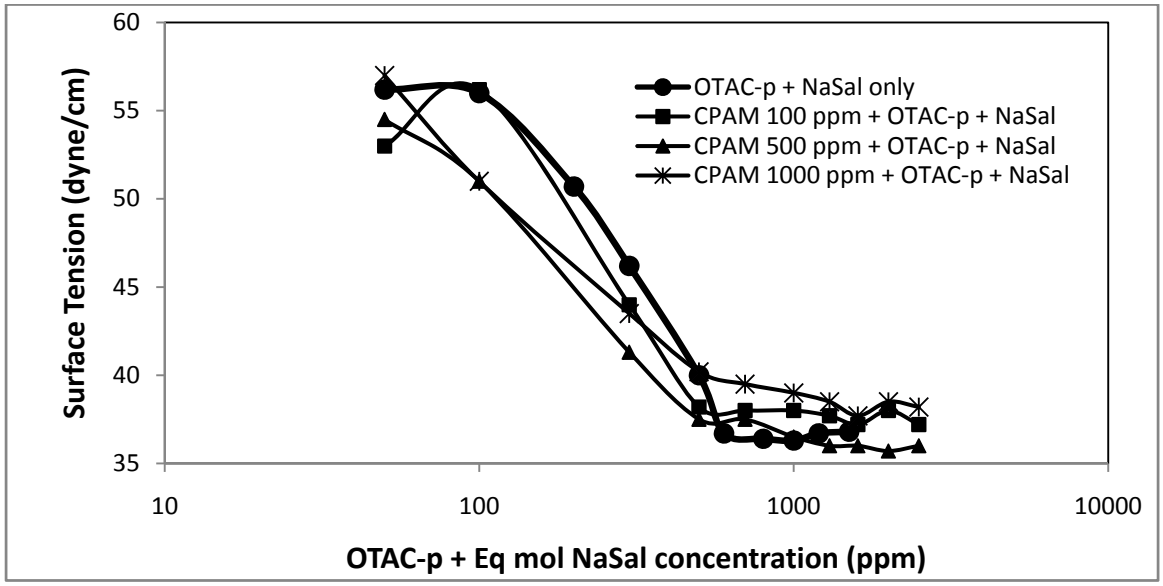

Figure 4.30 Surface tension data of CPAM / OTAC-p + NaSal solution in TAP WATER vs. OTAC-p concentration

4.4.3.2 Relative Viscosity

Figure 4.31 shows the relative viscosity data of CPAM / OTAC-p solution in tap water. The viscosity data clearly indicates that tap water is a poor solvent for anionic CPAM compared to DI water. The Na^+ ions present in tap water shield the anionic charge of CPAM. Therefore, the electrostatic repulsive forces responsible for full extension of polymer chain disappear resulting in a low viscosity of polymer solution. The relative viscosity of 1000 ppm CPAM is about 48 in DI water; in tap water it is reduced to only 3.5.

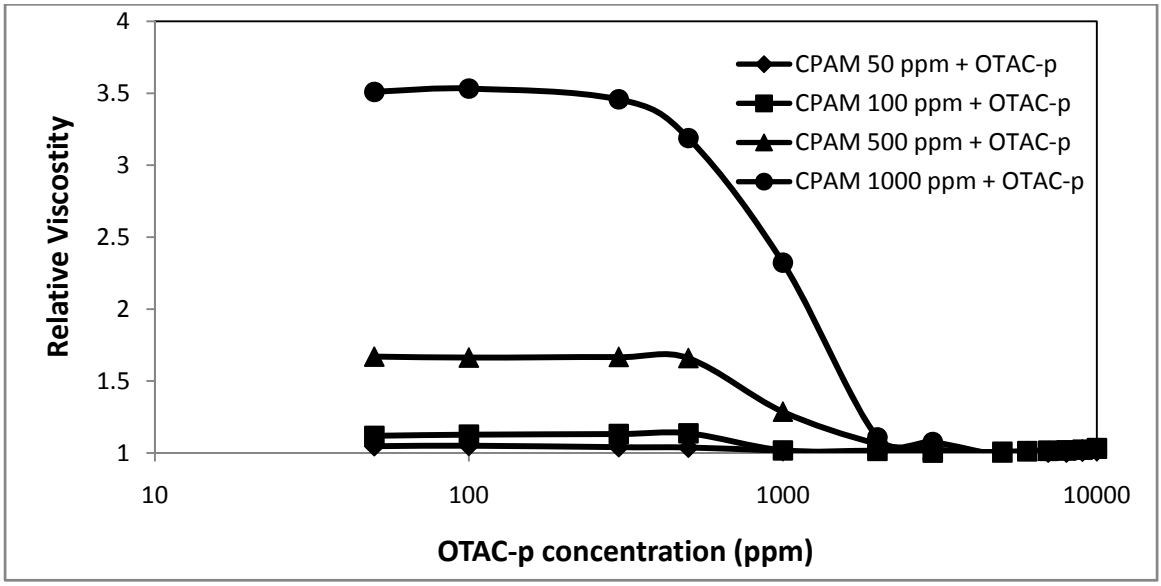

Figure 4.31 Relative viscosity of CPAM / OTAC-p solution in TAP WATER vs. OTAC-p concentration

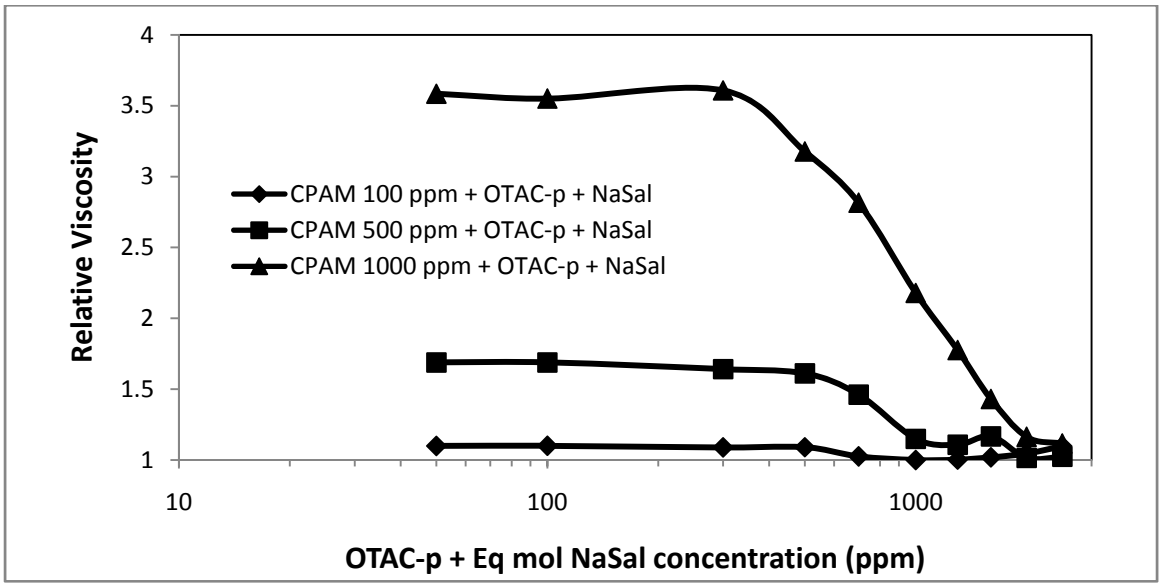

Figure 4.32 Relative viscosity of CPAM / OTAC-p + NaSal solution in TAP WATER vs. OTAC-p concentration

Another striking difference between the viscosity results obtained from DI water (see ***Figure 4.17***) and from tap water (see ***Figure 4.31***) is that the interaction between OTAC-p and CPAM starts well below 50 ppm OTAC-p in the case of DI water whereas in tap water, the

interaction begins at 500 ppm OTAC-p concentration. The presence of NaSal seems to have little effect on the viscosity of CPAM / OTAC-p solution in tap water (see ***Figure 4.32***). The cac point is about 500 ppm in presence of NaSal. Since tap water is a poor solvent, the anionic CPAM chains are highly coiled. This makes the diffusion of OTAC-p monomers to the charged sites of polymer chain difficult. Therefore, no interaction between CPAM and OTAC-p is observed upto 500 ppm. After about 500 ppm OTAC-p, the concentration gradient of OTAC-p is sufficiently high value to start diffusion of OTAC-p monomers into the coiled CPAM chains. The neutralization of remaining anionic charge on CPAM chains leads to further collapse of CPAM chains resulting in further reduction of relative viscosity.

It can also be seen from ***Figure 4.31*** and ***Figure 4.32*** that the cac point is around 400 ppm OTAC-p for a solution containing 1000 ppm CPAM. At lower CPAM concentrations, the cac point is around 500 ppm OTAC-p. In 1000 ppm CPAM solution, the coiling of CPAM in tap water is comparatively less due to the presence of a large number of charged sites. Therefore, the diffusion of OTAC-p monomers to the polymer charged sites starts at a comparatively lower concentration. It would be interesting to study the effect of water quality (tap water, DI water) on the drag reduction behavior of CPAM / OTAC-p solutions.

4.4.3.3 Turbidity

Figure 4.33 and ***Figure 4.34*** show the turbidity data. The turbidity data indicates that the interaction between OTAC-p and CPAM starts around 400 – 500 ppm OTAC-p, which is in agreement with the viscosity data of CPAM / OTAC-p in the presence and absence of NaSal. Due to the precipitation of CPAM / OTAC-p aggregates after the maximum turbidity point, some of the turbidity data exhibit unusual behavior (see ***Figure 4.34***).

Figure 4.35 shows the comparison of relative viscosity, turbidity and physical appearance of the samples on the same plot. The relative viscosity remains fairly constant up to 500 ppm OTAC-p. Also, the solution remains clear in this concentration range, indicating no interaction between CPAM and OTAC-p due to the shielding effect of NaCl present in the

tap water. The decrease in turbidity after 3000 ppm OTAC-p is mainly due to the phase separation of the CPAM / OTAC-p aggregates.

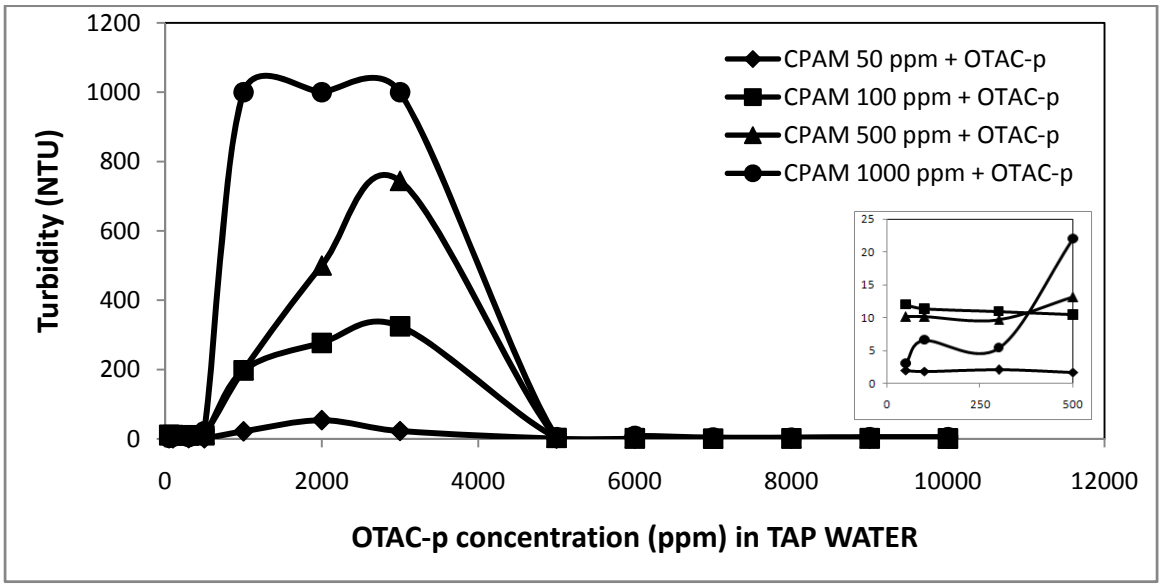

Figure 4.33 Turbidity data of CPAM / OTAC-p solution in TAP WATER vs. OTAC-p concentration

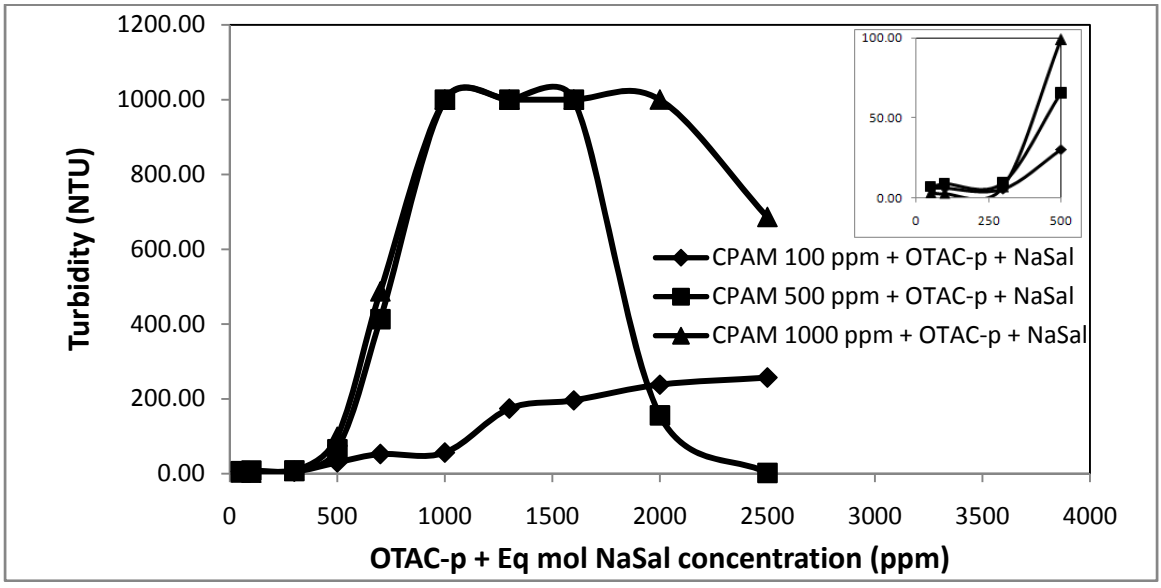

Figure 4.34 Turbidity data of CPAM / OTAC-p solution concentration in TAP WATER vs. OTAC-p

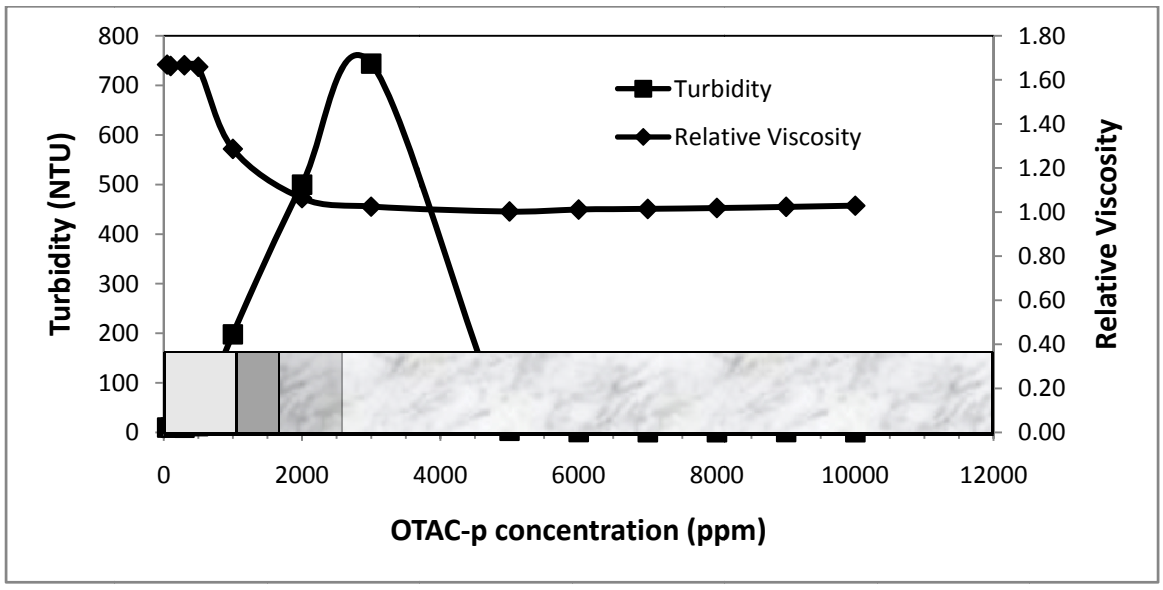

Figure 4.35 Relative viscosity, Turbidity and physical appearance box-plot of 500 ppm CPAM / OTAC-p solution in TAP WATER

4.5 Drag reduction study

To study the effect of mixed polymer and surfactant system on drag reduction, the anionic CPAM and cationic OTAC-p were mixed in tap water and the flow behavior of these mixed systems were studied in a pipeline flow loop. The pipeline flow experiments were carried out by Prof. Rajinder Pal's Ph. D. student Ali Mohsenipour. The experimental results are shown in ***Figure 4.36*** to ***Figure 4.39***.

As can be seen from ***Figure 4.36*** and ***Figure 4.37***, both the cationic OTAC-p and anionic CPAM are good drag reducers in tap water. The solid line represents the Blasius equation for Newtonian fluids. The friction factor data fall below the Blasius equation indicating drag reduction. ***Figure 4.37*** shows that by increasing the CPAM concentration in the tap water, the friction factor reduces substantially from that of tap water alone. A similar effect is seen in the case of OTAC-p in ***Figure 4.36***. The cmc value of OTAC-p + NaSal (1:1 mol ratio) is around 750 ppm. An increase in the NaSal content can further lower the cmc value. As

shown in ***Figure 4.36***, by changing the OTAC-p / NaSal mol ratio from 1:1.5 to 1:2.0, the drag reduction ability improves significantly. With the increase in the NaSal content, the number of micelles increases resulting in better drag reduction.

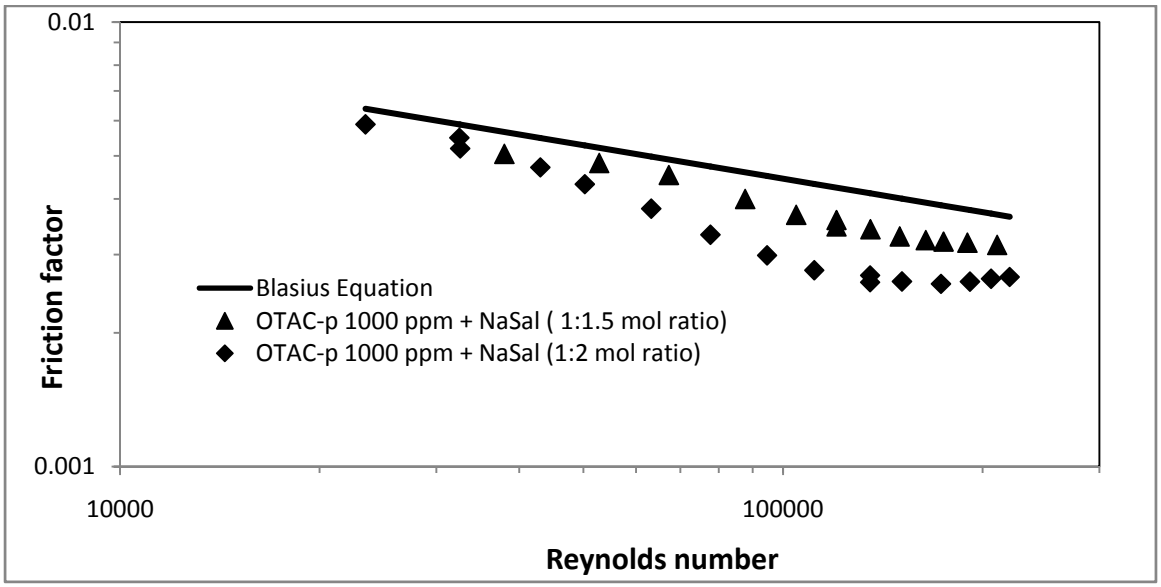

Figure 4.36 Friction factor of OTAC-p solution in TAP WATER with 1:15 and 1:2.0 mol ratio NaSal at 20 °C in 1" pipe flow

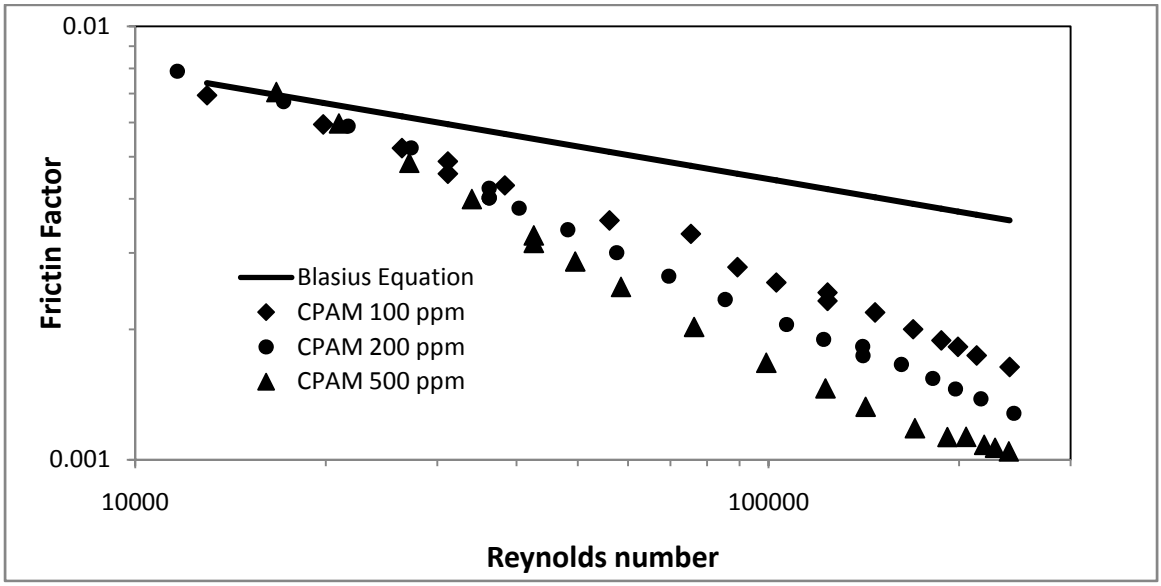

Figure 4.37 Friction factor vs. Reynolds number of CPAM solutions in TAP WATER in 1" pipe flow

Figure 4.38 shows the effect of interaction between CPAM and OTAC-p on drag reduction in 1" pipe flow. As mentioned earlier, the interaction between CPAM and OTAC-p in tap water begins at around 500 ppm OTAC-p. Therefore, no change in the drag reduction behavior of CPAM is seen upon addition of 100 and 300 ppm OTAC-p. As tap water is a poor solvent for anionic CPAM, the CPAM chains exist as partially collapsed in tap water. The polymer chains of CPAM are expected to collapse further upon the addition of 800 ppm OTAC-p. However, the degree of further shrinkage is not very appreciable at 800 ppm. Therefore, there does not occur much change in the drag reduction ability of 500 ppm CPAM solution in tap water upon the addition of OTAC-p.

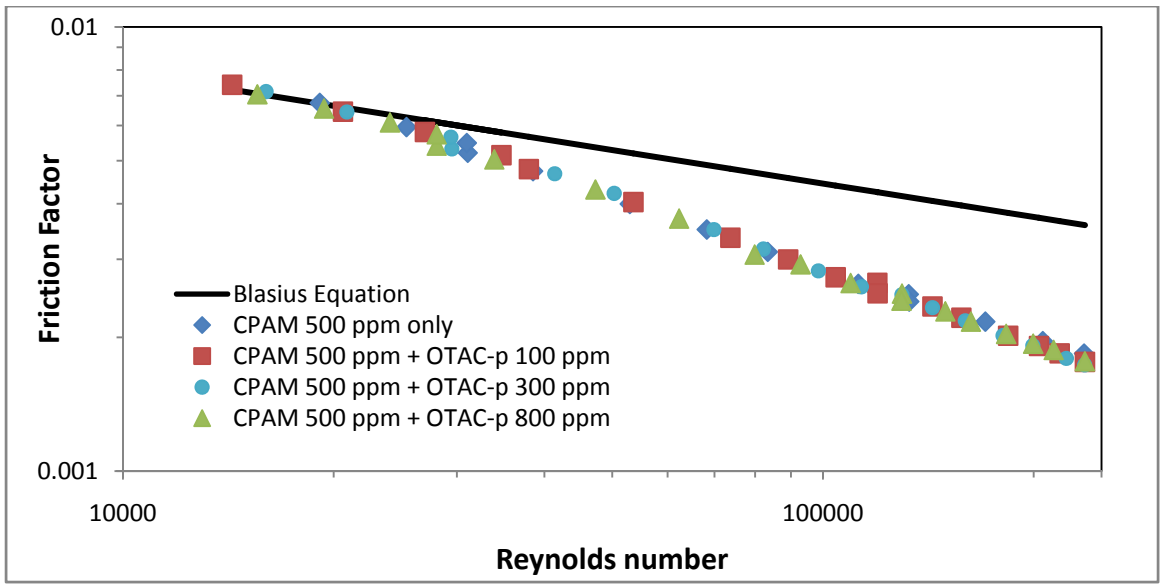

Figure 4.38 Friction factor vs. Reynolds number of CPAM / OTAC-p solutions in TAP WATER in 1" pipe flow

The maximum OTAC-p concentration tried in this experiment was 800 ppm, which is far below the cmc of OTAC-p in tap water (4800 ppm). At such a low surfactant concentration, no micelle formation takes place. Therefore, no contribution of OTAC-p towards drag reduction is expected.

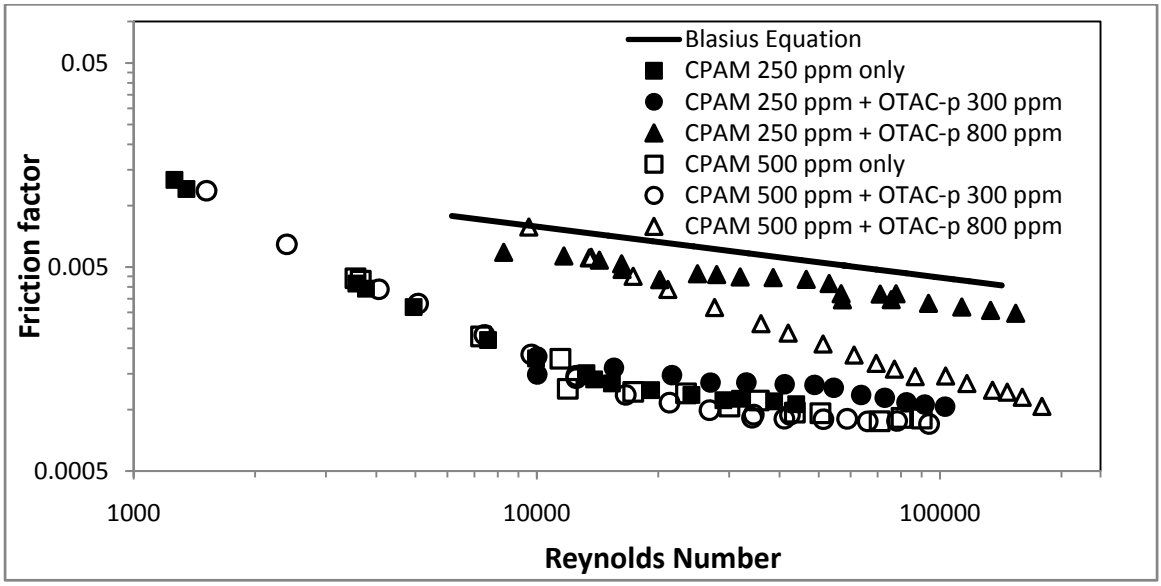

Figure 4.39 Friction factor vs. Reynolds number of CPAM / OTAC-p solutions in DI WATER in 1" pipe flow

A significant change in the drag reducing ability of CPAM in DI water solution is observed upon the addition of OTAC-p (see ***Figure 4.39***). The addition of OTAC-p to the CPAM / DI water solution reduces the drag reduction ability of CPAM, especially when OTAC-p is 800 ppm.

The reduction in the drag reducing ability of anionic CPAM upon the addition of cationic OTAC-p is expected. Due to charge neutralization, the polymer chains collapse upon the addition of OTAC-p to the aqueous solution of anionic CPAM. As a consequence, the polymer chains lose their drag reduction ability.

Chapter 5
Conclusion and Recommendations

5.1 Conclusions

1. Weak interactions were observed between nonionic polymer PEO (polyethylene oxide) and nonionic surfactant EA (ethoxylated alcohol). Due to the attachment of EA monomers to the PEO chain, the viscosity increased initially. With further addition of EA, the viscosity reduced to a certain minimum value due to "wrapping" of PEO chain around the developing micelles of EA. At high concentrations of EA, the viscosity increased again due to the formation of free micelles in the solution.

2. For the mixed system of nonionic polymer PEO and cationic surfactant OTAC-p (Octadeycltrimethylammonium chloride in powder form), the viscosity data indicated weak interactions. Opposite behaviors were observed for PEO concentrations below and above critical entanglement concentration C*. The relative viscosity reduced to a minimum value due to intramolecular interactions when the polymer concentration was below C*. When the polymer concentration was above C*, the relative viscosity increased to a certain maximum value due to the formation of intermolecular three-dimensional structure. These results are similar to those reported by Nilsson (1995) for the nonionic polymer / anionic surfactant system. At high concentrations of OTAC-p, the viscosity increased again due to the formation of free micelles of OTAC-p in the solution.

   In the presence of counterion NaSal (sodium salicylate), stronger interactions between PEO and OTAC-p were observed. With the increase in temperature, the interactions between PEO and OTAC-p became stronger. The conductivity plots indicated that binding between PEO and OTAC-s (OTAC in solvent form) was better than the binding between PEO and OTAC-p (OTAC in powder form) at the same temperature.

3. The relative viscosity of anionic polymer CPAM (copolymer of polyacrylamide and sodium polyacrylate) reduced to a certain minimum value upon addition of nonionic surfactant EA (ethoxylated alcohol). The Na^+ bridging bond between anionic CPAM and EO (ethylene oxide) units of EA led to shielding of electrostatic repulsive forces between the charged sites of the anionic polymer chain. The relative viscosity increased at higher EA concentrations due to the formation of free micelles of EA in the solution.

4. Strong interactions were observed between anionic polymer CPAM (copolymer of polyacrylamide and sodium polyacrylate) and cationic surfactant OTAC-p (Octadecyltrimethylammonium chloride). The cationic OTAC-p molecules neutralized the charge on anionic CPAM. The presence of CPAM in the solution increased the cmc value due to the "loss" of free OTAC-p molecules to CPAM chains. The increase in the cmc value was not in stoichiometric proportion. At higher CPAM concentrations, parts of the CPAM chains became inaccessible to OTAC-p.

   Due to charge neutralization, the electrostatic repulsive forces responsible for full extension of CPAM chains disappeared. The shrinkage of CPAM chains resulted in a large drop in the relative viscosity. The shrinkage in polymer chains also caused a decrease in the intrinsic viscosity. Due to charge neutralization, the polymer chains became less polar and insoluble, resulting in the phase separation of CPAM / OTAC-p aggregates. This was reflected in the turbidity data. In the presence of NaSal counterion, the OTAC-p monomers were stabilized leading to formation of free micelles in the solution well before the complete charge neutralization of CPAM.

5. From drag reduction point of view, the shrinkage of CPAM chains due to the addition of OTAC-p is not favorable. The pipeline results indicated that the drag reducing ability of CPAM / OTAC-p solution was reduced due to the shrinkage of polymer chains.

5.2 Recommendations for future work

Following are some of the recommendations for future work:

1. Out of the four polymer – surfactant systems studied here, the nonionic PEO / cationic OTAC-p system seems to be most suitable for drag reduction. OTAC-p used in this study did not exhibit strong interactions. However, better interactions between PEO and OTAC-s were observed at elevated temperatures and in presence of counterion NaSal. There is no significant chain size reduction of PEO due to interaction with OTAC-p and no precipitation is observed even at very high OTAC-p concentration. Therefore, this combination of polymer and surfactant can bring out the advantages of both polymer and surfactant – full extension of polymer chain and shear induced structures of surfactant under turbulent flow conditions. This could result in better drag reduction when surfactant concentration is above the cmc point.

2. Although the shrinkage of anionic CPAM in the presence of cationic OTAC-p is not a desired effect from drag reduction point of view, the presence of NaSal can mitigate this negative effect to a certain extent. Due to presence of NaSal, micelles of OTAC-p are formed in the solution well before the complete charge neutralization of CPAM chains. The coexistence of micelles and partly collapsed CPAM chains can produce some interesting results. Although the shrinkage of CPAM chains can lead to poor drag reducing ability, other aspects such as reduced mechanical degradation of the polymer may be beneficial. For example, if the polymer chains are collapsed, then the extent of mechanical degradation may be less.

3. Due to time limitations, a detailed study of the interaction of nonionic PEO and cationic OTAC-s at different temperatures could not be carried out. The preliminary results suggested that at high temperatures, the interactions between nonionic polymer and cationic surfactant could be as cooperative as those observed between nonionic polymer and anionic surfactant. More experiments in this direction could help to identify the underlying mechanisms of interaction between polymer and surfactant.

Appendix A

Drag reducing surfactants and polymers

Type of Surfactant	Name of surfactant	Reference
Anionic	Sodium oleate with KCl	Savins (1967, 1968, 1969)
Nonionic	Ethoxylated alcohol $C_xH_y(OCH_2CH_2)_nOH$ x=12 – 18, y=2x+1 or 2x-1, z≈0.5x Ethoxylated fatty acid ethanolamide $C_nH_{2n-1}CONHC_2H_4(OC_2H_4)_mOH$ n=18 – 22, m=3-8	Zakin & Chiang (1972) Zakin & Lui (1983) DeRoussel (1993) Chang & Zakin (1985) Hellsten & Harwigsson (1994)
Zwitterionic	N-alkylbetaines $CH_3(CH_2)_n\text{-}N^+(CH_3)_2CH_2COO^-$ n=15-17	Harwigsson (1995) Harwigsson & Hellsten (1996) Hellsten et al. (1996)
Cationic	Cetyltrimethylammonium bromide with 1-naphthol C16TAC, C18TAC, C22TAC with sodium salicylate Alkyl trimethyl ammonium chloride, alkyl bis-hydroxyethyl ammonium chloride and tris-hydroxyethyl ammonium chloride Ethoqaud O-12 with sodium salicylate Cetyltrimethylammonium salicylate	White (1967) Zakin et al. (1971) Chou et al. (1987, 1988) Chou et al. (1989) Chou (1991) Chou et al. (1989, 1991) Roes et al. (1984, 1989)

Table A.1 List of some of the Surfactants used as drag reducing agents in water (Zakin et al., 1998)

Solute	Reference	Molecular weight per backbone chain link ($x10^6$)	Degradation Resistance
Sodium Carboxymethyl Cellulose	Dodge (1958); Dodge and Metzner (1959) Escudier et. al. (1999) Shaver (1957); Shaver and Merrill (1959)	0.7 ^{w}	High
Hydroxyethylcellulose	Gadd (1966); Wang, (1972)	0.68 ^{v}	High
Guar Gum	Gadd (1965 and 1966); Wang (1972)	1.7 ^{w}	High
Xanthan Gum	Escudier et. al. (1999)		Low
Polyethyleneoxide	Gadd (1965); Virk (1962); Virk et al. (1967); Virk and Baher (1970) Patterson and Abernathy (1970 and 1972) Fortuna and Hanratty (1972)	0.1 ~ 8.0 ^{w}	Low
Polyacrylamide	Dodge (1958); Virk and Haher (1970) Chang and Darby (1983) Sellin and Ollis (1983) Escudier et. al. (1999) Fortuna and Hanratty (1972)	4.7 ~ 12.5 ^{w}	Low
Polyisobutylene	Shaver (1957); Lescarboura et al. (1971)	-	Low
Polyacrylic acid	White and Gordon (1975)	10	Low

Note) Subscript *w* means its MW is a weight-average value and *v* a viscosity-average.

Table A.2 List of some of the polymers successfully used as a drag reducing agent in water (Seonwook, 2003)

Appendix B
Experimental Data

Sample #	EA conc. (ppm)	t_p (sec)	t_p (sec)	t_p (sec)	t_p (sec)	Surface Tension (dyne/cm)
1	10	126	124	122		38.5
2	25	125	123	122		36.0
3	50	127	125	121		33.1
4	100	126	124	122		32.3
5	200	128	126	123	122	32.3
6	500	119	119	118		32.2
7	1000	126	123	123		32.2
8	1500	125	124	123		32.2
9	2000	128	125	123		32.3
10	3000	128	126	124		32.3

Table B.1 PEO 100 ppm solution in DI water with EA

Sample #	EA conc. (ppm)	t_p (sec)	t_p (sec)	t_p (sec)	t_p (sec)	t_p (sec)	t_p (sec)	Surface Tension (dyne/cm)
1	10	174	176	171	175	175		40.5
2	20	189	185	183	181	180	179	36.2
3	30	195	188	184	183	182		35
4	50	191	186	183	182	184	183	34.5
5	100	191	186	183	182	181	180	33.3
6	300	191	187	184	181	181		32.9
7	500	189	183	180	182	180		32.3
8	700	190	182	181	180	179		32
9	1000	189	183	182	181			32
10	1500	193	186	184	184			32.1
11	2500	193	186	183	183			32.5

Table B.2 PEO 500 ppm solution in DI water with EA

Sample #	EA conc. (ppm)	t_p (sec)	t_p (sec)	t_p (sec)	t_p (sec)	t_p (sec)	t_p (sec)	Surface Tension (dyne/cm)
1	10	290	293	294	294			45.0
2	20	302	300	297	293	293		37.0
3	30	291	295	295				34.9
4	50	316	295	295				34.9
5	100	300	298	298				33.5
6	300	305	304					32.4
7	500	283	284					32.5
8	700	294	289	286	283	282	284	32.0
9	1000	284	282	282				32.1
10	1500	305	294	295				32.0
11	2500	311	299	299				32.0

Table B.3 PEO 1000 ppm solution in DI water with EA

Sample #	OTAC-p conc. (ppm)	Conductivity (µS/cm)	t_p (sec)	t_p (sec)	t_p (sec)	t_p (sec)	t_p (sec)	t_p (sec)	t_p (sec)	t_p (sec)	t_p (sec)	t_p (sec)
1	50	24.64	122	122	122	122						
2	100	40.8	121	122	121	121	121					
3	200	71.9	123	126	123	123	122	122				
4	500	180.2	121	122	123	121	120	120				
5	800	279.2	123	125	123	123	122	123				
6	1000	350	123	126	124	122	121	122				
7	2000	682	120	117	120	120	121	120				
8	3000	998	123	124	123	123	122	122				
9	5000	1623	123	126	125	124	123	123	122	122	121	122
10	7000	2100	121	121	121	120	120	121				
11	10000	2466	124	123	124	124	123	124				
12	13000	2857	128	131	129	128	127	127	127			
13	16000	3220	127	126	126	127	127	129	127	127		
14	20000	3750	135	139	135	133	136	133				
15	25000	4410	139	140	139	138	138					

Table B.4 PEO 100 ppm solution in DI water with OTAC-p

Sample #	OTAC-p conc. (ppm)	Conductivity (µS/cm)	t_p (sec)	t_p (sec)	t_p (sec)	Surface Tension (dyne/cm)
1	100	39.8	213	211	211	64.7
2	500	176	209	208	207	59.6
3	1000	342	204	204		58.2
4	3000	976	210	208	209	52.8
5	5000	1574	210	210		47.8
6	7000	2046	210	210		46.8
7	10000	2420	215	215		47.1
8	13000	2790	217	215	216	46.9
9	16000	3160	220	219	219	46.6
10	20000	3670	225	223	224	46.5
11	25000	4330	231	231		46.5

Table B.5 PEO 500 ppm solution in DI water with OTAC-p

Sample #	OTAC-p conc. (ppm)	Conductivity (µS/cm)	t_p (sec)	t_p (sec)	t_p (sec)	t_p (sec)	t_p (sec)	Surface Tension (dyne/cm)
1	50	41.8	1044	1059	1070	1062		65
2	100	57.8	1016	1070	1080	1072		64.8
3	200	95.3	1091	1101	1102			64.6
4	500	188.4	1088	1099	1103			62.6
5	800	283.2	1109	1168	1160			59.2
6	1000	363	1160	1160	1171			58
7	2000	680	1215	1203	1184	1185		55.8
8	3000	986	1172	1167	1165			52.6
9	5000	1590	1189	1169	1168			47.5
10	7000	2041	1151	1148	1149			47
11	10000	2422	1168	1173	1172			47
12	13000	2795	1175	1173	1157	1170		47
13	16000	3160	1179	1159	1149	1162		46.7
14	20000	3680	1194	1196	1201			46.3
15	25000	4330	1241	1224	1217	1207	1218	46.3

Table B.6 PEO 2500 ppm solution in DI water with OTAC-p

OTAC-p + equimolar NaSal conc. (ppm)	Conductivity (µS/cm)	t_p (sec)	t_p (sec)	t_p (sec)	t_p (sec)	t_p (sec)	Surface Tension (dyne/cm)
25	16.49	118	120	121	121	121	63.7
50	33.1	123	122	121	121	120	56.1
100	61.6	118	118	119	119		50.8
200	116.8	121	119	119	119		49.5
300	172.4	119	118	118			47.1
500	281.1	123	121	120	118	119	43.5
650	363	117	117	117	118		37.8
800	439	128	125	122	121	121	37.0
950	493	124	123	122	123	122	37.5
1100	556	130	126	124	125	123	36.5
1200	595	131	129	125	125	124	37.8
1500	707	133	129	126	126	125	37.6

Table B.7 PEO 100 ppm solution in DI water with OTAC-p + equimolar NaSal

Sample #	OTAC-p + equimolar NaSal conc. (ppm)	Conductivity (µS/cm)	t_p (sec)	t_p (sec)	t_p (sec)	Surface Tension (dyne/cm)
1	50	41.5	363	361		59.7
2	100	71	360	360		54.2
3	200	128.4	367	366	365	52.3
4	300	183.4	357	358	357	47.3
5	400	240.4	358	357		45
6	500	294.1	354	358	356	41.1
7	600	350	358	341	344	37.7
8	700	405	347	345	345	35.3
9	800	457	348	347		35.3
10	900	499	351	348	349	35.7
11	1000	539	370	365	367	36
12	1200	618	369	371		35.9
13	1500	733	377	376		36.1
14	2000	929	391	390	390	35.6
15	2500	1113	404	403		36

Table B.8 PEO 1000 ppm solution in DI water with OTAC-p + equimolar NaSal

Sample #	OTAC-p + equimolar NaSal conc. (ppm)	Conductivity (µS/cm)	t_p (sec)	Surface Tension (dyne/cm)
1	50	54.4	1009	42.6
2	100	83.9	1030	42.8
3	200	141.6	1034	54.9
4	300	197	1048	50.1
5	400	253.9	1029	45.2
6	500	308	1032	43.4
7	600	362	1041	40.0
8	700	418	1062	37.5
9	800	468	1064	37.8
10	1000	553	1079	38.0
11	1200	631	1092	37.8
12	1500	747	1092	37.8

Table B.9 PEO 2500 ppm solution in DI water with OTAC-p + equimolar NaSal

Sample #	EA conc. (ppm)	t_p (sec)	t_p (sec)	t_p (sec)	t_p (sec)	t_p (sec)	Surface Tension (dyne/cm)
1	10	187	186				47.5
2	20	189	186	184	182	181	37.4
3	30	181	178	179			35.8
4	50	176	176				35
5	100	180	179	179			32.5
6	300	190	181	181			32
7	500	182	181	178	180		31.9
8	600	185	181	182	182		32
9	1000	185	183	183			31.9
10	1500	182	181				31.9
11	2500	185	184	184			32

Table B.10 CPAM 50 ppm solution in DI water with EA

Sample #	EA conc. (ppm)	t_p (sec)	t_p (sec)	t_p (sec)	t_p (sec)	t_p (sec)	Surface Tension (dyne/cm)
1	10	387	390	390			44.5
2	20	390	391				39.1
3	30	391	392				35.9
4	50	387	387				35
5	100	380	382				34.1
6	300	387	384	387	388		32.5
7	500	388	388	380	379	383	32.5
8	600	378	384	390	389		32.5
9	1000	383	386	387			32.5
10	1500	383	386	388			32.5
11	2500	389	391	391	398		32.5

Table B.11 CPAM 200 ppm solution in DI water with EA

Sample #	EA conc. (ppm)	t_p (sec)	t_p (sec)	t_p (sec)	t_p (sec)	t_p (sec)	Surface Tension (dyne/cm)
1	10	1174	1195	1195			45.5
2	20	1176	1180	1179			41.5
3	30	1162	1162				34.9
4	50	1168	1169				33.8
5	100	1126	1130	1134			33.8
6	300	1078	1073	1082			32.9
7	500	1131	1112	1101	1163	1118	32.7
8	700	1098	1100				32.2
9	1000	1137	1121	1114	1110		32.5
10	1500	1134	1113	1104	1115		32.1
11	2500	1096	1078	1068	1065		32.1

Table B.12 CPAM 500 ppm solution in DI water with EA

Sample #	OTAC-p conc. (ppm)	Conductivity (µS/cm)	Surface Tension (dyne/cm)	t_p (sec)	Turbidity (NTU)	Physical appearance
1	100	158.2	53.7	1267	1.1	clear
2	500	283.1	49.2	267	49.6	clear
3	1000	417	48	117	102	cloudy
4	3000	1038	47	106	328	cloudy
5	5000	1595	46.4	106	0.54	phase separation
6	9000	2416	45.8	105	15.9	phase separation
7	13000	2901	46	108	1.04	phase separation
8	18000	3550	45.5	112	24.1	phase separation
9	21000	3880	45.5	113	7.05	phase separation
10	25000	4420	45	113	89.6	phase separation

Table B.13 CPAM 500 ppm solution in DI water with OTAC-p

Sample #	OTAC-p conc. (ppm)	Conductivity (µS/cm)	Surface Tension (dyne/cm)	t_p (sec)	Turbidity (NTU)	Physical appearance
1	100	280.5	47	4832	3.15	clear
2	500	388	47.1	1695	26.7	cloudy
3	1000	522	46.9	537	101	cloudy
4	3000	1106	45.7	119	921	precipitations
5	5000	1703	45.2	112	6.89	phase separation
6	9000	2556	44.9	111	0.43	phase separation
7	13000	3050	45	113	0.45	phase separation
8	18000	3660	44.8	118	0.39	phase separation
9	21000	4040	44.4	118	0.38	phase separation
10	25000	4560	44.4	120	0.45	phase separation

Table B.14 CPAM 1000 ppm solution in DI water with OTAC-p

Sample #	OTAC-p conc. (ppm)	Conductivity (µS/cm)	t_p (sec)	Turbidity (NTU)	Physical appearance
1	50	494		2.4	clear
2	100	507		2.36	clear
3	200	542	18101	2.64	clear
4	400	591		9.06	clear
5	600	644		36	opaque
6	800	687		47.26	opaque
7	1000	744	4636	96.9	opaque
8	1500	878	2669	191	cloudy
9	2000	1017	1019	560	cloudy
10	2500	1152	338	1000	very minute precipitates
11	3000	1290	175	1000	some precipitates
12	4000	1636	129	658	phase separation
13	6000	2149	107	10.8	phase separation

Table B.15 CPAM 2000 ppm solution in DI water with OTAC-p

Sr. No.	OTAC-p + equimolar NaSal conc. (ppm)	Conductivity (µS/cm)	Surface Tension (dyne/cm)	t_p (sec)	Turbidity (NTU)	Physical appearance
1	100	74.1	51.2	125	1.4	clear
2	200	128.9	47.5	114	10.9	clear
3	300	184.4	44.0	114	19.5	cloudy
4	500	292.4	40.7	113	62.3	cloudy
5	700	393	38.5	111	243.0	cloudy
6	800	444	37.8	109	228.0	cloudy
7	900	494	38.2	109	11.1	Phase separation
8	1000	542	37.9	105	10.0	Phase separation
9	1200	619	37.8	107	12.8	Phase separation
10	1500	735	38.0	110	8.9	Phase separation

Table B.16 CPAM 50 ppm solution in DI water with OTAC-p + equimolar NaSal

Sr. No.	OTAC-p + equimolar NaSal conc. (ppm)	Conductivity (µS/cm)	Surface Tension (dyne/cm)	t_p (sec)	Turbidity (NTU)	Physical appearance
1	50	60.2	51.3	172	0.9	clear
2	100	92.1	50.8	161	2.3	clear
3	200	132.5	54.5	107	0.3	cloudy
4	400	255.1	43.3	116	51.0	cloudy
5	600	360	40.5	114	158.0	cloudy
6	700	409	39.9	113	266.0	cloudy
7	800	459	38.6	112	461.0	cloudy
8	1000	555	37.4	112	126.0	phase separation
9	1200	646	37.6	115	128.0	phase separation
10	1500	762	37.4	115	136.0	phase separation
11	2000	960	37.4	118	127.0	phase separation
12	2500	1146	37.5	127	116.0	phase separation

Table B.17 CPAM 100 ppm solution in DI water with OTAC-p + equimolar NaSal

Sr. No.	OTAC-p + equimolar NaSal conc. (ppm)	Conductivity (µS/cm)	Surface Tension (dyne/cm)	t_p (sec)	Turbidity (NTU)	Physical appearance
1	200	144.8	47.5	120	8.2	clear
2	400	254.9	43.0	111	39.2	clear
3	600	358	40.0	112	165.0	cloudy
4	800	458	38.3	112	537.0	cloudy
5	1000	552	37.6	111	7.0	phase separation
6	1200	646	37.3	108	18.0	phase separation
7	1400	720	37.6	108	26.0	phase separation
8	1600	797	37.5	107	20.0	phase separation

Table B.18 CPAM 100 ppm solution in DI water with OTAC-p + equimolar NaSal (Repeat run 1)

Sr. No.	OTAC-p + equimolar NaSal conc. (ppm)	Conductivity (µS/cm)	Surface Tension (dyne/cm)	t_p (sec)	Turbidity (NTU)	Physical appearance
1	50	61.5	45.7	203	2.9	clear
2	100	88.4	48.0	172	3.9	clear
3	300	195.6	45.9	117	29.6	cloudy
4	500	302	42.0	111	71.3	cloudy
5	700	402	39.0	112	259.0	cloudy
6	900	499	38.0	112	832.0	cloudy
7	1100	593	37.5	109	7.4	phase separation
8	1300	676	37.6	106	10.0	phase separation
9	1500	753	37.9	106	16.0	phase separation
10	2000	944	37.9	106	22.9	phase separation

Table B.19 CPAM 100 ppm solution in DI water with OTAC-p + equimolar NaSal (Repeat run 2)

Sr. No.	OTAC-p + equimolar NaSal conc. (ppm)	Conductivity (µS/cm)	Surface Tension (dyne/cm)	t_p (sec)	Turbidity (NTU)	Physical appearance
1	200	187.9	44.90	317	18.90	clear
2	400	292.6	41.70	167	68.40	cloudy
3	600	390	39.60	130	192.00	cloudy
4	700	438	38.50	128	243.00	cloudy
5	800	487	37.90	126	524.00	cloudy
6	900	529	38.10	120	736.00	cloudy
7	1000	574	38.60	125	1000	cloudy
8	1100	620	37.00	117	1000	precipitates
9	1500	794	35.80	110	786	phase separation
10	2000	1005	36.00	108	808	phase separation

Table B.20 CPAM 300 ppm solution in DI water with OTAC-p + equimolar NaSal

Sr. No.	OTAC-p + equimolar NaSal conc. (ppm)	Conductivity (µS/cm)	Surface Tension (dyne/cm)	t_p (sec)	Turbidity (NTU)	Physical appearance
1	50	159.3	52.6	1305	1.7	clear
2	100	184.6	48.4	1099	1.5	clear
3	300	289.3	47.3	554	18.9	cloudy
4	500	395	44.3	336	64.7	cloudy
5	700	495	42.9	195	98.5	cloudy
6	1000	641	40.6	134	259.0	cloudy
7	1300	776	40.4	126	560.0	precipitates
8	1600	896	39	121	1000.0	phase separation
9	2000	1089	38.2	114	994.0	phase separation

Table B.21 CPAM 500 ppm solution in DI water with OTAC-p + equimolar NaSal

Sr. No.	OTAC-p + equimolar NaSal conc. (ppm)	Conductivity (µS/cm)	Surface Tension (dyne/cm)	t_p (sec)	Turbidity (NTU)	Physical appearance
1	50	157	55.9	1297	1.85	clear
2	100	180.9	54.7	1102	2.47	clear
3	300	278.6	47.5	496	22.10	cloudy
4	500	379	45.9	296	42.80	cloudy
5	700	481	43.8	182	96.60	cloudy
6	900	568	41.4	125	250.00	cloudy
7	1100	657	40.1	123	661.00	cloudy
8	1300	741	40.2	125	1000.00	precipitates
9	1500	824	40	124	1000.00	phase separation
10	2000	1031	38	111	1000	phase separation

Table B.22 CPAM 500 ppm solution in DI water with OTAC-p + equimolar NaSal

Sr. No.	OTAC-p + equimolar NaSal conc. (ppm)	Conductivity (µS/cm)	Surface Tension (dyne/cm)	t_p (sec)	Turbidity (NTU)	Physical appearance
1	50	271.4	57.60	4589	1.41	clear
2	100	301	54.10	3602	1.87	clear
3	200	349	48.20	2761	3.31	clear
4	400	451	45.50	1643	25.90	cloudy
5	600	550	44.30	1095	67.70	cloudy
6	800	644	43.00	790	97.30	cloudy
7	1000	738	40.80	564	101	cloudy
8	1300	878	40.50	327	208	precipitates
9	1600	1002	40.00	211	321	precipitates
10	2000	1165	40.00	149	641	phase separation
11	2500	1369	39.20	132	946	phase separation
12	3000	1564	39.10	133	1000	phase separation

Table B.23 CPAM 1000 ppm solution in DI water with OTAC-p + equimolar NaSal

Sr. No.	OTAC-p conc. (ppm)	Conductivity (µS/cm)	Surface Tension (dyne/cm)	Turbidity (NTU)	t_p (sec)	Physical appearance
1	50	648	58.5	1.99	121	clear
2	100	663	51	1.78	122	clear
3	300	727	48	2.02	121	clear
4	500	786	45.5	1.65	120	clear
5	1000	948	47	21.7	118	cloudy
6	2000	1260	44.5	53.9	115	cloudy
7	3000	1565	45.5	22.8	115	some precipitates
8	5000	2157	45.7	0.81	115	phase separation
9	6000	2402	45.5	0.38	116	phase separation
10	7000	2560	46.5	0.35	116	phase separation
11	8000	2700	46.1	0.41	116	phase separation
12	9000	2835	46.2	0.39	117	phase separation
13	10000	2960	46.7	0.49	118	phase separation

Table B.24 CPAM 50 ppm solution in TAP WATER with OTAC-p

Sr. No.	OTAC-p conc. (ppm)	Conductivity (µS/cm)	Surface Tension (dyne/cm)	Turbidity (NTU)	t_p (sec)	Physical appearance
1	50	727	52.6	12	132	clear
2	100	742	52.2	11.3	133	clear
3	300	809	47.3	10.9	133	clear
4	500	871	44.6	10.4	134	clear
5	1000	1031	45.4	198	120	cloudy
6	2000	1349	45.5	277	120	cloudy
7	3000	1635	45.8	325	118	precipitates
8	5000	2242	45.7	2.94	119	phase separation
9	6000	2489	45.8	2.43	119	phase separation
10	7000	2647	45.7	1.08	120	phase separation
11	8000	2786	45.6	1.84	120	phase separation
12	9000	2925	45.9	2.24	121	phase separation
13	10000	3050	45.8	1.97	122	phase separation

Table B.25 CPAM 100 ppm solution in TAP WATER with OTAC-p

Sr. No.	OTAC-p conc. (ppm)	Conductivity (µS/cm)	Surface Tension (dyne/cm)	Turbidity (NTU)	t_p (sec)	Physical appearance
1	50	723	56.8	10.1	194	clear
2	100	737	51	10.1	193	clear
3	300	804	48	9.65	193	clear
4	500	867	45.6	13.1	192	clear
5	1000	1035	47.2	198	149	cloudy
6	2000	1368	48.1	500	123	precipitates
7	3000	1671	44.6	744	119	precipitates
8	5000	2266	46.4	3.51	116	phase separation
9	6000	2542	44.8	1.01	117	phase separation
10	7000	2719	46.9	0.61	118	phase separation
11	8000	2860	46.1	0.78	118	phase separation
12	9000	3000	46.2	1.02	119	phase separation
13	10000	3140	45.2	0.67	119	phase separation

Table B.26 CPAM 500 ppm solution in TAP WATER with OTAC-p

Sr. No.	OTAC-p conc. (ppm)	Conductivity (µS/cm)	Surface Tension (dyne/cm)	Turbidity (NTU)	t_p (sec)
1	50	811	52.5	3.04	414
2	100	831	51	6.54	417
3	300	894	46.8	5.37	408
4	500	956	46.9	22	376
5	1000	1120	48.2	1000	274
6	2000	1443	46.9	1000	131
7	3000	1758	47	1000	127
8	5000	2335	46.8	5.13	115
9	6000	2598	46.7	8.69	114
10	7000	2838	46.9	4.06	115
11	8000	2990	46.5	3.91	116
12	9000	3130	46.5	5.3	117
13	10000	3260	46.5	5.3	117

Table B.27 CPAM 1000 ppm solution in TAP WATER with OTAC-p

Sr. No.	OTAC-p + equimolar NaSal conc. (ppm)	Conductivity (µS/cm)	Surface Tension (dyne/cm)	t_p (sec)	Turbidity (NTU)	Physical appearance
1	50	720	53	125	6.09	clear
2	100	746	56.2	125	6.00	clear
3	300	851	44	124	5.52	clear
4	500	957	38.2	124	30.00	cloudy
5	700	1053	38	117	52.40	cloudy
6	1000	1192	38	114	56.30	precipitates
7	1300	1313	37.7	114	174.00	precipitates
8	1600	1424	37.2	116	196.00	precipitates
9	2000	1571	38	119	238.00	precipitates
10	2500	1752	37.2	125	257.00	precipitates

Table B.28 CPAM 100 ppm solution in TAP WATER with OTAC-p + equimolar NaSal

Sr. No.	OTAC-p + equimolar NaSal conc. (ppm)	Conductivity (µS/cm)	Surface Tension (dyne/cm)	t_p (sec)	Turbidity (NTU)	Physical appearance
1	50	755	54.5	195	6.79	clear
2	100	777	51	195	8.57	clear
3	300	883	41.3	189	9.1	clear
4	500	988	37.5	186	65.4	cloudy
5	700	1088	37.5	168	413	cloudy
6	1000	1216	36.5	132	1000	precipitates
7	1300	1356	36	128	252	precipitates
8	1600	1485	36	130	1000	precipitates
9	2000	1642	35.7	118	156	Phase separation
10	2500	1851	36	117	2.16	Phase separation

Table B.29 CPAM 500 ppm solution in TAP WATER with OTAC-p + equimolar NaSal

Sr. No.	OTAC-p + equimolar NaSal conc. (ppm)	Conductivity (µS/cm)	Surface Tension (dyne/cm)	t_p (sec)	Turbidity (NTU)	Physical appearance
1	50	795	57	413	2.99	clear
2	100	822	51	409	2.58	clear
3	300	931	43.5	416	6.78	clear
4	500	1031	40.2	366	98.9	cloudy
5	700	1125	39.5	324	487	cloudy
6	1000	1263	39	251	1000	precipitates
7	1300	1386	38.5	205	1000	precipitates
8	1600	1521	37.7	165	1000	precipitates
9	2000	1691	38.5	134	1000	precipitates
10	2500	1896	38.2	129	686	precipitates

Table B.30 CPAM 1000 ppm solution in TAP WATER with OTAC-p + equimolar NaSal

PEO conc. (gm / dL)	t_p (sec)
0.5	7168
0.4	3556
0.3	1692
0.25	1173
0.2	804
0.15	540
0.1	353
0.08	286
0.06	229
0.04	192
0.02	150

Table B.31 PEO Viscosity in DI water at 25 °C to calculate C*

CPAM conc. (gm / dL)	t_p (sec)
0.1	5182
0.09	4310
0.08	3452
0.07	2628
0.06	2014
0.05	1480
0.04	1113
0.03	724
0.02	505
0.015	405
0.01	273
0.009	266
0.008	247
0.007	232
0.006	212
0.004	181
0.002	144

Table B.32 CPAM viscosity in DI water at 25 °C to calculate C*

OTAC-p conc. (ppm)	Conductivity (µS/cm)
0	5.6
249	100.7
522	221
818	333
1112	425
1381	518
1599	588
1865	677
2105	752
2368	842
2605	921
3077	1068
3568	1222
4054	1375
4512	1512
4966	1652
5437	1793
5904	1912
6345	1992
6868	2076
7322	2136
7770	2191
8215	2248
8655	2305
9070	2362
9482	2411
9890	2466
10314	2516

Table B.33 OTAC-p solution in DI water continuous conductimetry data at 25 °C for finding cmc point

OTAC-p conc. (ppm)	Surface Tension Ring method (dyne/cm)	OTAC-p conc. (ppm)	Surface Tension Pendant drop method (dyne/cm)
100	75.2	100	67.5
198	73.7	500	66.14
296	72.8	2000	48.66
392	71.8	5000	41.35
488	71.1	6000	40.64
723	68.5		
952	66.1		
1395	62.1		
1818	58.6		
2222	55		
2609	54.6		
2979	52		
3333	48.5		
3673	45.6		
4000	39.1		
4314	37.2		
4615	36.5		
4906	35.5		
5185	35.5		
5455	36.5		
5714	35.8		
5965	36.6		

Table B.34 OTAC-p solution in DI water surface Tension data using Du Nouy ring method and pendant drop method for finding cmc point

Sample #	OTAC-p + equimolar NaSal conc. (ppm)	Conductivity (µS/cm)	Surface Tension (dyne/cm)
1	50	32.8	53.2
2	100	60.1	52.5
3	200	117.7	51.8
4	300	172.2	47.6
5	500	284.1	40
6	600	335	36.3
7	800	438	36.2
8	1000	517	37
9	1200	593	36.8
10	1500	706	36.9

Table B.35 Conductivity and Surface tension of OTAC-p + equimolar NaSal solution in DI water for finding cmc point

EA conc. (ppm)	Surface Tension (dyne/cm)
12.5	39.4
24.9	35.6
37.2	33
49.5	33.1
61.7	32.9
122.0	32.5
180.7	32.5
238.1	32.5

Table B.36 Surface Tension data of EA solution in DI water using Du Nouy ring method for finding cmc point

OTAC-p conc. (ppm)	Conductivity at 48.5 °C (µS/cm)	OTAC-p conc. (ppm)	Conductivity at 48.5 °C (µS/cm)
0	2.92	4314	1410
100	36	4615	1505
198	70.3	4906	1592
296	105.3	5185	1675
392	138.6	5455	1763
488	172.2	5714	1840
723	253.3	5965	1913
952	331	6207	1976
1176	405	6441	2032
1395	477	6667	2080
1609	548	6885	2126
1818	615	7097	2167
2022	682	7302	2200
2222	747	7500	2235
2609	872	7786	2287
2979	990	8060	2330
3333	1103	8321	2370
3673	1208	8571	2408
4000	1312		

Table B.37 OTAC-p solution in DI water continuous conductimetry data at 48.5 °C

OTAC-p conc. (ppm)	Conductivity at 48.5 °C (µS/cm)	OTAC-p conc. (ppm)	Conductivity at 48.5 °C (µS/cm)
0	16.41	4906	1599
100	48.8	5185	1683
198	82.9	5455	1768
296	116	5714	1845
392	148.5	5965	1918
488	181.1	6207	1982
723	264.9	6441	2035
952	341	6667	2085
1176	417	6885	2130
1395	486	7097	2170
1609	558	7402	2227
1818	627	7692	2273
2222	769	7970	2319
2609	881	8235	2362
2979	994	8571	2415
3333	1109	8920	2469
3673	1215	9189	2512
4000	1316	9474	2555
4314	1415	9744	2596
4615	1509	10000	2632

Table B.38 PEO 1000 ppm solution in DI water conductimetry data at 48.5 °C

OTAC-s conc. (ppm)	Conductivity (µS/cm)	OTAC-s conc. (ppm)	Conductivity (µS/cm)
0	2.06	123	18.75
4	2.72	138	20.74
8	3.27	153	22.78
12	3.86	167	24.51
16	4.36	180	26.31
20	4.89	194	27.98
23	5.42	206	29.5
27	5.9	219	31
31	6.43	231	32.4
35	6.94	242	33.6
38	7.42	254	34.7
46	8.39	265	35.5
53	9.39	275	36.3
60	10.36	286	37
67	11.28	306	38.3
74	12.26	324	39.5
81	13.16	342	40.6
88	14.08	359	41.7
94	14.95	375	42.7
101	15.85	398	44
107	16.71	425	45.8

Table B.39 OTAC-s solution in DI water continuous conductimetry at 25 °C to find cmc point

OTAC-s conc. (ppm)	Conductivity at 48.5 °C (µS/cm)	OTAC-s conc. (ppm)	Conductivity at 48.5 °C (µS/cm)
0	2.62	319	44.6
20	5.6	347	47
39	8.38	361	48.3
58	11.1	381	49.9
78	13.68	400	51.4
97	16.45	431	53.8
113	18.58	462	56
131	20.91	491	58.2
148	23.14	519	60.1
165	25.6	571	63.9
182	27.73	621	67.2
206	31	667	70.2
230	34	730	74.3
253	36.8	788	78
276	39.5	857	82.4
298	42.1		

Table B.40 OTAC-s solution in DI water continuous conductimetry data at 48.5 °C

OTAC-s conc. (ppm)	Conductivity at 48.5 °C (µS/cm)	OTAC-s conc. (ppm)	Conductivity at 48.5 °C (µS/cm)
0	15.82	431	60.3
21	18.35	462	62.8
44	21.31	491	65.2
58	23.1	519	67.3
77	25.45	545	69.3
95	27.71	571	71.2
113	29.9	596	73
131	32	621	74.6
148	34	667	77.7
165	35.8	710	80.5
182	37.5	750	83
206	40	788	85.1
230	42.4	824	87.1
257	44.9	857	88.7
276	46.7	889	90.4
298	48.8	919	91.8
319	50.8	947	93.2
340	52.6	974	94.6
361	54.4	1000	95.8
381	56.1	1059	98.6
400	57.7	1111	101.1

Table B.41 PEO 1000 ppm solution in DI water continuous conductimetry data at 48.5 °C

Appendix C

Specifications Datasheet

Properties

Typical Properties	1216-1.5	1214GC-2	1214GC-3	1412-3
Average Molecular Wt.	258	284	327	341
Color, APHA	10	10	15	10
Water, Wt. %	0.03	0.03	0.03	0.03
Hydroxyl Number, mg KOH/g	217	197	175	170
Glycol, Wt. %	0.47	0.50	0.43	0.72
Specific Gravity 22°C/22°C	0.869	0.900	0.920	0.920
Flash Point, (PM) °C	127	138	149	160
Melting Range, °C	3 to 4	7 to 11	4 to 7	8 to 13
Pour Point, °C	4	7	4	8
Cloud Point				
mls of Water@25°C	21.9	23.4	37.1	36.7
Viscosity, cSt	17	14.6	15	52
Temperature,°C	37.8	40	37.8	21
Appearance, 25°C	Clear, colorless liquid	Clear, colorless liquid	Clear, colorless liquid	Clear, colorless liquid
pH, 5% in H_2O/IPA	6.4	6.8	6.9	7.0
Avg. EO content, moles	1.3	2.0	2.8	3
Avg. EO content, Wt. %	22	30	40	40
HLB	4.4	6	8	8

Typical Properties	1618-5	1216CO-7	1412-7	1218-8	1412-9
Average Molecular Wt.	469	508	513	525	601
Color, APHA	25	15	20	15	20
Water, Wt. %	0.04	0.02	0.04	0.02	0.02
Hydroxyl Number, mg KOH/g	125	114	110	100	93
Glycol, Wt. %	-	-	0.92	-	1.24
Specific Gravity 22°C/22°C	-	0.985	0.98	0.989	0.995
Flash Point, (PM) °C	-	147	166	241	171
Melting Range, °C	28 to 31	7 to 18	19 to 25	-	20 to 25
Pour Point, °C	-	18	19	-	22
Cloud Point 1% in Water, °C	-	54.2	53.9	68.0	79.2
Viscosity, cSt	-	15	35	38	37.9
Temperature, °C	-	37.8	37.8	40	40
Appearance, 25°C	White solid	Cloudy liquid	Cloudy liquid	White solid	White solid
pH, 5% in H_2O/IPA	7.0	6.8	6.7	6.8	6.7
Avg. EO content, moles	5.1	7	7	7.4	9
Avg. EO content, Wt. %	46	60	60	62	66
HLB	9	12	12	12.4	13.2

EA specifications (Source: Sasol North America, USA)

Molekula S.a.r.l.
Z.I. du Chapelier
St. Jean-de-Soudain
38110 La Tour du Pin
France
Tel: +33 (0) 6 19 11 96 97
Fax: +33 (0) 4 74 97 43 68

Molekula Ltd.
Technology House, Old Forge Road
Ferndown Industrial Estate
Wimborne Dorset BH21 7RR
United Kingdom
Tel: +44 (0) 1202 86 3000
Fax: +44 (0) 1202 86 3003

Molekula Life Sciences (P) Ltd
'Kanchan', 10, Umanagar
Begumpet,
Hyderabad 500 016
A.P. India
Tel: +91 (0) 40 6662 6366
Fax: +91 (0) 40 6682 6366

Molekula GmbH
Werk Nienburg
Grosse Drakenburger Str. 93-97
31582 Nienburg/Weser
Deutschland
Tel: +49 (0) 5021 988 341
Fax: +49 (0) 5021 988 342

Certificate of Analysis

Product	Octadecyltrimethylammonium chloride
Product Number	61986888(M67752390)
CAS Number	112-03-8
Batch Number	60802
Physical Appearance	White Powder
Purity(HPLC)	98.65%
Moisture	0.2%

molekula July 2007

internet : www.molekula.com email : info@molekula.com

Octadecyltrimethylammonium Chloride certificate of Analysis (Source : Molekula Ltd., UK)

Bibliography

Aloulou, F., Boufi, S., Chakchouk, M.; Adsorption of octadecyltrimethylammonium chloride and adsolubilization on to cellulosic fibers; *Colloid and Polymer Science*, 282(7), pp-699, 2004

Anthony, O., Zana, R.; Effect of temperature on the interactions between neutral polymers and a cationic and a nonionic surfactant in aqueous solutions; *Langmuir,* 10 (11), pp 4048-4052, 1994

Benkhira, A., Lachhab, T., Bagassi, M., & François, J.; Interactions of polyethers with a cationic surfactant; Polymer, 41(7), pp. 2471-2480, March, 2000

Bewersdorff, H., Frings, B., Lindner, P., Oberthur, R. C.; The conformation of drag reducing micelles from small-angle-neutron-scattering experiments; *Rheologica Acta,* 25(6), 642-646, 1986

Bewersdorff, H., Ohlendorf, D.; Behaviour of drag-reducing cationic surfactant solutions; *Colloid and Polymer Science*, 266(10), 941-953, 1988

Bewersdorff, H. W., Dohmann, J., Langowski, J., Lindner, P., Maack, A., Oberthur, R., et al.; SANS- and LS-studies on drag-reducing surfactant solutions; *Physica B*,Vol.156-157,pp.508-511,Jan.-Feb. 1989; *4th International Conference on Neutron Scattering* (ICNS 88), 12-15 July 1988, *Grenoble, France*. , 156-157 508-511, 1989

Bewersdorff, H.; Drag reduction in surfactant solutions; *Progress in Colloid and Polymer Science*, 81, 248-249, 1990

Brackman, J. C., van Os, N. M., Engberts, J. B. F. N.; Polymer-nonionic micelle complexation formation of poly(propylene oxide)-complexed n-octyl thioglucoside micelles; *Langmuir*, 4(6), 1266-1269, 1988

Cabane, B.; structure of some polymer-detergent aggregates in water; *Journal of physical chemistry,* 81 (17), pp 1639-1645, 1977

Carlsson, A., Lindman, B., Watanabe, T., Shirahama, K; Polymer-surfactant interactions: binding of N-tetradecylpyridinium bromide to ethyl(hydroxyethyl)cellulose; *Langmuir*, 5(5), 1250-1252, 1989

Deo, P., Deo, N., Somasundaran, P., Moscatelli, A., Jockusch, S., Turro, N.J., Ananthapadmanabhan, K., Ottaviani, M.; Interactions of a hydrophobically modified polymer with oppositely charged surfactants; *Langmuir*, 23 (11), pp 5906-5913, 2007

Ezrahi, S., Tuval, E., & Aserin, A.; Properties, main applications and perspectives of worm micelles; *Advances in Colloid and Interface Science*, 128-130, suppl. Complete, pp. 77-102, December, 2006.

Feitosa, E., Brown, W., Vasilescu, M., Swanson-Vethamuthu, M.; Effect of temperature on the interaction between the nonionic surfactant C 12 E 5 and poly(ethylene oxide) investigated by dynamic light scattering and fluorescence methods; *Macromolecules*, 29(21), pp. 6837-6846, October,1996

Ge, L., Zhang, X., Guo, R.; Microstructure of Triton X-100/poly (ethylene glycol) complex investigated by fluorescence resonance energy transfer; *Polymer* 48, (9), pp 2681-2691, 2007

Goddard, E. D.; Polymer—surfactant interaction part I. uncharged water-soluble polymers and charged surfactants; *Colloids and Surfaces*, 19(2-3), pp. 255-300, August, 1986

Goddard, E. D.; Polymer—surfactant interaction part II - polymer and surfactant of opposite charge; *Colloids and Surfaces*, 19(2-3), 301-329, 1986

Goddard, E. D., Ananthapadmanabhan, K.; Interactions of Surfactants with Polymers and Proteins; *CRC Press, Boca Raton,* 1993

Goddard E. D.; Polymer / Surfactant Interaction: Interfacial Aspects; *Journal of Colloid and Interface Science*; 256, 228 – 235, 2002

Guillot, S., McLoughlin, D., Jain, N., Delsanti, M., Langevin, D.; Polyelectrolyte-surfactant complexes at interfaces and in bulk; *Journal of Physics Condensed Matter*, 15 (1), pp. S219-S224, 2003

Hayakawa, K., Kwak, J.C.T.; Surfactant-polyelectrolyte interactions-1-Binding of dodecyltrimethylammonium ions by sodium dextran sulfate and sodium poly(styrenesulfonate) in aqueous solution in the presence of sodium chloride; *Journal of Physical Chemistry*, 86 (19), pp. 3866-3870,1982

Hayakawa, K., Santerre, J.P., Kwak, J.C.T.; Study of surfactant-polyelectrolyte interactions, Binding of dodecyl- and tetradecyltrimethylammonium bromide by some carboxylic polyelectrolytes; Macromolecules, 16 (10), pp. 1642-1645, 1983

Hinch, E. J.; Mechanical models of dilute polymer solutions in strong flows; *Physics of Fluids*,Vol.20,no.10,pp.S22-S30,Oct. 1977; Structure of Turbulence and Drag Reduction, 7-12 June 1976, Washington, DC, USA. , 20(10) S22-S30, 1977

Ikawa, Takeo, Abe, Koji, Honda, Kenji, Tsuchida, Eishun; Interpolymer complex between poly (ethylene oxide) and poly (carboxylic acid); *J Polym Sci Polym Chem* Ed, 13 (7), pp. 1505-1514, 1975

Jones, M. N.; The interaction of sodium dodecyl sulfate with polyethylene oxide; *Journal of Colloid and Interface Science*, 23(1), pp. 36-42, January, 1967

Kang K., Kye-Hong , Kim, H. , Lim, K.; Effect of temperature on critical micelle concentration and thermodynamic potentials of micellization of anionic ammonium dodecyl sulfate and cationic octadecyltrimethylammonium chloride; *Colloids and Surfaces A: Physicochemical and Engineering Aspects*, 189(1-3), 113, 2001

Kurata, M., Tsunashima, Y.; Chapter VII; Polymer Handbook 3rd edition, edited by Brandrup, J., Immergut E. H.; Willey interscience publication, pp VII 8, 22, 1989

Lissi, E., Abuin, E.; Aggregation numbers of sodium dodecyl sulfate micelles formed on poly(ethylene oxide) and poly(vinyl pyrrolidone) chains; *Journal of Colloid and Interface Science*, 105(1), pp 1-6, May, 1985

Liu, J., Takisawa, N., Shirahama, K., Abe, H., Sakamoto, K.; Effect of polymer size on the polyelectrolyte-surfactant interaction; *Journal of Physical Chemistry,* 101 (38), pp 7520-7523, 1997

Lumley, J. L.; Drag reduction in turbulent flow by polymer additives; *Journal of Polymer Science*, 7, 263-290, 1973

Mata, J., Patel, J., Jain, N., Ghosh, G., Bahadur, P.; Interaction of cationic surfactants with carboxymethylcellulose in aqueous media; *Journal of Colloid and Interface Science*, 297 (2) pp 797-804, 2006

Matras, Z., Malcher, T., & Gzyl-Malcher, B.; The influence of polymer-surfactant aggregates on drag reduction; *Thin Solid Films*, 516 (24), pp 8848-8851, October, 2008

Metzner, A., Metzner, A.; Stress levels in rapid extensional flows of polymeric fluids; *Rheologica Acta*; 9,(2), pp 174-181, 1970

Moroi, Y., Akisada, H., Saito, M., & Matuura, R.; Interaction between ionic surfactants and polyethylene oxide in relation to mixed micelle formation in aqueous solution; *Journal of Colloid and Interface Science,* 61(2), pp 233-238, September, 1977

Mukerjee, P., Mysels, K.; Critical Micelle concentrations of Aqueous surfactant systems; *National Bureau of standards, United States Department of commerce,* NSRDS-NBS 36, p-137, 1971

Mya, K. Y., Jamieson, A. M., & Sirivat, A.; Interactions between the nonionic surfactant and polyacrylamide studied by light scattering and viscometry; *Polymer*, 40(21), pp 5741-5749, October, 1999

Mya, K.Y., Jamieson, A.M., Sirivat, A.; Effect of temperature and molecular weight on binding between poly (ethylene oxide) and cationic surfactant in aqueous solutions; *Langmuir,* 16 (15), pp 6131-6135, 2000

Mya, K.Y., Sirivat, A., Jamieson, A.M.; Effect of ionic strength on the structure of polymer-surfactant complexes; *Journal of Physical Chemistry B,* 107 (23), pp 5460-5466, 2003

Nilsson, S.; Interactions between water-soluble cellulose derivatives and surfactants. 1. The HPMC/SDS/water system; *Macromolecules,* 28 (23), pp 7837 -7844, 1995

Pal R.; Rheology of Emulsions Containing Polymeric Liquids; Encyclopedia of Emulsion Technology vol. 4, Edited by Becher P.; Marcel Dekker Inc., NY, pp 93-112, 1996

Patterson, R. L., Little, R. C.; The drag reduction of poly(ethylene oxide)-carboxylate soap mixtures; *Journal of Colloid and Interface Science*, 53(1), pp 110-114, October, 1975

Povkh, I. L., Stupin, A. V., Aslanov, P. V.; Structure of turbulence in flows with surfactant and polymeric additives; *Fluid Mechanics - Soviet Research*, 17(1), pp 65-79, 1988

Qiao, L., Easteal, A. J.; The interaction between triton X series surfactants and poly (ethylene glycol) in aqueous solutions; *Colloid & Polymer Science*, 276(4), pp 313-320, 1998

Rodenhiser A. P., Kwak J. C. T.; Polymer-surfactant systems: Introduction and overview; *Polymer surfactant systems edited by* Kwak J., *Surfactant science series vol. 77*; *Marcel Dekker Inc.,* pp - 1-20, 1998

Saito, S.; Solubilization properties of polymer-surfactant complexes; *Journal of Colloid and Interface Science,* 24(2), pp 227-234, June, 1967

Saito S., Taniguchi, T.; Effect of nonionic surfactants on aqueous polyacrylic acid solutions *Journal of Colloid And Interface Science*, 44 (1), pp 114-120, 1973

Saito S.; Polymer-surfactant interactions; Nonionic surfactants physical chemistry Edited by Schick, M. *Surfactant science series; Marcel Dekker Inc.*, 23, pp 881-926, 1987

Savins, J.; "A stress-controlled drag-reduction phenomenon"; *Rheologica Acta,* 6,(4), pp 323-330, 1967

Schwuger, M.; Mechanism of interaction between ionic surfactants and polyglycol ethers in water; *Journal of Colloid and Interface Science*, 43(2), pp 491-498, May, 1973

Seonwook, K.; Turbulent drag reduction behavior of pseudoplastic fluids in straight pipes; *PhD thesis, University of Waterloo*, 2003

Sirivat, A., Suksamranchit, S.; Influence of ionic strength on complex formation between poly(ethylene oxide) and cationic surfactant and turbulent wall shear stress in aqueous solution; *Chemical Engineering Journal*, 128(1), pp 11-20, 2007

Suksamranchit, S., Sirivat, A., & Jamieson, A. M.; Influence of polyethylene oxide on the rheological properties of semidilute, wormlike micellar solutions of hexadecyltrimethylammonium chloride and sodium salicylate; *Journal of Colloid and Interface Science*, 304(2), pp 497-504, December, 2006[1]

Suksamranchit, S., Sirivat, A., & Jamieson, A. M.; Polymer-surfactant complex formation and its effect on turbulent wall shear stress. *Journal of Colloid and Interface Science*, 294(1), pp 212-221, February, 2006[2]

Tabor, M., de Gennes, P. G.; A cascade theory of drag reduction; *Europhysics Letters*, 2(7), pp 519-522, 1986

Tesauro, C., Boersma, B. J., Hulsen, M. A., Ptasinski, P. K., Nieuwstadt, F. T. M.; Events of high polymer activity in drag reducing flows. *Flow, Turbulence and Combustion*, 79(2), pp 123-132, September, 2007

Trabelsi, S., Raspaud, E., & Langevin, D.; Aggregate formation in aqueous solutions of carboxymethylcellulose and cationic surfactants; *Langmuir*, 23(20), pp 10053-10062, September, 2007

Virk, P. S.; Drag reduction fundamentals; *AICHE Journal*, 21(4), pp 625-656, July, 1975

Vlassopoulos, D., Schowalter, W. R.; Steady viscometric properties and characterization of dilute drag-reducing polymer solutions. *Journal of Rheology*, Vol.38,no.5,pp.1427-1446,Sept.-Oct. 1994; *Boston Symposium on Liquid Crystals, Oct. 1993, Boston, MA, USA.* , 38(5) pp 1427-1446, 1994

Wallin, T., Linse, P.; Monte Carlo simulations of polyelectrolytes at charged micelles. 1. Effects of chain flexibility; *Langmuir*, 12 (2), pp 305-314, 1996

White, C., Mungal, M.; Mechanics and Prediction of Turbulent Drag Reduction with Polymer Additives; *Annual Review of Fluid Mechanics*; 40, pp 235-256, 2008

Winnik, F. M.; Interaction of fluorescent dye labeled (hydroxypropyl)cellulose with nonionic surfactants; *Langmuir*, 6(2), 522-524, 1990

Winnik, F. M., Regismond, S. T. A.; Fluorescence methods in the study of the interactions of surfactants with polymers; *Colloids and Surfaces A: Physicochemical and Engineering Aspects*, 118(1-2), pp 1-39, November, 1996

Zakin, J., Lu, B., Bewersdorff; Surfactant drag reduction; *Reviews in Chemical Engineering*; 14, 4-5, pp 253-320, 1998